

COMPACTION EQUIPMENT

THEORY AND PRACTICE



SAKAI®

PREFACE

The first edition of this book was published in English in 1985 entitled "COMPACTION EQUIPMENT and Practice". It has since been used by overseas road engineers as a guide for roadway building. During the last decade from its publication, research and development have been undertaken in the fields of compacting machinery, technology of their use and construction method. The case is the same the world over.

With the 20th century approaching an end, technology in the area concerned is still developing towards the coming 21st century. At this period, we reviewed the first edition, arranged the data obtained during the past 10 years and are now publishing this revised edition, both in Japanese and English versions, with newly added information.

The added items are:

- ① **Analysis by elasto-plasticity finite element method for compacting results of steel rollers**
- ② **Prevention of mix pick up on roll surfaces**
- ③ **Development of a roller for RCD**
- ④ **Development of a roller for RCCP**
- ⑤ **Nutating roller**
- ⑥ **Automatic control for compaction process**
- ⑦ **Inductive estimate of compaction results**

The construction of compaction test facilities has been completed at Sakai's laboratory in February, 1995. They will facilitate more efficient experimental investigation for the development of both compacting equipment and compacting technology.

March, 1996

Koyama Fujio
Sakai Heavy Industries, Ltd.

CONTENTS

PREFACE

I. MECHANIZATION OF COMPACTION	1
II CLASSIFICATION OF COMPACTION MACHINES	3
III. COMPACTING CHARACTERISTICS	4
1. Compacting by Steel Rollers	4
(1) Experimental analysis	4
(2) Analysis by elasto-plasticity finite element method	12
2. Compacting by Pneumatic Tired Rollers	19
(1) Characteristics of pneumatic tire.....	19
(2) Compaction operation by pneumatic tired rollers	35
(3) Prevention of mix pick-up on wheels.....	37
3. Compacting by Tamping Rollers	41
IV. COMPACTING BY VIBRATING ROLLERS	46
1. Compactive Characteristics of Vibrating Rollers	46
2. Applications of Vibrating Rollers	60
(1) Adaptability to granular material	60
(2) Vibratory compaction of low-slump cement concrete (RCD)	65
3. Development of a Roller (SD450) for RCD	81
(1) Specification decision	81
(2) Vibrating system.....	82
(3) Soil compaction tests.....	83
(4) RCD compaction tests.....	88
4. Development of a Roller for RCCP	96
(1) RCCP pavement	97
(2) Expanding the application field	100
V. NUTATING ROLLER (HORIZONTAL VIBRATING ROLLER)	101
1. Background of the Development	101
2. Principle of Nutating Motion	103
3. Characteristics of Nutating Roller	104
4. Power Consumption to Drive Vibrator	107
5. Experimental Comparison Between Compaction Effects	108

6. Field Tests to Determine Compacting Effects	110
(1) Weight and travel speed of test machines	110
(2) Settlement rate and number of passes	110
(3) Degree of compaction.....	111
(4) Compaction characteristics	112
7. Summation of Features	113
VI. AUTOMATIC CONTROL OF COMPACTION PROCESS	114
1. Evaluation of Compaction Operation	114
2. Compaction Meter	114
3. Compaction Simulation	117
4. Automated Control of Compaction Process	119
VII. INDUCTIVE ESTIMATE OF COMPACTION RESULTS	120
1. Prediction Formulas of Dry Density (for General Vibrating Rollers)	120
(1) Basic formula	120
(2) Basic coefficient formulas.....	121
(3) Modified coefficient formulas.....	121
2. Prediction Formulas of Dry Density (for Small-sized Rollers under 2 tons)	122
(1) Basic formula	122
(2) Basic coefficient formulas.....	122
(3) Modified coefficient formulas.....	123
3. Prediction Formulas of CBR (for General Vibrating Rollers)	124
(1) Prediction formula.....	124
(2) Calculation example.....	124
(3) Comparison between the test data and prediction value	125
(4) Other examples.....	125
4. Summary.....	125
CONCLUSION	127
Definitions	129
References	134
APPENDIX	
Application range for SAKAI conpaction equipment • Specifications	



Midnight paving work in Matsuyama City

I. MECHANIZATION OF COMPACTION

History tells us that mechanical power was applied much earlier to the road roller than to other types of road construction tools. Of them, the road roller was the pioneer in the domain of construction, having a history of more than a century.

Over a long period, up to years before World War II, the road roller was the one and only powered compacting tool for road building that performed major processes of road construction. In this infancy, many soil engineering scholars including Terzaghi and Atterberg laid down the foundation of compaction theory. In 1930, R. R. Proctor built the basis for standard density tests known as the Proctor Test. With the Proctor method having come into wide application to evaluate the quality of compacted soil, it became evident from experience that compaction with the road roller alone was not adequate, and that the whole process of road construction, from earth excavating and filling to paving, had to be rationalized. To achieve effective compaction of dams or huge embankments, etc., the so-called "sheep's foot roller" (general term of rollers having many projections on their drum surfaces) came into existence, and have developed to self-propelled and vibratory types.

During World War II, the sudden need for large-scale military airfields gave rise to pneumatic tired rollers, some weighing as much as 200 tons. Self-propelling smooth-tire rollers in popular use today are all outcomes of the wartime tired rollers employed in the rush construction of air field runways.

Roads and highways as public properties are built by contractors to the specifications laid down by the public authority. In this regard, the development of uniform criteria on the quality of compaction was slow in coming. In some cases the practice of specifying the compaction machinery was prevalent while in others the method of compaction based on the use of certain types of machinery with or without the specification of the end results was laid down to the contractor. Three typical types of specification required the contractor to use:

- ① **Specified construction materials and machinery.**
- ② **Specified machinery as compaction method**
- ③ **Any materials, machinery or method but to the stated end results.**

There were other combinations, but these three stood out as representative ones.

In the United States, this state of affairs persisted for long among the various regional and local authorities and, consequently, the manufacturers of compaction machinery competed with one another by designing various types of machines to meet the diversified requirements.

In the domain of earthworks for road construction, there is a widely-accepted conception that the stability and strength of base courses or subgrade largely depend upon how satisfactorily compaction operation is performed. This notion also applies to asphalt pavement building.

Efforts of engineers concerned have been directed to how economically and effectively finish rolling should be conducted to realize high grade and uniform quality pavement.

To cope with this problem, every trial has been made and various types of machines have been employed particularly for asphalt pavement construction. Some paving technologies and equipment have developed highly to those we have today. A few of them were questionable and have since faded into oblivion.

New trials still continue, particularly in the field of vibratory roller applications. In the course of these periods of trial and error, construction methods by combined use of steel, pneumatic and vibratory rollers were adopted and have taken root particularly in asphalt pavement building. This is greatly attributable to a guide, "Manual for Asphalt Pavement" prescribed by the Japan Road Association, and other construction guides related.

The guide recommends as follows:

- Breakdown rolling ⇨ 2 passes with 10- to 12-ton steel roller
- Intermediate ⇨ With 8- to 20-ton pneumatic tired roller or 6- to 10-ton vibratory roller. In some cases, vibratory roller is preferable to pneumatics.
- Finish ⇨ 2 passes with pneumatic tired or steel roller

Today, construction works are conducted, in general, based upon the guide as mentioned above.

However, the guide does not necessarily stipulate the strict use of work methods and related equipment as stated in it, but prescribes the quality of resulting pavement structure.

For this reason, it is an appointed task for both construction technology and construction equipment technology to build pavements that satisfy quality requirements under given conditions and at minimum costs.

To achieve this, investigations must be made from both aspects, theory and practice, to seek the contact point of construction technology and equipment technology.

This book is intended to serve as a guide to this task.

II. CLASSIFICATION OF COMPACTION MACHINES

Compressive force for compaction can be produced in several ways. Broadly viewed, there are two basic modes of compressing the earth. One makes use of weight or force due to gravity and is static; the other utilizes momentum and is dynamic. According to these basic modes, compaction machines are in two groups:

① Machines utilizing gravity

- ex) Road rollers (steel rollers)
Pneumatic tired rollers
Tamping rollers and the like

② Machines utilizing dynamic force

- ex) Vibrating rollers
Tampers
Rammers and the like

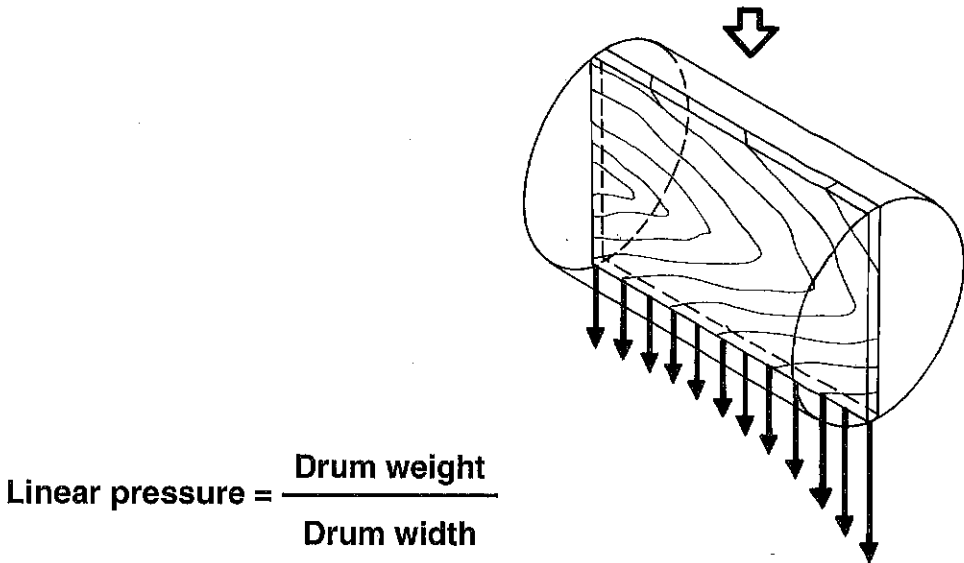
Pages that follow discuss compacting characteristics of typical types of compacting equipment; steel, pneumatic, tamping and vibrating rollers.

III. COMPACTING CHARACTERISTICS

1. Compacting by Steel Rollers

(1) Experimental analysis

As a solid cylinder rolls on the material spread out on the ground surface, the weight of the drum acts at the line of contact to compress the earth (Fig. 3-1). Imagine such a drum in steady rolling motion: we may picture the line of contact as if it were the bottom edge of a plate being pushed down. This gives rise to the concept of “linear pressure” or “line intensity”.



$$\text{Linear pressure} = \frac{\text{Drum weight}}{\text{Drum width}}$$

Fig. 3-1 Pressure under a solid drum

The linear pressure, or the drum weight per unit width, means far more than what this definition signifies. If this pressure is too large, that is, if the drum is too heavy, the bottom edge of the imaginary plate will thrust itself into the earth. As this plate advances continuously (as drum rolls), the bottom edge will then push the material ahead into a “wave”. This tendency is prominent with material high in plasticity.

The “shoving” or “waving” tendency eats into the compacting efficiency of the roller and suggests a certain mutually limiting or optimum relationship among drum diameter, width and weight. This relationship is illustrated most eloquently in the curves plotted by Garbotz to show the dry density (t/m^3) of compacted soil as a function of the linear pressure for different diameters of drums.

The experimental data compiled by Garbotz into curves, in Fig. 3-2, clearly indicate that, for each drum diameter, there is a certain optimum linear pressure that can produce the highest attainable compaction.

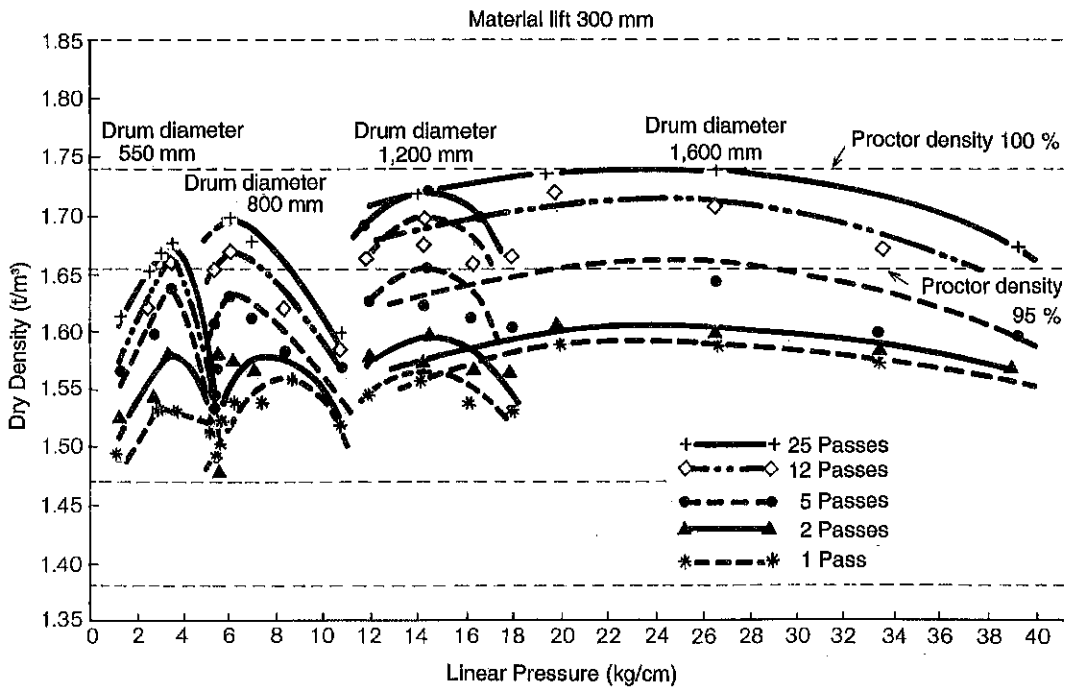


Fig. 3-2 Relationship between drum diameter, linear pressure and dry density of compacted material (Towed drum)

Let's consider the distribution of pressure in the soil under the roller, by bringing the imaginary plate back into play. In the soil under the bottom edge of the plate, pressure is transmitted in a distributive way. This came out with the equi-pressure curves by Boussinesq shown in Fig. 3-3.



Concentrated work for construction of an
expressway in a suburb of Takamatsu City

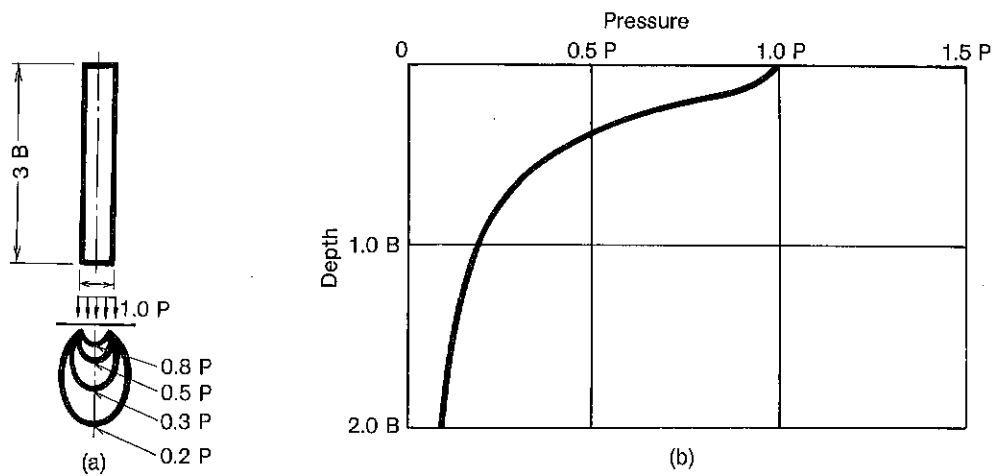


Fig. 3-3 Pressure distribution under solid plate

From this graphic representation, we can readily see that the pressure is concentrated at the surface directly below the edge and that this concentration accounts for the tendency, under certain conditions, of the roller to shove the material ahead into waves.

Boussinesq's distribution pattern presupposes the roller to be in static condition. The same roller in rolling motion modifies the distribution pattern, as will be seen in the following illustration based on the results of an investigation of the hot-asphalt mixture being compacted by steel roller.

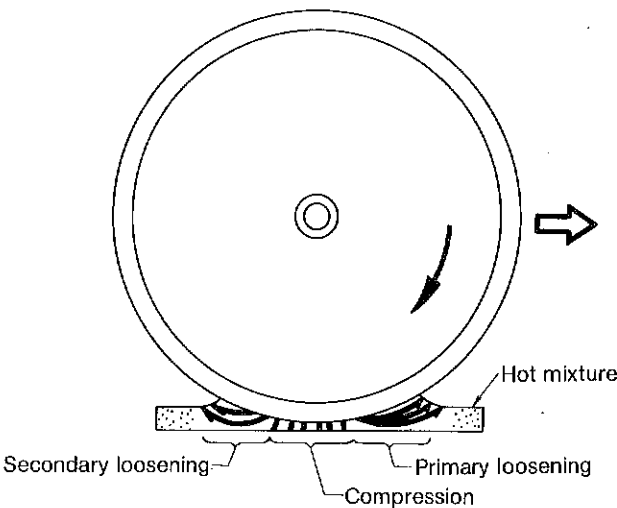
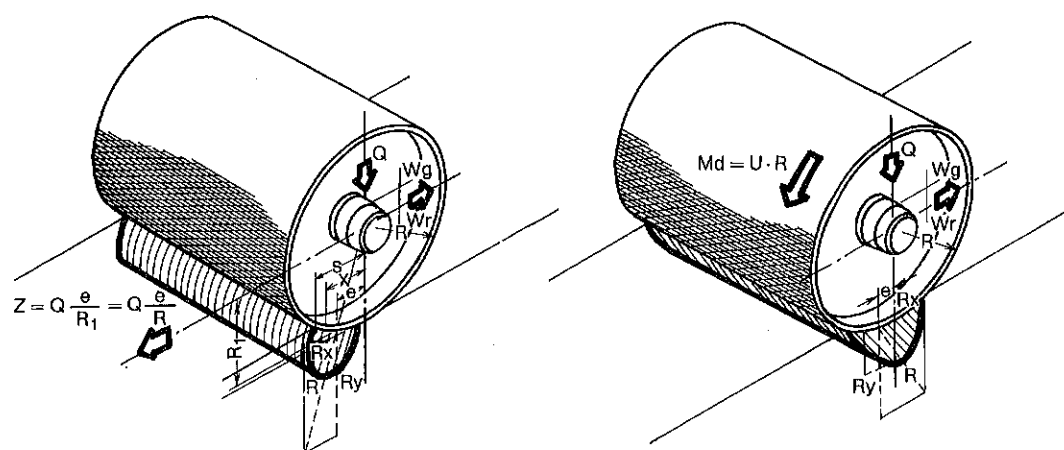


Fig. 3-4 Behavior of asphalt hot mix under drum in motion

The drum is advancing to the right. The portion of the surface immediately ahead of the localized area under direct pressure is momentarily shoved and becomes loosened because the shoved volume is not confined: it bulges upward slightly. A moment later, the surface of the drum rides onto that bulge to compress it while the drum parts with the previously compacted portion. The portion now being compressed affects the compacted portion behind it to loosen the latter portion somewhat.

This loosening is indicated as "secondary" in the illustration, and may be thought of as the effect of reaction of the passing drum to the compacted surface. Just how much the primary (ahead of the point of contact) and secondary loosening occurs is determined by a number of factors, of which the dominant one is whether the drum is towed (non-driving) or driven, the others being the linear pressure of the drum, the properties of the material (which is an asphalt hotmix in the above illustration) and the bearing capacity of the subbase or further subgrade.

Two cases of compaction by solid drum are analyzed in the next illustration: one for towed and the other for driven (propelled) drum:



(a) Towed drum

(b) Self-propelled drum

r : Drum radius
 e : Arm of rolling resistance
 Q : Drum weight
 W_g = Bearing friction = μQ
 W_r = Rolling resistance = eQ
 Z : Tractive force
 $R_x = Z = W_g + W_r$
 $R_y = Q$

U : Tangential force
 $R_x = U = W_g + W_r$
 $R_y = Q$

Fig. 3-5 Difference in compacting performance between towed and self-propelled drums

Force involves action and reaction and we may regard the drum as acting or reacting, depending on the point of view. Now, if we view the ground surface as reacting and the drum as acting, the reactive force in the above two instances is roughly equal to the resistance of soil against the external force acting on it. The predominant factor governing the magnitude of this reaction is the linear pressure: this explains the phenomena of "wave" formation and cracking for the surface.

Another factor, besides weight Q , comes into play where the drum is a self-propelling drum, not a towed one. It is expressed in terms of driving torque M_d . If the reaction from the surface is inordinately large, cracks by shearing could occur in the compacted layer. This phenomenon is attributable to the fact that the drum is not merely riding on the surface but is kicking it.

In the case of a towed drum, a large reaction in excess of an optimized intensity of linear pressure is likely to induce shifts between layers. In this connection, Garbotz has published a useful reference for explaining the relationship between dry density and linear pressure: one previously shown as Fig. 3-2 and this as Fig. 3-6 for a self-propelling drum; parameters differing in drum diameters are taken up for each case.

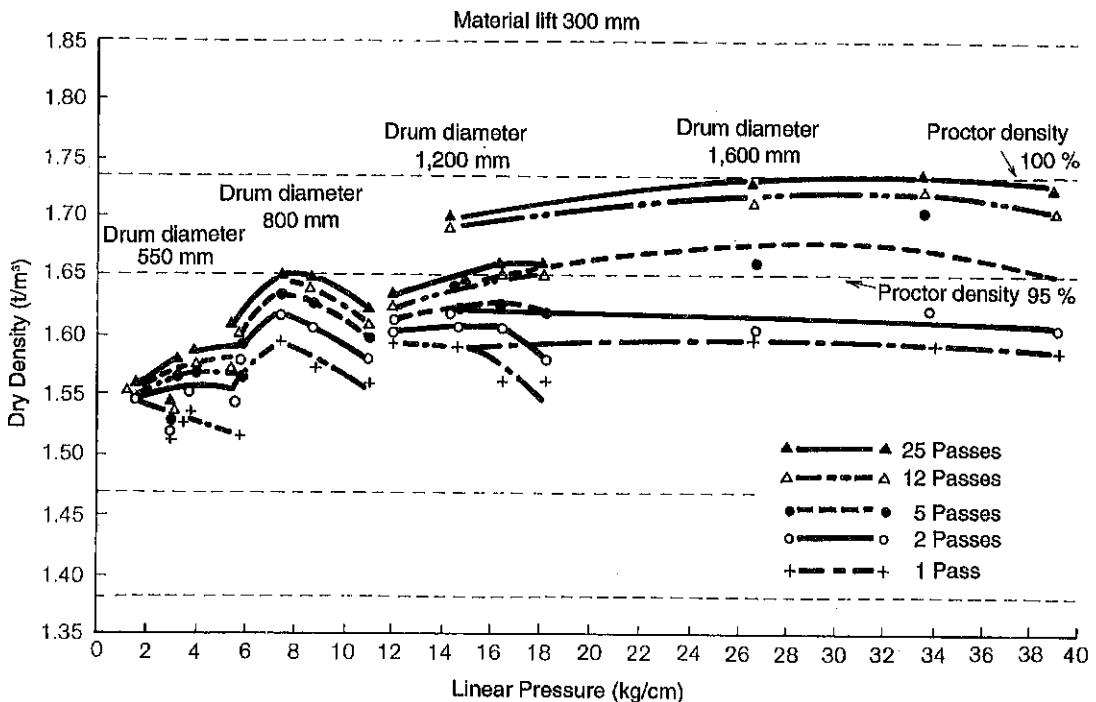


Fig. 3-6 Relationship between drum diameter, linear pressure and dry density of compacted material (Self-propelled drum)



Overlaying operation on Tohoku Expressway

From the comparison of these curves by Garbotz, we may assume that the self-propelling drum permits the linear pressure to be designed higher, without regard to drum diameter. The latter indicates higher dry density than the former. As compared with those curves, the latter curves are not so acutely bent: this signifies that changes in linear pressure do not affect dry density so much with a drive drum as with a towed one.

From all these relationships, we can conclude as follows:

- ① With a towed drum, the range of optimum linear pressure for maximizing the density cannot be widened.
- ② With a self-propelled drum, the range is generally wide and can be determined flexibly.

These conclusions are supported by the results of an investigation conducted by us on an asphalt pavement finished with an all-drum-drive tandem roller in order to check its degree of compaction and Marshal stability. The results are represented by Fig. 3-7 and Fig. 3-8 shown here.

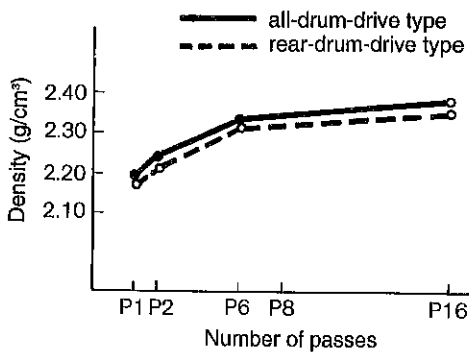


Fig. 3-7 Relationship between number of passes and density of all-drum-drive and rear-drum-drive types

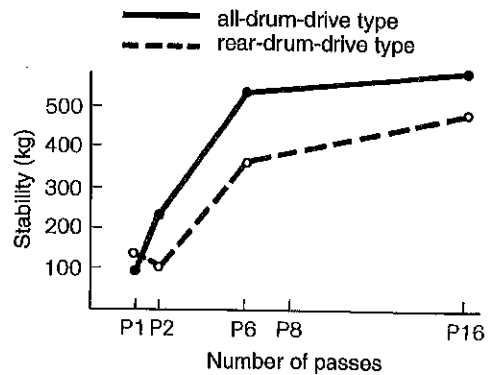


Fig. 3-8 Relationship between number of passes and stability of all-drum-drive and rear-drum-drive types

The difference between the two in stability or strength is appreciable, though the two do not differ much in density. In overall consideration of the two, there is no denying that the all-drum-drive type is definitely superior. What has been said thus far was the theoretical and engineering guidepost under which the model R-1 and R-2 were developed since 1970.

In summary, the compacting characteristic of the steel static roller may be expressed in these terms:

- ① **Generally compacts the layers closer to surface to higher densities, thereby rendering it easier for a following heavier roller to make secondary compaction process.**
- ② **The depth of compaction is generally small.**
- ③ **The surface does not become sufficiently dense.**
- ④ **Drum diameter and linear pressure have a very important relativity on compacting performance.**
- ⑤ **By its solid face, granular material can be properly crushed and thrust into the surface.**

(2) Analysis by elasto-plasticity finite element method

In the previous pages, we have seized characteristics of static drum rollers by integrating the rules of thumb after analyzing a number of test results.

To grasp the dynamic factors related to compacting plants on a qualitative basis, it is practically impossible to rely upon conventional physical and measurement engineering methods alone.

The analysis aided by elasticity finite element method developed by professor Zienkiewics and others concerned in Wales University for analyzing such factors as the structures of machinery has rapidly extended its range of application boosting reliability to the analyzed results with the development of computers.

The application of this method ranges from the dynamic and static structures of a variety of vehicles, ships and airplanes, etc. to the design of materials for spacecrafts that utilize combinations of various materials with different dynamic characteristics. This widely applicable analysis method is indispensable to designing modernized machinery.

Simply explained, the elasto-plasticity finite element method is a means of analysis in which the object to be analyzed is divided into mesh-like elements, each forming a quadrilateral with four nodes of framework. Factors such as stress and strain in each node are calculated based upon unique formulae.

Because the number of nodes and analysis accuracy are in a proportional relationship, enormous amount of calculations may be required. This will make it impossible to perform the analysis without the use of computers.

To ascertain whether this method is practically applicable to analysis of compaction results gained by use of rollers, experiments were performed with the use of the test equipment as shown in Fig. 3-9. The experiment results agreed well with the calculated values.

1) Characteristics of analysis program with elasto-plasticity finite element method.

The indispensability of this method as a effective means of analysis for designing machines or their component parts is as described above. However, in the domain of compaction utilizing rollers where soils are targets of analysis, this method is still outside practical use. The reason is that the solution of this problem is not only limited to the calculating technology of this method, but also it involves more comprehensive and high-degree research work in a specialized domain, as described in a later chapter, "Automated Control".

Such being the case, for in-depth description of the method, consult other books dealing with the subject. Summation is only given as below:

To discuss the dynamic behavior of a soil, it is necessary to determine the stress-strain relationships. For roller-compacted simulation, the elasto-plasticity equations that enable expression of cyclic loading are the best alternative today. Features of this program are:

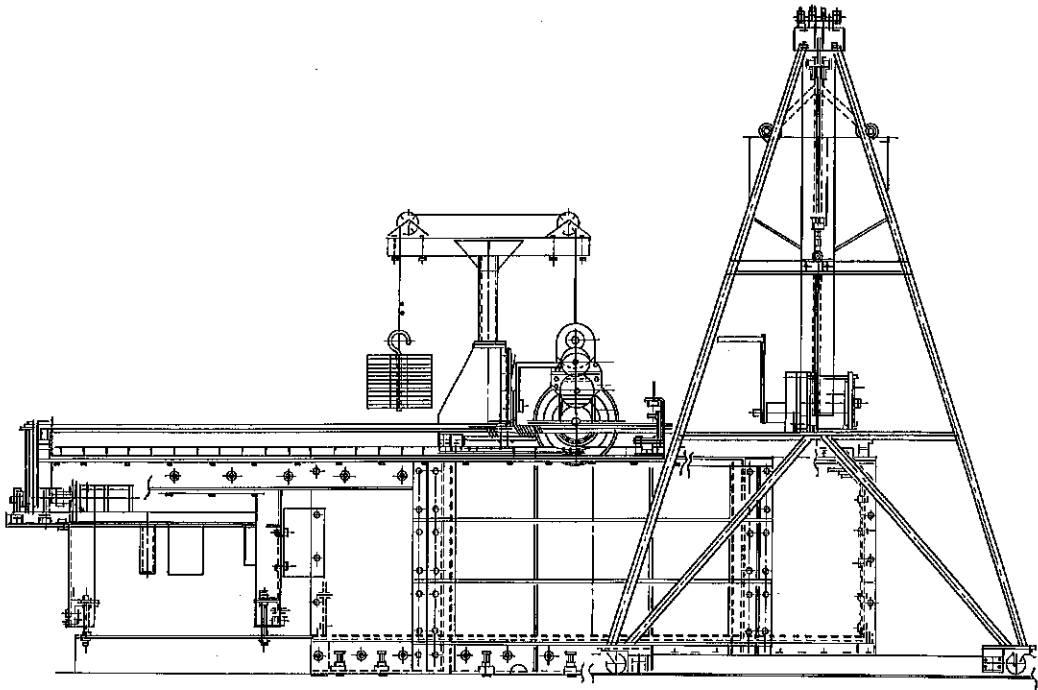


Fig. 3-9 Test equipment for elasto-plasticity finite element method

① **Boundary conditions**

- Roller \Rightarrow Regarded as rigid body
- Soil \Rightarrow Regarded as elasto-plastic body
- Roller-soil contact area \Rightarrow Coulomb's friction condition is applied.
- Elements' restriction \Rightarrow 2-dimension strain condition is applied.

② **Constitutive rule of soil**

Elasto-plastic constitutive equation (Subloading-Surface-Model) is applied.

☆ Cyclically loaded

☆ Hardening and softening pheomena can be expressed.

③ **Experiment equipment**

An experiment equipment made up of a soil-contained tank that enables 2-dimensional strain, and a drum unit mounted on the tank in such a manner that it enables a precision rolling movement control and measurement of various factors.

2) Application of the method to roller-compaction analysis

The pages that follow continue the discussion for the above-mentioned program applied to analysis of compaction results with a steel wheel (rigid body) roller. Figure 3-10 illustrates divided elements. The divided elements total 204, each forming a quadrilateral element with 4 nodes of framework. Nodes between neighboring elements number 245 in all. The division covers the whole area assumed to be under the influence of outer forces exerted by the test roller. Dimensions of the drum of the test machine were equal to those of the drum in the experimental apparatus. The soil sample was relatively dense, air-dried standard sand with a void ratio of 0.62. The friction coefficient between the soil and drum (steel) was 0.38.

Drum diameter:	300 mm	Lift thickness:	60 mm
Drum width:	412 mm	Friction factor:	0.05 mm
Drum travel distance:	370 mm		

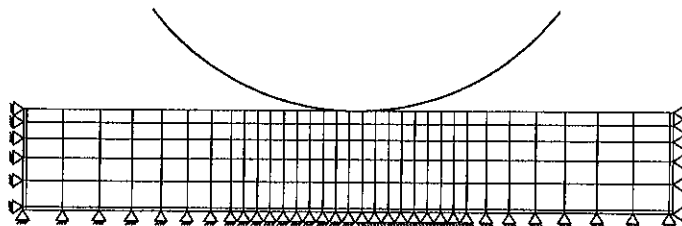


Fig. 3-10 Divided elements

3) Static compression settlement

Figure 3-11 shows the relationship between the static linear pressure and settlement when a 30 cm diameter drum was forcibly settled with the static linear pressure increased from zero to about 2 kg/cm.

The figure shows that the settlement increases smoothly with increasing static linear pressure. Marked differences between the theoretical and experimental values in low linear pressure domains are attributable to the difficulty in adequate determination of material constants under the low confining pressure conditions in the surface layers when the initial conditions were set.

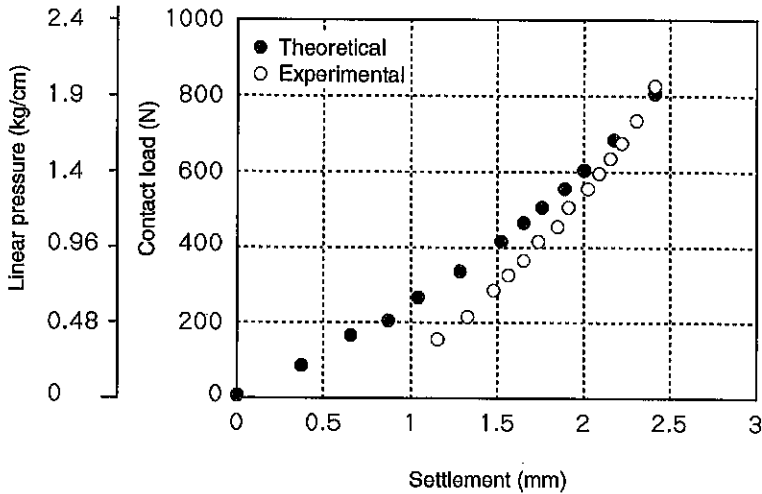


Fig. 3-11 Relationship between linear pressure and settlement

4) Volumetric strain distribution in the soil under the same condition as above.

Figure 3-12 indicates volumetric strain distributions under a loads of 216N with the drum not rolling for theoretical analysis.

Settlement under static load: Load 216 N Lift thickness: 60 mm (Steel drum)
 Volumetric strain: Positive —△— Volumetric strain: Max. +0.01439
 Volumetric strain 0 ——— Min. -0.01797
 Volumetric strain: Negative —○—

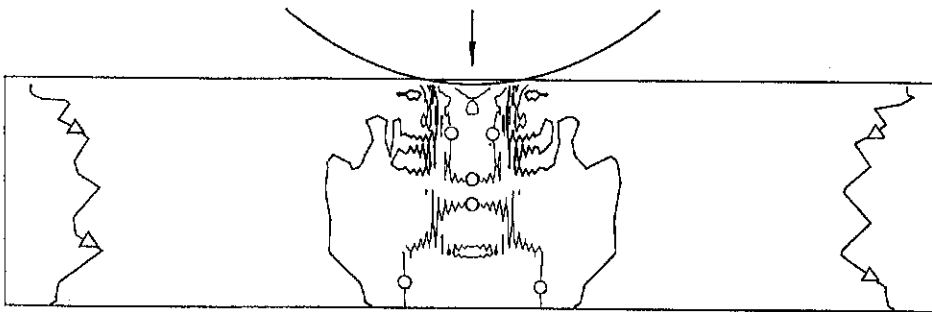


Fig. 3-12 Volumetric strain distributions under a load of 216 N with drum stationary (Theoretical results)

5) Behavior of ground under drum in motion

The previous section has discussed the theoretical and experimental results on the compression settlement and shearing strain with the drum not self-propelled. Stress analyses have also been made with the drum stalled and self-propelled under the same load conditions as above. Figures 3-13a and 3-13b show vertical/lateral stress (σ_y) distributions with the drum stationary and being driven respectively.

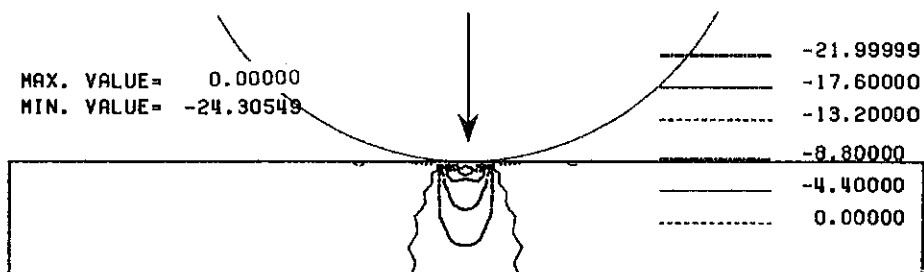


Fig. 3-13a Vertical/lateral stresses (σ_y) under a load of 216 N with drum stalled

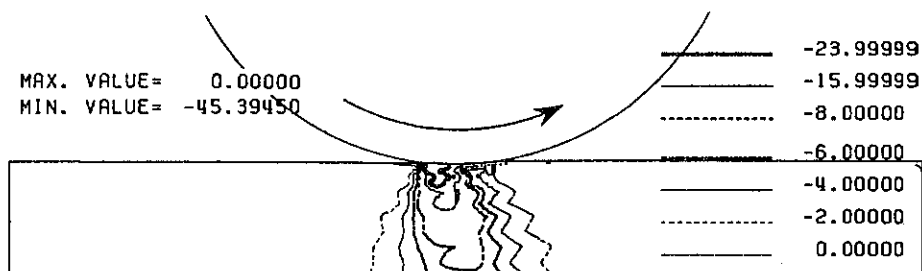


Fig. 3-13b Vertical/lateral stresses (σ_y) under a load of 216 N with drum self-propelled

In Figs. 3-13a and 3-13b, stresses σ_y in the compressive direction are expressed in minus (-) quantities. When the drum rolls, the stress distributions change that were symmetrical with respect to the vertical line running through the rotating axis center. High stress domains move ahead of the drum's contact area with the symmetrical axis inclining forward. In Fig. 3-13b, stress domains representing about -22 kPa that can be seen in front and behind the drum's contact area, expand

diagonally rearward and downward while moving towards the front end of the drum's contact area. Compression domains expand more rearward than forward. On the other hand, stresses decrease in the surface layers at rear of the drum's contact area, approaching to zero.

Further, Figs. 3-14a and 3-14b indicate horizontal/vertical stress (σ_x) distributions with the drum stationary and self-propelled respectively with the load conditions unchanged. The slip was assumed 0.05.

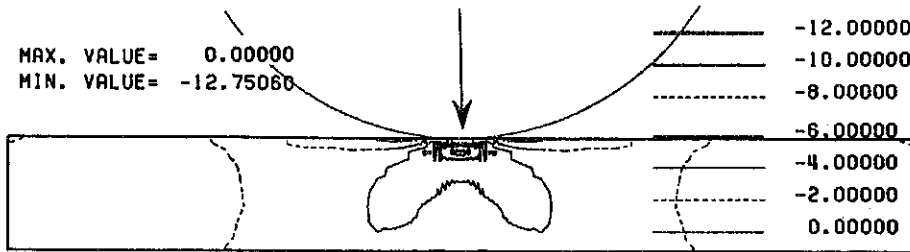


Fig. 3-14a Horizontal/vertical stresses (σ_x) under a load of 216 N with drum stationary



Fig. 3-14b Horizontal/vertical stresses (σ_x) under a load of 216 N with drum driven

The horizontal/vertical stress (σ_x) distributions, as shown in Fig. 3-14b, have the same tendency as the vertical/lateral stress (σ_y) distribution patterns. That is: Maximum stress domains move ahead of the drum contact area, with stresses on the rear side approaching to zero. The compression domains in the lower part on the front side become smaller and retreat, however, they significantly expand and grow on the rear side. This expansion in the compression domains on the rear side explains qualitatively an increase in settlement caused by the propulsion of the drum, and also an increase in traction consequent with the increasing settlement.

Figures 3-15a and 3-15b make a comparison between the theoretical and experimental results of the horizontal/vertical and vertical/lateral stress distributions as described above.

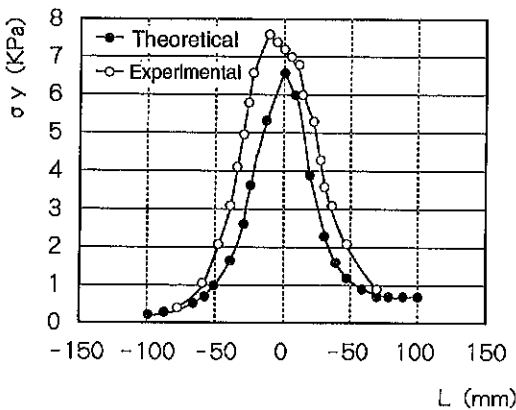


Fig. 3-15a Vertical/lateral stresses (σ_y) under a load of 216 N with drum in motion

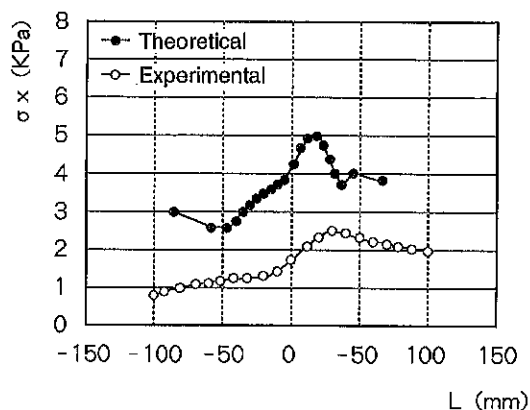


Fig. 3-15b Horizontal/vertical stresses (σ_x) under a load of 216 N with drum in motion

In the horizontal axis in Figs. 3-15a and 3-15b, distances from the drum center on the ground on the rear side area of the rolling drum are expressed in plus (+) quantities for ease of comparison. Figure 3-15a shows that stresses σ_y are in good accord for both theoretical and experimental values, with the maximum value falling on the front side of the vertical line running through the rotating center. This trend agrees with the theoretical results of normal and tangential stress distributions as shown below: Figures 3-16a and 3-16b illustrate theoretical analyses on normal and tangential stresses acting on the ground when the drum is stationary and self-propelled respectively under a contact load of 216 N with a slip ratio of 0.05 and a friction factor 0.38.

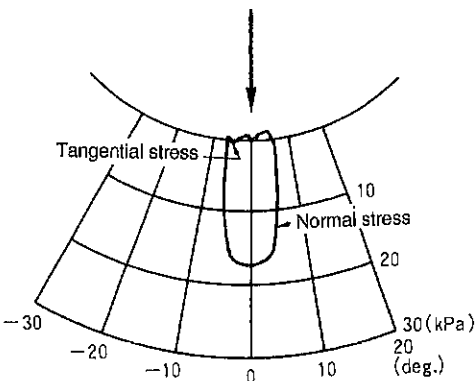


Fig. 3-16a Normal and tangential stresses under a load of 216 N with drum not in motion (Theoretical)

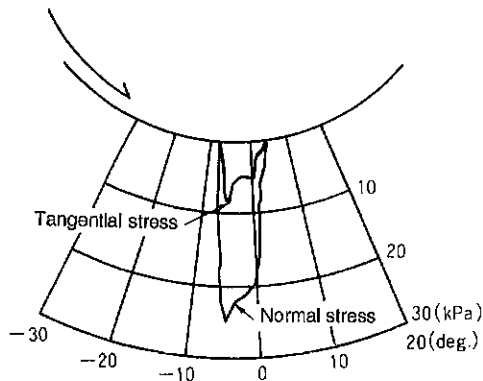


Fig. 3-16b Normal and tangential stresses under a load of 216 N with drum in motion (Theoretical)

Figure 3-17 shows stress distributions for test results.

It can be said that a variety of theoretical and test results described above are theoretical and experimental verifications of the technological descriptions carried at the beginning of this chapter, "Compaction Characteristics".

Max. tangential stress: 5.705 kPa/-0.061 rad.
 Max. normal stress: 21.505 kPa/-0.044 rad.

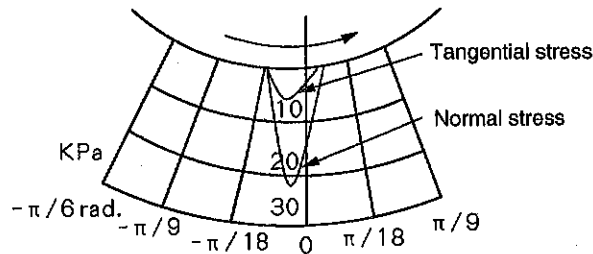


Fig. 3-17 Normal and tangential stresses under a load of 216 N with drum in motion (Experimental)

2. Compacting by Pneumatic Tired Rollers

(1) Characteristics of pneumatic tire

Wheels with pneumatic tires perform compaction in a manner quite different from the steel roller discussed before. While the steel roller permits its own compacting characteristic to be controlled only by varying its weight or ballast, the pneumatic tired roller permits its characteristics to be provided two-dimensionally by means of wheel load (ballast adjustment) and tire inflating pressure: this versatility feature of the latter roller can be analytically comprehended by resorting to the research by Boussinesq again.

Imagine the level surface of a semi-infinitely elastic material, and assume a flat-bottomed metallic disc placed on the surface. That surface under the disc is subjected to a pressure which is equal to the weight of the disc divided by the bottom area. This pressure is transmitted into the material layer in vertical direction and, at the same time, spreads out in a distributive manner. This hypothetical material being elastic, the pressure is countered by the varied stresses induced in it. The pattern of the pressure or stress distribution is similar to that indicated previously: the equi-pressure diagram looks like the cross section of an onion, as shown in Fig. 3-3 and the following. Note the pattern of equi-stress lines. The pattern is referred to as a "pressure bulb".

Suppose we enlarge the bottom area of the imaginary disc, keeping its

thickness unchanged. According to experimental findings, the bulb density does not change but the bulb itself becomes larger in size. Conversely, make the plate thicker while keeping its bottom area unchanged. This will not change the bulb size but the bulb density will be higher.

The foregoing relationship is illustrated in the following curves plotted with actually measured values.

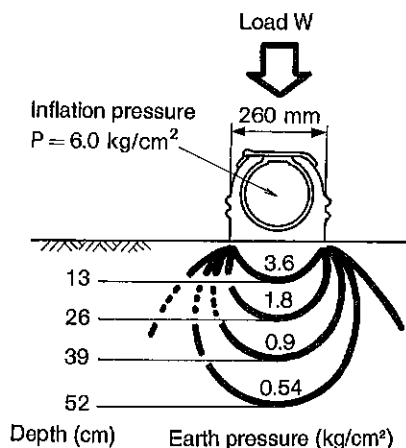
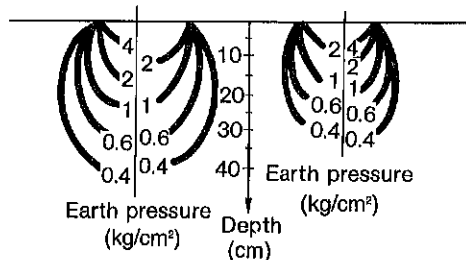


Fig. 3-18 Pressure bulb at 6 kg/cm² in inflation pressure

Tire load	1.7 t	0.9 t
Inflation pressure	8.0	2.0
Contact area	34.2	58.5
Average contact pressure	5.0	2.9



Tire size: 11.20-20 12PR

Fig. 3-19 Pressure bulb with tire load changed 1700 kg and 900 kg

Note here that, in Fig. 3-19, the tire is of 11.00-20 size. This tire statically compacted the earth in four different ways: first with wheel load of 1.7 tons and inflating pressure of 8 kg/cm²; second with the same load of 1.7 tons and pressure of 2 kg/cm²; third with a load of 0.9 ton and pressure of 8 kg/cm²; and fourth with the same load of 0.9 ton and pressure of 2 kg/cm².

Quadrupling the inflating pressure (from 2 to 8 kg/cm²) under the same load did not appreciably change the depths of equi-pressure line (magnitude of compacting force), but these depths became multiplied by 1.5 times when the wheel load was doubled (from 0.9 to 1.7 ton).

This tells us that, where the tire is used as the compacting means, the primary factor for determining the magnitude of compacting energy extended in the earth is the wheel load as obviously shown also in Fig. 3-20.



Finish rolling of pavement surface course near Matsuyama City

Inflation pressure $P = 0.8 \text{ kg/cm}^2$

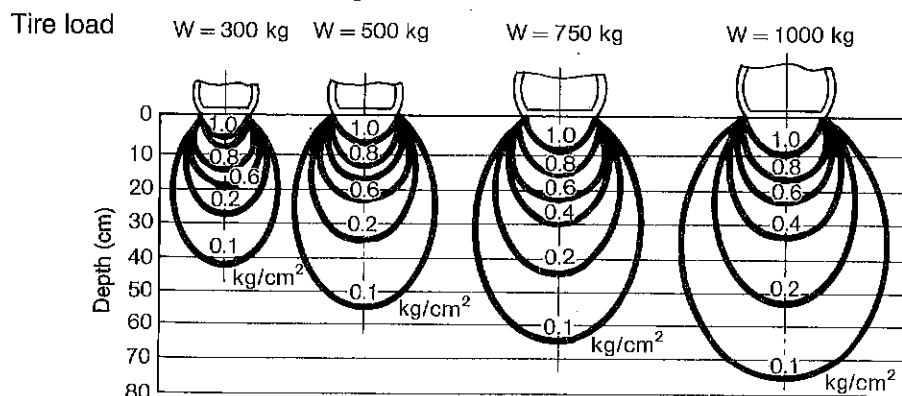


Fig. 3-20 Relationship between tire load and pressure penetration

In Fig. 3-21, each curve is a parameter and represents a given tire inflating pressure. For all these parameters, the wheel load is given (2.5 tons). The curves indicate that changes in inflating pressure practically do not affect the vertical pressure gradient at greater depths but, at the surface, compacting pressure varies almost directly with the inflating pressure.

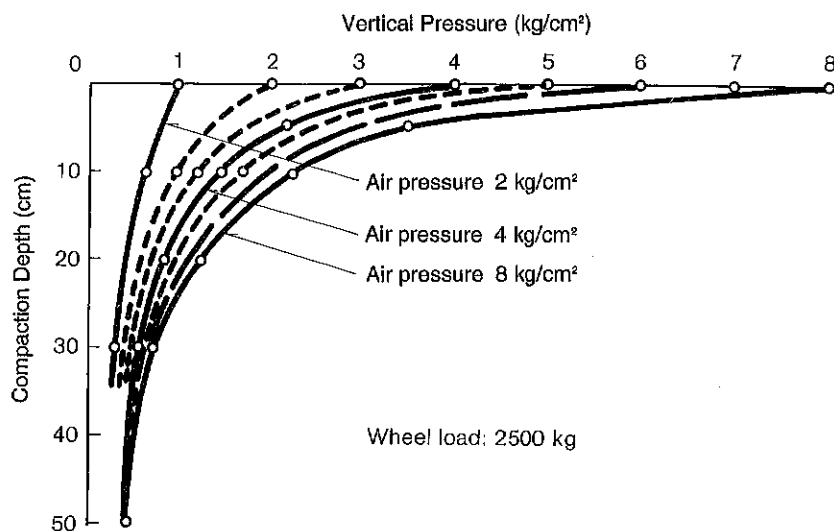


Fig. 3-21 Relationships between air pressure, and surface pressure under constant wheel load with air pressure on various parameters

Figure 3-22 is a test result that represents relationships between moisture content, bearing capacity and degree of compaction with lifts 30 cm and 50 cm thick before compaction.

It is a widely accepted notion, in moisture content examinations, that variations in test results corresponding to different test conditions are less on the wet side (i.e. right side area of optimum moisture content) than the dry side (i.e. left side area of optimum moisture content).

An example shown in Fig. 3-22 indicates the same tendency. Test results on the dry side indicate noticeable differences between lifts of 30 cm and 50 cm thick, and also between top and bottom layers.

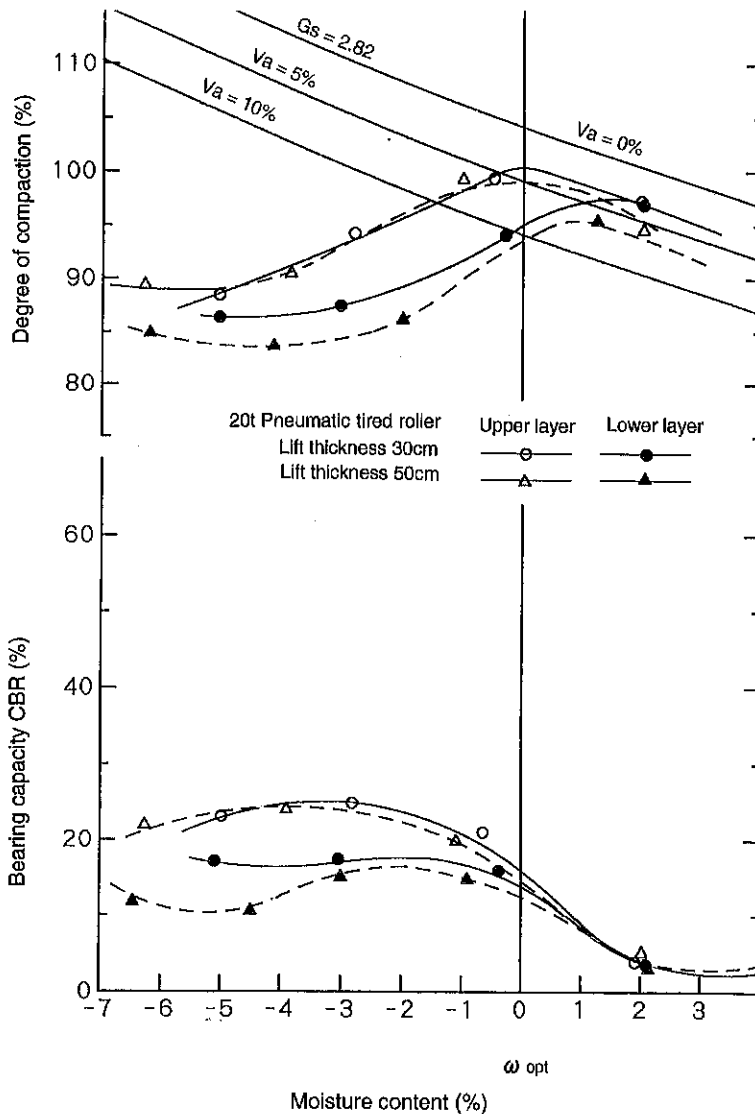


Fig. 3-22 Relationship between moisture content, bearing capacity and degree of compaction for lifts 30 cm and 50 cm thick before compaction

When a tire is in contact with the ground, conditions on the contact area vary with factors like cross sectional structure, tire load and inflation pressure. Parameters that govern the variation are modulus of deformation of tire, that of the ground and width of ground contact.

Quoting from a thesis presented by Fujii and Watanabe who developed their theory from Herz's thesis:

$$\ell = 2.16 \sqrt{\frac{Pr}{b} \left(\frac{1}{E_t} + \frac{1}{E_s} \right)}$$

where, ℓ = Tire contact length
 P = Tire load
 r = Tire radius
 b = Tire contact width
 E_t = Modulus of deformation of tire
 E_s = Modulus of deformation of ground

Let ground contact area ℓb be a , then mean ground contact pressure q is:

$$q = P/a$$

$$q = \frac{\ell}{2.16} \sqrt{\frac{E_t \cdot E_s \cdot P}{r \cdot b \cdot (E_t + E_s)}}$$

Supposing the soil property and roller speed are kept constant, E_t , E_s , r , b are considered to be constant.

$$\text{That is: } q \propto \sqrt{P}$$

This signifies that the mean ground contact pressure q remains invariable if tire load P is maintained constant.

Uniformity of tread pressure at the contact area between the tire and the earth depends greatly upon its tread pattern and design of tire carcass and, in general, is not necessarily uniform. Needless to say, an optimum tire for compaction use bears on the surface with uniform tread pressure.

Let **a** (cm²) stand for the tread contact area of the tire and **P** (kg) for the wheel load, then;

$$\frac{P}{a} = q \text{ (kg/cm}^2\text{)}$$

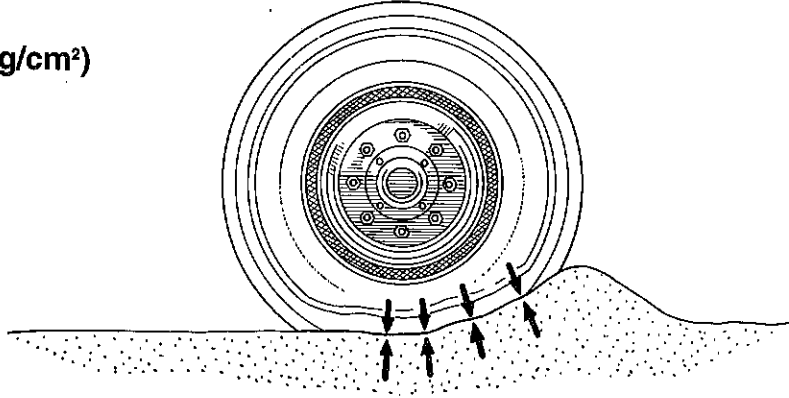


Fig. 3-23 Tire contact area

This **p** can be a theoretical mean pressure and this has not much practical meaning because the contact area cannot be measured precisely in practice and, besides, the actual area is a three-dimensionally curved surface as usual at which unit tread pressure (downward) and a countering supporting pressure (upward) are balanced in equilibrium. Theoretically and at the same time practically, the pressure acting on this curved face is more uniform than that which exists between the tire and a flat, solid surface on which the tire stands. Thus, we may regard that pressure as equal to the tire inflating pressure:

p = Tire tread pressure

Pa = Tire air pressure

$$p = Pa$$

There is no denying that we need a tire which, when rolling over the material, presents a flat tread face at the spot of contact. Such a tire is particularly desirable for highly plastic material like an asphalt hotmix. If the tire does not present a flat treading face in its compaction process, it will leave a tire mark in its wake which will be very difficult to eliminate. The remedy is to reduce the inflating pressure but, importantly, a tire with an overreduced air pressure will not be able to increase the surface density of the material under compaction.

Generally speaking, the decisive points on the pneumatic tired roller, regardless of the material to be compacted, are:

- ① **Appropriate wheel loading**
- ② **Suitable inflating pressure control**
- ③ **Uniform tread pressure distribution**

Points ① and ② can be controlled for each compacting job and should be controlled in consideration of what has been said thus far. When the three points are optimized, one can be sure of compacting to the specification.

As to control over the inflating pressure, the idea of starting the initial compacting pass with a lower pressure and successively raising the pressure for the subsequent passes is not practical because it entails a number of problems.

The first problem occurs in a large-scale job site involving a number of pneumatic tired rollers, each having its tires set at a particular pressure level. Pressure adjustment and control of the fleet of rollers responding to quick needs of job operation is hardly practical.

Some types of pneumatic tired rollers are designed to allow tire pressure to be variable under centralized control. To increase the pressure at short intervals, each machine has to be provided with an impractical large-capacity compressed air tank: this is the second but not last problem.

Useful information concerning compaction with the pneumatic tire has been made available by some researchers. We shall consider what **Belyaev** came up with through his research concerning the relationship between tire inflation pressure, tire load and maximum tread pressure. Here is his equation:

$$P_{max} = \sqrt{\frac{S}{\pi^2 \cdot D} \cdot (E_1 + E_2)} \dots\dots\dots(1)$$

- where, **P_{max}** = Maximum tread pressure (kg/cm²)
S = Load per unit width of tread (kg/cm)
D = Wheel diameter (cm)
E₁ = Coefficient of elasticity of tire (kg/cm²)
E₂ = Deformation coefficient of soil (kg/cm²)

Coefficient “**E₂**” concerns the properties of the material, which is soil in the present case, and represents the strain caused by stress set up in the material. Its value changes broadly for a range of soil properties. Since, in actual job operation, the soil properties have to be and are adjusted to suit the compacting process, we may consider a certain limited range of practical “**E₂**.”



Overlaying for cold milled surface on Tohoku Expressway

Soil taken up in the present discussion is generally elasto-plastic. According to the theory of elasticity, " E_2 " can be expressed in terms of " E " for elastic range of the soil, " E " being the coefficient of elasticity:

$$E_2 = \frac{E}{0.405} \dots\dots\dots(2)$$

Now, what constitute the coefficient " E_1 " of the tire are mainly tire diameter, load and tread width. These three, plus inflating pressure, can be equated to " E_1 " by the theory of Hertz (concerning the contact area, ball diameter, pressure and elastic coefficient of two elastic balls being pressed together) and by the empirical equation proposed by Hedikeli concerning tire strain as follows:

$$E_1 = \frac{P}{0.055} \sqrt{\frac{PD^2B}{W \sqrt{DB}}} \dots\dots\dots(3)$$

P = Tire air pressure (kg/cm²)

W = Tire load (kg)

D = Tire diameter (cm)

B = Tread width (cm)

By using the foregoing equations (1), (2) and (3), we can correlate tire air pressure, tire load and maximum tread pressure.

The next topic is the degree and depth of compaction. Fig. 3-24 indicates the relation of the degree to the depth with tire air pressure taken as the parameter.

$$\text{Specific density} = \frac{\text{Density of test result}}{\text{Density by standard compaction}}$$

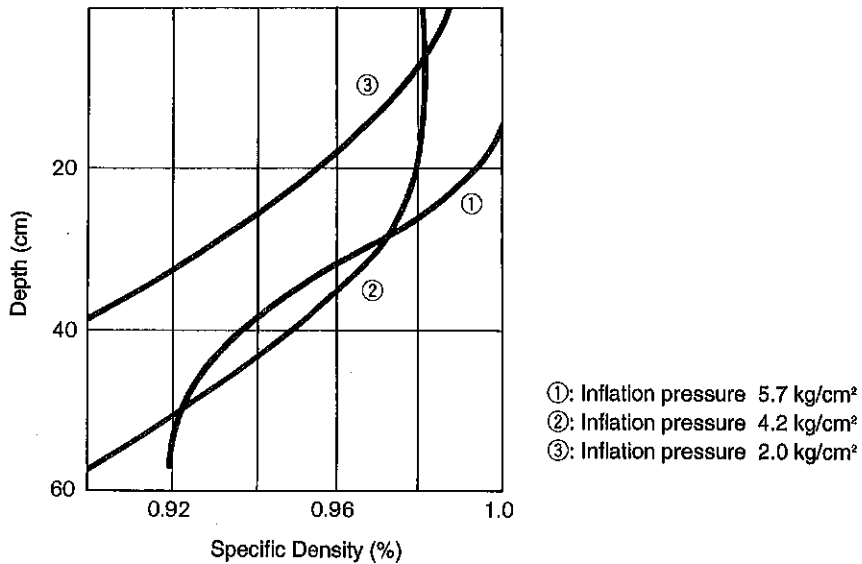


Fig. 3-24 Relationship between depth of compaction and specific density

These curves were obtained from an actual operation with 3.5 t tire load, 60 cm depth with 10 passes.

It can be seen in Fig. 3-24, above, that with a low pressure, the number of passes has to be greatly increased if the given degree of compaction is to be attained. This relationship is supported by the results of our experiment with an asphalt hotmix. The results are shown graphically in Fig. 3-25.

The given test conditions were as follows:

Material:	0/25, 4% asphalt content
Lift:	6 cm
Preliminary compaction:	2 passes by steel roller at 140°C
Applied tire size:	12:00-20
Air pressure:	2 kg/cm ² , 5 kg/cm ² and 8 kg/cm ²
Wheel load:	1,700 kg
Temperature of hotmix:	105 to 95°C

Here it is also explained that the low-pressure initial compaction leaves behind such a layer structure of the material as will retain a self-locking strength – resistance to subsequent compacting action – which interferes with compacting action in the following roller passes. To be appreciated is the importance of controlling the air pressure where the job is performed with pneumatic tired rollers.

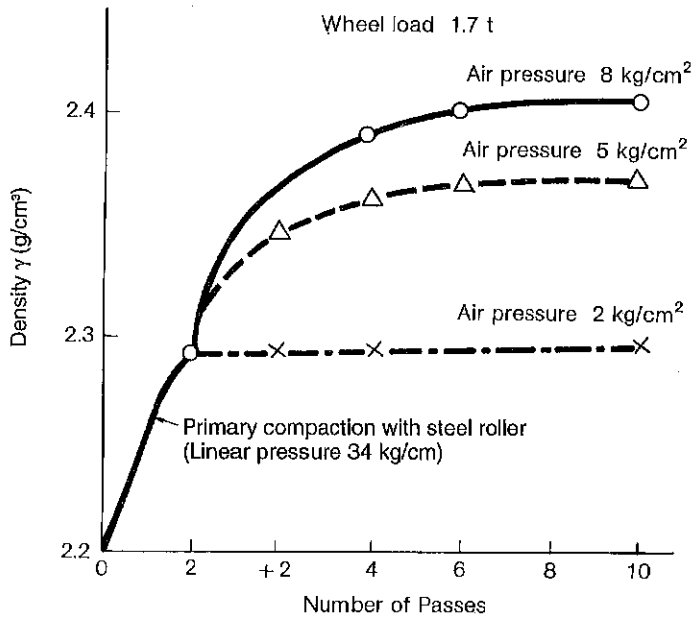


Fig. 3-25 Relationship between number of passes and density

What has been said thus far strikes up the difference in compacting characteristics between steel roller and pneumatic tired roller. The tired roller has additionally two peculiar characteristics as follows:

- ① **Sealing (watertight) effect**
- ② **Kneading (manipulating) effect**

It is clear from experience that these two effects are due to the elastic property of rubber. They are noticeable not only in asphalt mixes, but in silty and loamy soils. The “kneading action” in such viscous materials differs from that seen in asphalt mix compaction. The former is created when trailing tires compress high rises on both edges of the tire tracks formed by the treads of leading wheels. This kneading action is quite similar to that noticeable when, for example, working dough by hand.

Figure 3-26 is a result of a test in which a soil sample was compacted with different moisture contents to gain relationships between the bearing capacity and the degree of compaction for air pressures of 3.5 kg/cm² and 9 kg/cm².

As is accepted as a general trend, on the right side area of the optimum moisture content (on the wet side), differences in test results corresponding to different test conditions prove to be less than those on the dry side.

As shown in Fig. 3-26, marked differences in test results are noticeable on the dry side on bearing capacity in particular. Figure 3-26 also represents the

influence of inflation pressure on three layers of a mat 50 cm thick; top, intermediate and bottom. Though significant differences are not noticed, bearing capacity indicates high values at higher air pressure in the top layer. An increase in inflation pressure signifies that the tire has become more rigid (that means the tire has approached a steel drum in regard to compactive characteristics). As stated in earlier pages, a smooth steel roller tends to compress layers near the surface.

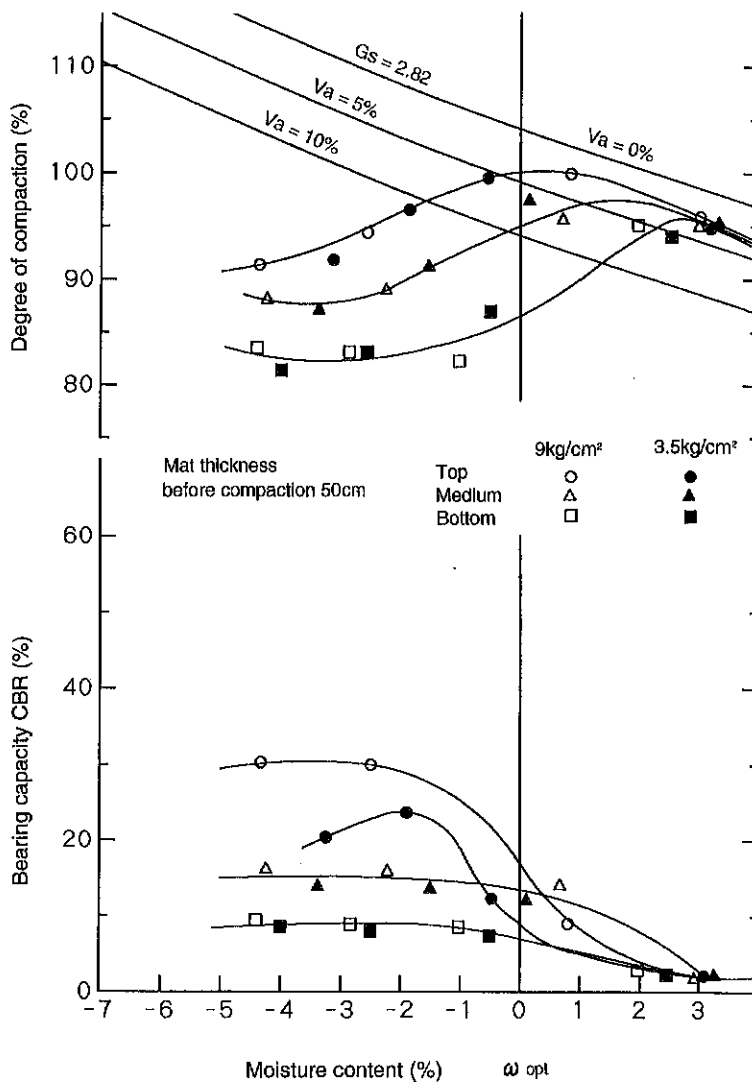


Fig. 3-26 Inflation pressure, moisture content and compaction effect in each layer

Earlier pages have described that the surface texture does not comparatively become dense with the steel roller. This means the surface layer is considerably more permeable. Let's see Fig. 3-27.

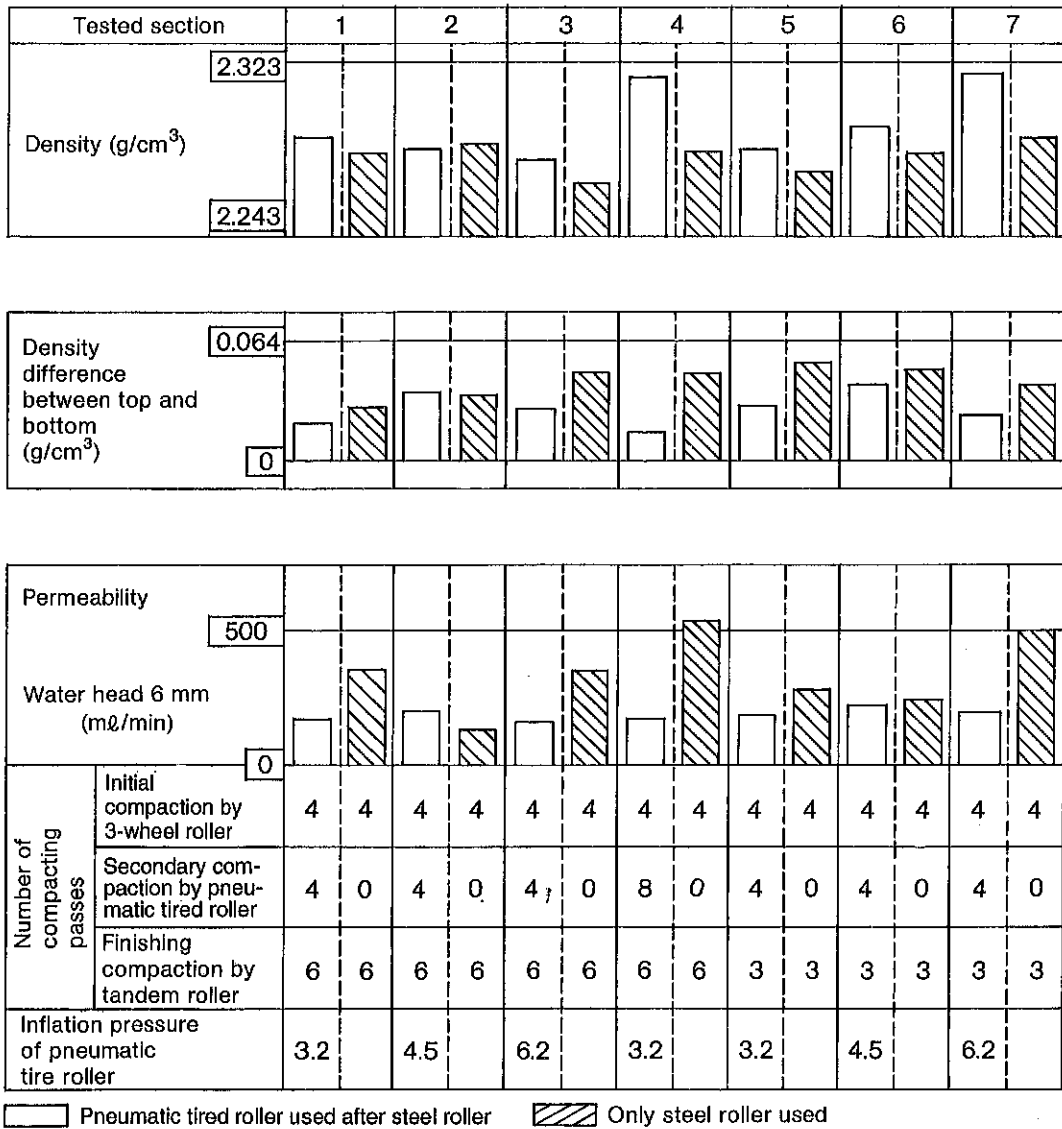


Fig. 3-27 Comparison of compaction effect between steel roller alone and combination of steel roller and pneumatic tired roller

Figure 3-27 is a comparison of compaction effect with respect to density and permeability between a steel roller alone and a combination of a steel roller and pneumatic tired roller.

Generally, there is no appreciable difference in density within the whole mat, however, significant difference exists between the top and bottom layers. This tendency is considerable in the permeability comparison. These findings reveal the mutually complementing relation between steel rollers and pneumatic tired rollers.

- This relationship accounts for the high popularity of combined use of steel rollers and pneumatic tired rollers in roadway building today.

In the above-mentioned test results, strict comparison is not reasonable, since the number of passes differs between the steel roller alone and a combination of a steel roller and a pneumatic tired roller. However, other experiment results also support the above-mentioned tendency.

In summary, the effects of the compacting characteristic of the pneumatic tired roller may be expressed as follows:

- ① Increased resistance of the surface to water penetration.
- ② Raising the inflation pressure increases surface density and boosts stability of the layer.
- ③ Increasing the wheel load increases the compaction for deeper layer.
- ④ Kneading effect is considerable in compaction of high plastic and wet soils.

Fig. 3-28 shows the range of proper wheel loads for lifts of soil and asphalt mixture.

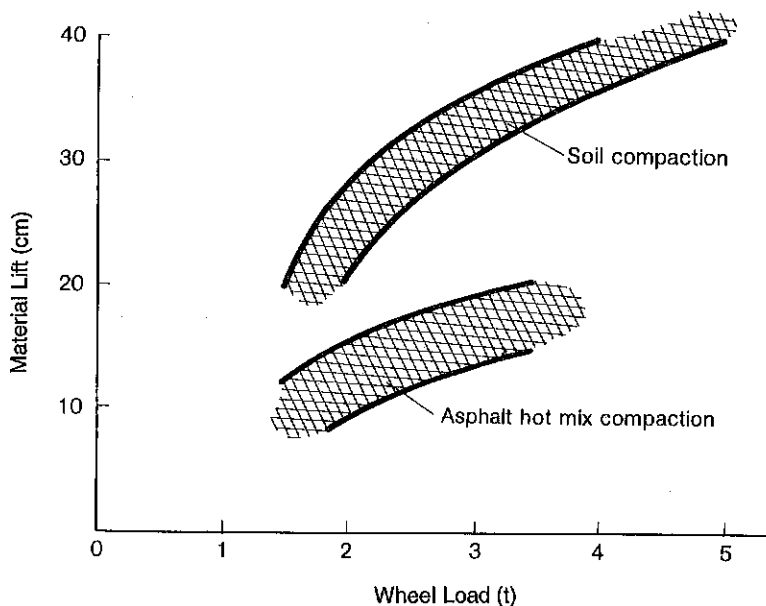


Fig. 3-28 Relationship between wheel load and applicable material lift



Overlaying operation on Tohoku Expressway

(2) Compaction operation by pneumatic tired rollers

As shown in Fig. 3-28, the pneumatic tired roller has also two domains of application; compaction of soils and asphalt mixes. For large-scale embankment, etc., large-sized heavy machines are employed. For pavement construction, surface course finish in particular, various sizes of pneumatics are utilized. In soil compaction work, the gross weight and condition of use of pneumatic tires on machines to be employed are designated at the stage of machine selection. For asphalt paving work, managements will be needed as described below:

In the asphalt paving work, the asphalt hotmix is laid down and spread over the prepared subgrade or subbase then the roller goes into action. Normally, the mixture is prepared under strict quality control at the mixing plant. All elements of quality are fixed at the plant including temperature of the mixture. On the part of the compacting procedure, none of the parameters are manageable anymore.

To obtain an asphalt pavement meeting the design specification, the importance of compaction work cannot be overemphasized, and this emphasis rests primarily on the compacting machine used.

Compaction work is easy or difficult depending on the required characteristics of the asphalt pavement, the composition, porosity and given temperature of the hotmix. Generally, the hotmix with a lower asphalt content is easy to compact even at a higher-than-average temperature. A mixture with a normal asphalt content is difficult to compact at higher temperature because of higher plasticity.

The purpose of compaction was stated at the onset. Compaction work has to achieve the stated purpose – high density and stability – more economically, and to produce a smooth compacted surface in specified evenness. In this regard, the paving work contractor must plan and execute the job under the following 5-point guideline:

- ① **Controlling the tire inflating pressure at the correct value.**
- ② **Determining the minimum required number of passes.**
- ③ **Carrying out the initial compaction run at 110 to 140°C of hotmix temperature, usually immediately after the asphalt finisher. If the mixture happens to be too soft to compact, the start of initial compaction must be held up until the mixture cools down to a proper consistency.**
- ④ **Carrying out the secondary compaction while the mixture is within the 70 to 90°C range: below this range, the maximum possible density can hardly be attained.**
- ⑤ **Making provisions on the tire tread to avoid adhesion of asphalt mortar to it.**

The texture of the finished surface is affected by point ⑤. According to

experience, the asphaltic mortar in the mixture begins to stick to the tire when the difference in temperature between tire tread and mixture exceeds 25°C or so. Once the tire picks up asphalt, it picks it up more and more as in snowballing.

The critical temperature difference, which is about 25°C , is usually absent when the temperature of the tread is 80°C or higher. Thus, provisions for avoiding asphalt sticking are necessary only until the heat flows into the tire to raise it to about 80°C . Here are suggested provisions:

- ① Clean water, diluted detergent or emulsified oil can be applied to the tire tread by spraying, brushing or daubing with a wad of gunny just before the machine is driven onto the hotmix. Kerosene may be used instead but excessive spray should be strictly avoided. Recently, a liquid has been developed for exclusive use of pick-up prevention.
- ② On sunny days, expose the tires to the sun to warm them.
- ③ On cool, windy days, put on skirts as windbreakers for the tires at work. The skirts will keep the tires from cooling off.
- ④ Infra-red heaters are useful in warming the tires when the machine is standing still. But this practice entails the danger of localized overheating.

In addition, the following consideration must be taken:

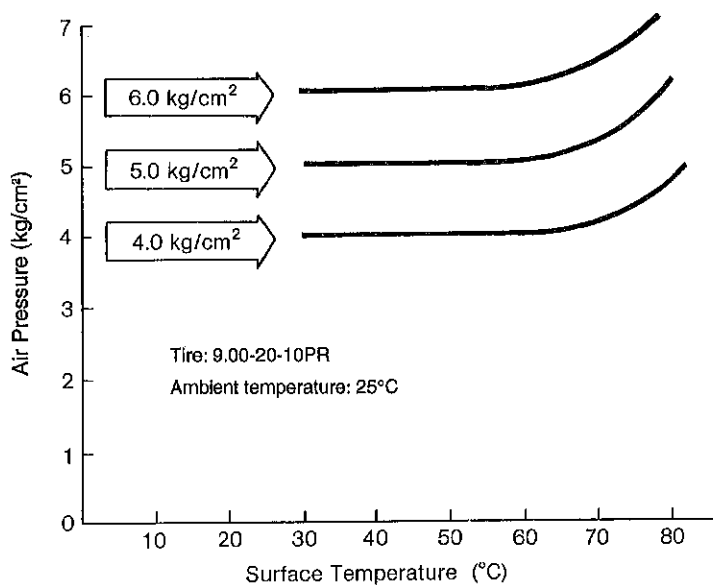


Fig. 3-29 Relationship between surface temperature and inflation pressure of tire

In the tire inflated to 5.0 kg/cm^2 , no appreciable change takes place in its inflating pressure until the tire temperature reaches a level of 60°C or so, when ambient temperature is 25°C . If the tire is heated further from that level, its pressure begins to rise and will be as high as 6 kg/cm^2 at 80°C . This relation is illustrated in Fig. 3-29.

Spraying cold water onto the tire surface to make it repel asphalt gains an additional useful effect: when the tire is already hot enough, it cools off the tire to a level at which its pressure will not be affected drastically by its own temperature.

(3) Prevention of mix pick-up on wheels

The surface texture of a finished road is one of the important factors that characterize the quality of a roadway. An important problem that exerts influence on the workmanship of a roadway is the prevention of mixture pick-up on the wheels. Experience-based preventive means are mentioned in a forgoing page. Recently, however, researches have made considerable progress on paving materials and new materials have come into use, giving rise for a need to handle them properly, particularly for plastic flow resisting asphalt or hot mixes whose binder is mainly composed of petroleum resin, and its allowable working process is limited. Furthermore, with these materials, spots not compacted to specification are difficult to rectify. These circumstances tend to demand stricter temperature control during paving work than before.

It is, therefore, impossible to proceed into a mat at specified rolling temperature unless pick-up preventive measures are taken. This, not only exerts a huge influences on the surface quality of a material rolled, but also extends traffic restriction hours, paralyzing traffic.

It is an established theory that the pick-up mechanism may be created by such factors as the contact stress of wheels and their surface conditions, and also by interaction between binder material and soil. Figure 3-30 illustrates major causes of pick-up and their interrelationship.

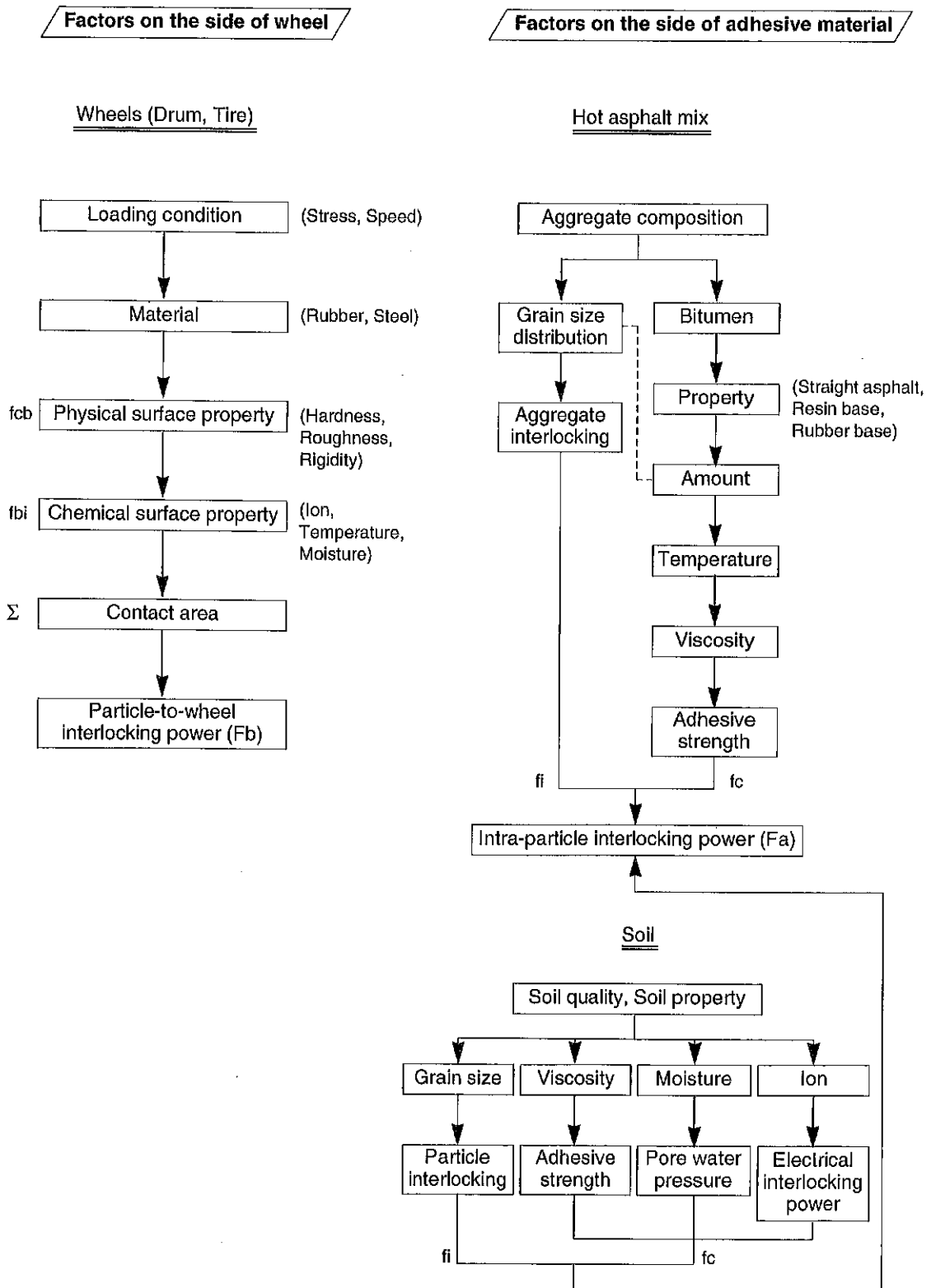


Fig. 3-30 Main factors to cause pick-up and their mutual relationships

In an asphalt mix, its adhesive strength is provided by interaction of binder's cohesion and the condition of the contact surface.

Intra-particle interlocking power **Fa** is the sum of **fc** and **fi** as described below:

Intra-particle cohesive strength (**fc**) offered by cohesive materials plus intra-particle interlocking power (**fi**) = **Fa**
and

Particle-to-wheel interlocking power **Fb** is the sum of **fc** and **fbi** as shown in the following:

Interlocking power influenced by physical surface property of tire or drum (**fc**) + interlocking power influenced by chemical surface property of tire or drum (**fbi**) = Particle-to-wheel interlocking power (**Fb**)

Pick-ups depend upon the power relationship between the two forces, **Fa** and **Fb**. That is:

$F_a < F_b$: Pick-ups occur

$F_a > F_b$: Pick-ups do not occur

As can be seen from the above relationships, pick-up can be avoided by retaining the value **Fb** at a low level. For this purpose, a variety of means are available as discussed in the foregoing pages. The use of a pick-up prevention liquid developed recently is also an effective alternative.

Whether the asphalt mixture can be easily compacted or not depends basically on the three properties of the mixture; namely,

- ① internal friction due to the nature of the aggregate
- ② adhesion due to the property of the asphalt
- ③ viscosity due mainly to the temperature

As a more basic prior condition:

- Flat subbase course with stable bearing power · Positive tack coat

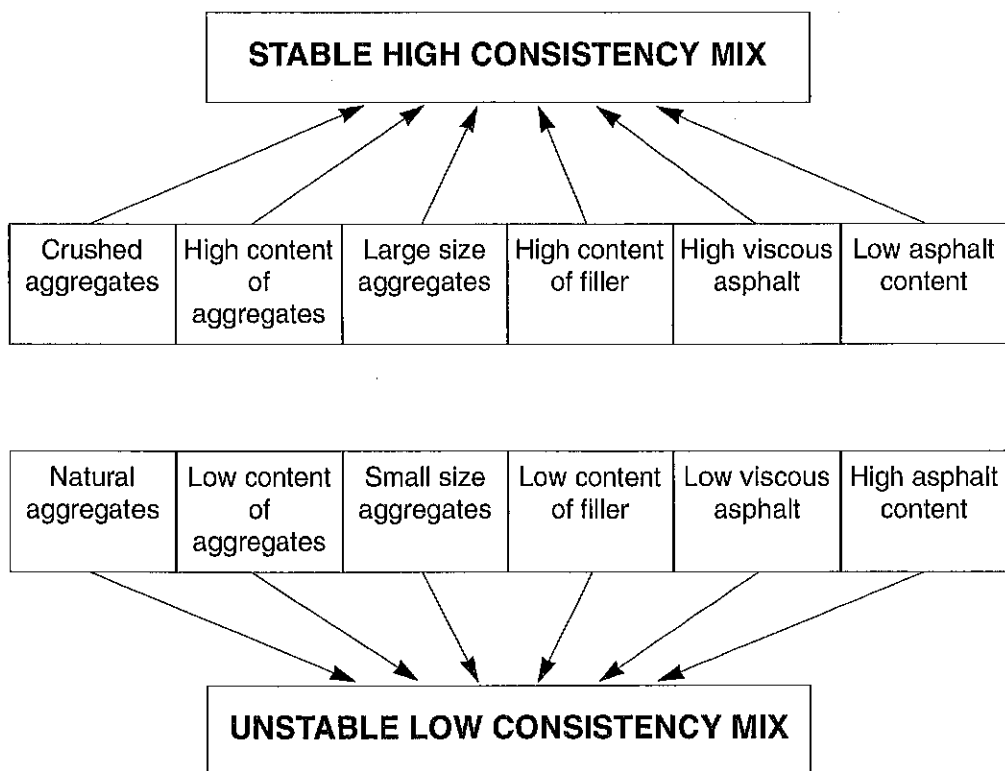


Fig. 3-31 Stable and unstable mixtures

Compactability, a term used in reference to asphalt mixture in a state ready to be compacted, is higher if the mixture is more stable, and lower if the mixture is more plastic. It is this correlation that the above depicts.

$$\text{COMPACTABILITY} = \frac{\text{STABILITY}}{\text{FLOW}}$$

Fig. 3-32 shows the attainable density of the mixture in regard to its temperature. In general an acceptable temperature of the mixture just after the finisher may be between 130°C and 160°C.

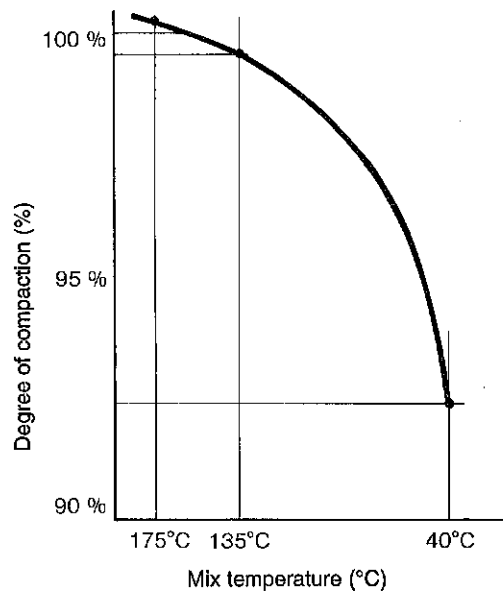


Fig. 3-32 Relationship between temperature of mix being compacted and degree of compaction

3. Compacting by Tamping Rollers

Tamping roller is a general term for rollers having a variety of projections (in the shape of club, knot and stub, etc.) on its drum surface to provide tamping effect. The tamping roller traces its origin to sheep's foot roller.

The projections are in club shape or in stubby pad shape and these are basic shapes of the so-called tamping roller. As the roller runs, its projections thrust into the earth, exerting pressure by their flat top and kneading the soil by their shanks. Characteristically, the effect of tamping reaches the upper layer from the bottom. Excessive kneading action plows and disturbs the surface, making it immune to compacting effects. Machine selection and moisture control on the job site should therefore be conducted with prudence.

A large majority of tamping rollers today are of vibration type, and are utilized with pneumatic tired rollers in compacting road embankments and rock-fill dam cores and for the RCD (Roller Compacted Dam) method of constructing dams with lean-mix cement concrete.

The protrusions, be they rod-like feet or stubby pads, revolve with the drum and, as they meet the loose soil surface, deliver impact. The faster the drum tumbles, the greater is the impact. Fast rolling, however, causes the feet to stir the surface and interfere with the compacting action.

Footprints that the pads leave behind on the surface should be no cause for concern, for they mix soil particles to curb the tendency of compacted soil to form

layers. As the compacting operation by tamping continues, footprints and other irregularities vanish gradually, turning the surface to a condition called "Walkout". This phenomenon brings the compacting effect from the bottom to the upper layer. State of the walkout is followed by compacting action with the pneumatic tired roller to "seal" the surface.

Fig. 3-33 shows the results of a study conducted on the compacted surface to ascertain the effect of tamping in terms of "pressure bulb" and the relation of the pad shape to the pressure distribution. On casual glance, pointed pads may appear more effective but the pressure bulbs in this figure indicate otherwise: flat-top square pads produce better results in that their bulbs are formed with more uniform pressure distributions and higher values of pressure.



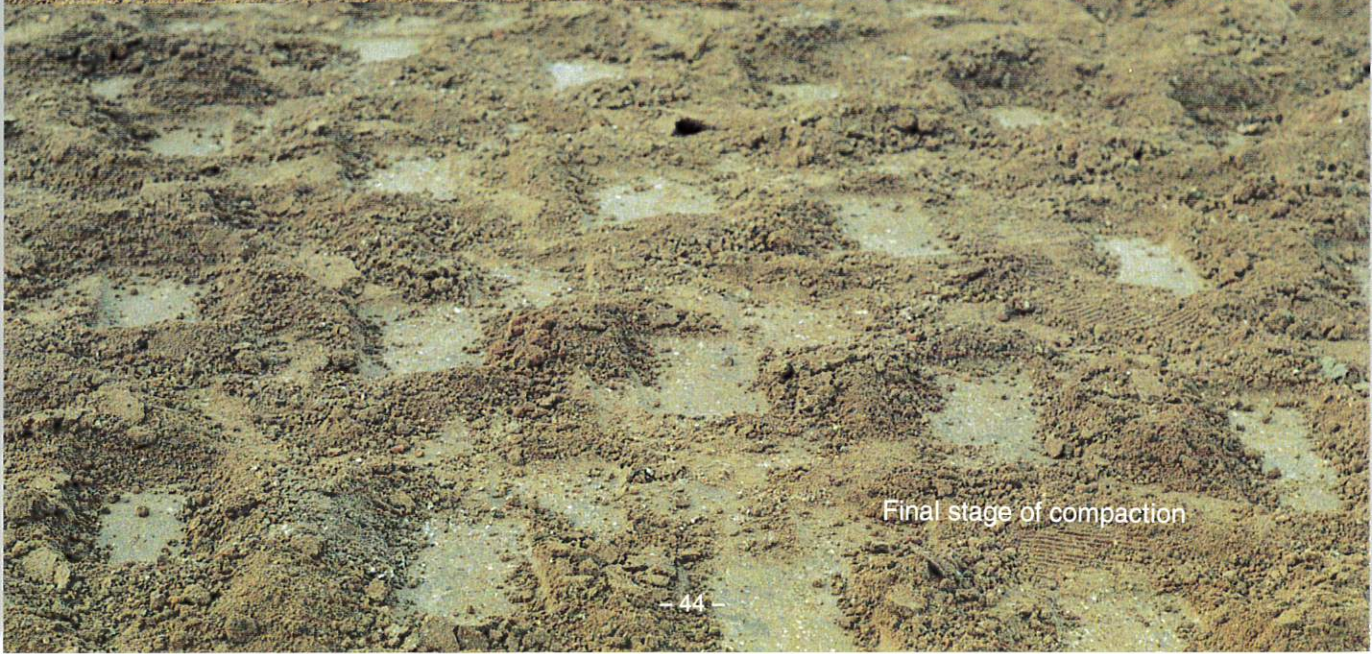
Subgrade compaction with a vibratory tamping roller



Penetration of padfeet of a tamping roller into a subgrade



Initial stage of compaction



Final stage of compaction

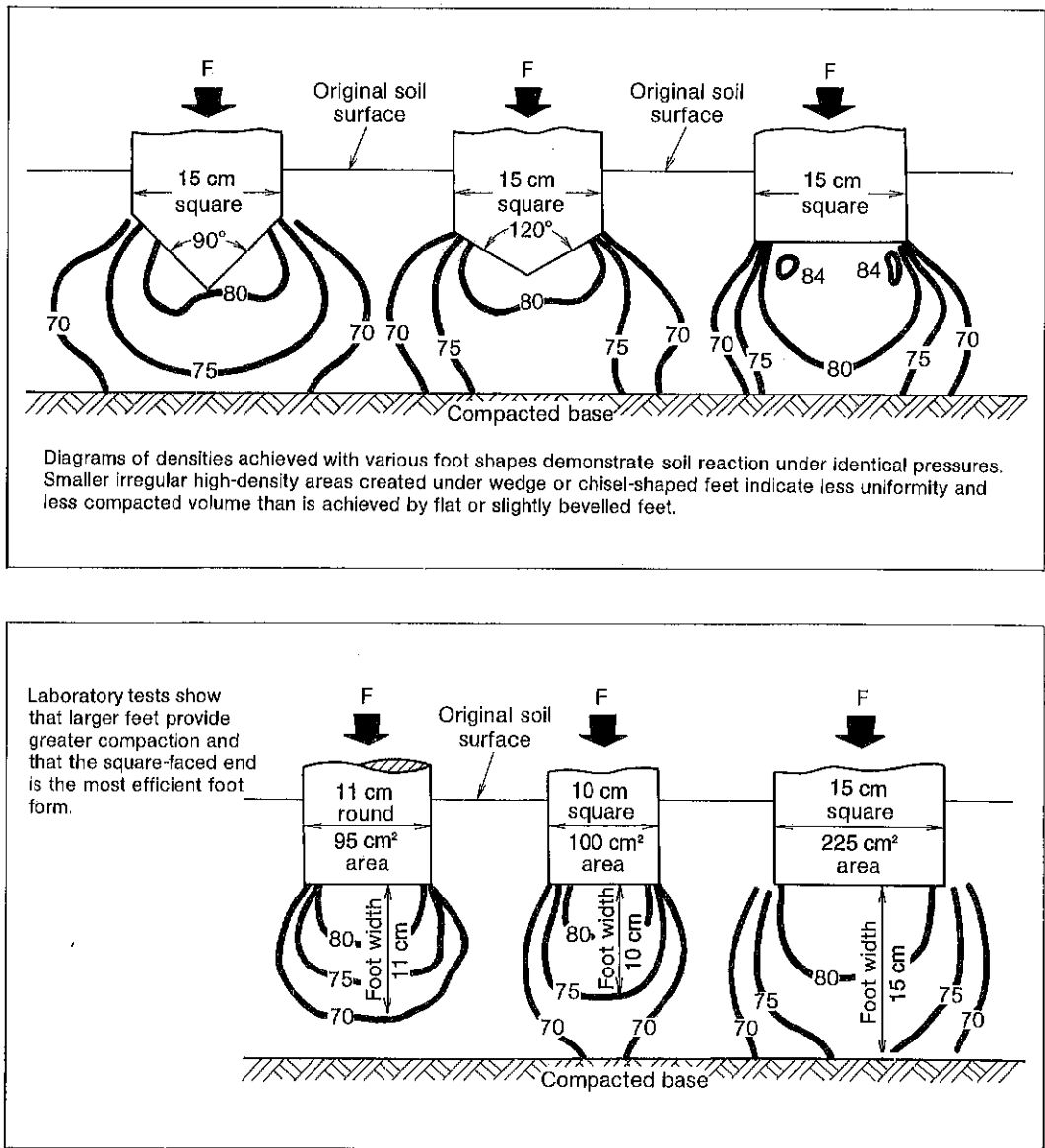


Fig. 3-33 Pad shape vs. pressure distribution by Colin Vallis;
Hyster "The Earthmover Nov. 1974"

IV COMPACTING BY VIBRATING ROLLERS

1. Compactive Characteristics of Vibrating Rollers

As its name implies, the vibrating roller exerts cyclic compacting force by its own vibrating dynamic motion. The mass of the machine under vibrating condition is cyclically hurled against the earth: the force due to the momentum can be as much as 5 times the weight (a gravity force) of the roller itself.

Modern vibrating rollers are the outcome of the research and development work initiated mainly in Europe shortly after the 2nd World War to find better ways of compacting soil for the rush of civil engineering projects. In those days, highways had to be extended, new airports had to be constructed, harbor facilities expanded, urban planning and re-planning promoted, not only in Europe but all over the world.

Studies have been continued by various quarters on the mechanics of soil compaction by vibratory force along with the development of vibration generating mechanisms. Recent years, it has become possible to analyze compaction processes by using such a means as the elasto-plasticity finite element method or through computer simulation. The application technology of their effects having been further developed, vibrating rollers are expected to be put to a wider gamut of applications. Besides, modern vibrating rollers have been put into practical use, such as ones capable of compressing very thick lifts, and ones having an entirely new mode for energy saving and environment protection.

The nominal size of a vibrating roller is expressed in terms of weight just as the other types of compacting rollers are, but this practice is somewhat misleading. In the vibrating roller, what counts is the vibratory force in the sense explained hereafter.

There are three classes of vibrating rollers:

- ① **Hand-guided vibrating rollers (up to 1.5 tons)**
- ② **Tow-type vibrating rollers (5 to 20 tons)**
- ③ **Self-propelling vibrating rollers (2 to 20 tons)**

The present state of the art is such that no practical rules can be laid down to match one type of vibrating roller to a particular set of working conditions and soil types. Selection of the type and size of vibrating roller for a particular contract should be made on the basis of the accumulated data on past jobs and by considering the functional capabilities of the candidate machines such as weight, compacting width, vibratory force, frequency and amplitude, static and dynamic linear pressures, type of driving, working speed and so on.

Before putting the selected machine to work, it should be tested preliminarily

in a particular site: how well it can perform and what its limits are should be checked and noted accurately enough for practical planning of the job on hand.

We shall now look into the way a vibration roller operates. The vibration is created by an eccentric mass rotating around a single or dual axes. This vibration generating principle is generally common to all types and makes of this type of machine.

Figure 4-1 represents the vibrating system of a vibrating roller. W_1 stands for the sprung weight of the roller mounted on the drum having a weight of W_2 by means of suspension damper with a spring constant K_1 . W_1 and W_2 are equal to the gross weight of the roller that exerts static load on the soil having a spring constant K_2 . The soil is regarded as an elastic substance. C_1 and C_2 are damping coefficients of the roller and soil respectively.

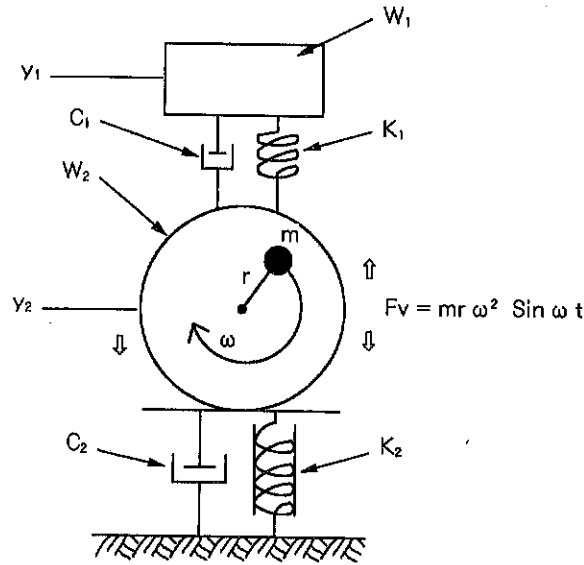


Fig. 4-1 Vibrating system of a vibrating roller

When the eccentric mass m revolves with a radius r and an angular velocity ω , mass m will exert a centrifugal force on the axis of rotation. Since mass m is rotating, this force revolves with it. This force contributes to compacting motion when it is in vertical direction.

The vibrating force (centrifugal force) F is given by:

$$F = m \cdot r \cdot \omega^2$$

In the vertical direction,

$$F_v = m \cdot r \cdot \omega^2 \cdot \sin \omega t$$

where, t = time



Foundation prepared by a heavy vibrating roller

The total generated force is:

$$\mathbf{P\ max = W_1 + W_2 + F}$$

This **Pmax** can be a scale of the capability of a vibrating roller. It is with this total force that the machine cyclically imparts compacting pressure to the soil. In general the higher the pressure, the higher is the resultant density of the compacted soil:

Figure 4-2 is a test result that shows the relationship between the pressure and degree of compaction. The density is roughly proportional to pressure, as will be seen in Fig. 4-2. The change in pressure with depth coincides with Boussinesq's theory. The soil pressure can be increased by increasing **Pmax**, but not without regard to the mutually optimizing relationship inherent between the components of **Pmax**, namely, **W₁**, **W₂** and **F**. We shall see what this relationship is and how it affects **Pmax**.

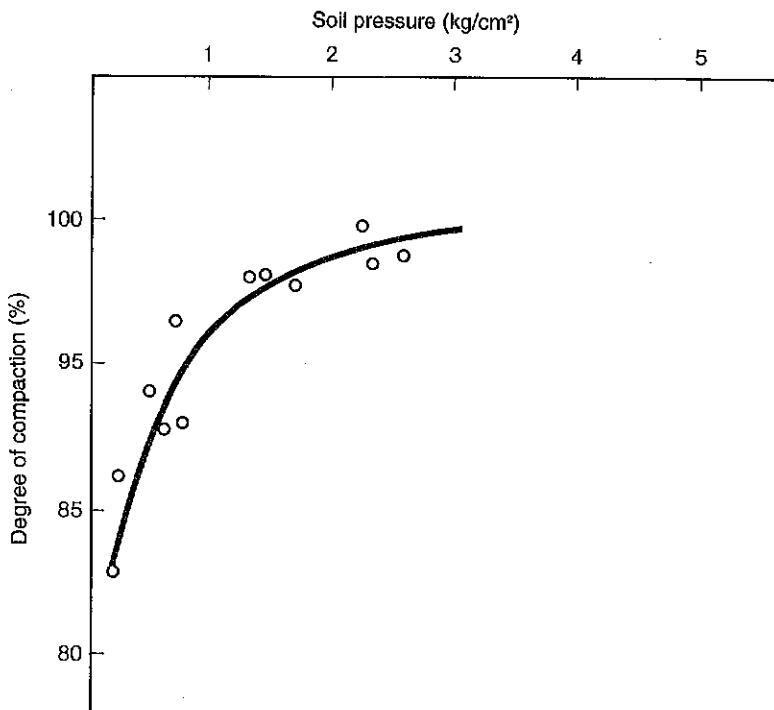


Fig. 4-2 Relationship between compacting pressure and degree of compaction

The vibratory generator for producing **F** has its own mass, which is **W₂**. This **W₂** is unsprung weight, and **W₁** is a sprung weight. Supposing **F** is kept constant, increasing **W₂** reduces the amplitude, but increasing **W₁** to a limited extent does not affect the amplitude of vibration. For this reason, the common practice for

intensifying the compacting action is to increase this weight, W_1 . We may be justified to view this sprung weight W_1 as functioning to push down the roll against the soil. Figure 4-3 shows a general transition of the soil pressure under a pass by a vibrating roller.

P_h = Maximum pressure by the static load $W_1 + W_2$

P_{max} = $W_1 + W_2 + F$

a = Amplitude

ℓ = Affected zone

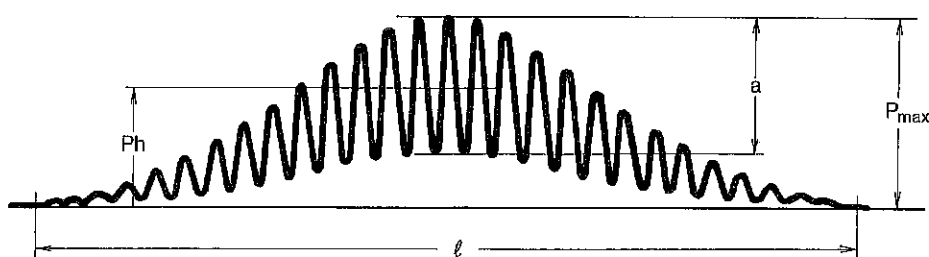


Fig. 4-3 Change in compacting pressure under roll in motion

In Fig. 4-1, the motion of W_1 and W_2 is expressed by the following equations:

$$\frac{W_1}{g} \ddot{y}_1 + C_1 (\dot{y}_1 - \dot{y}_2) + K_1 (y_1 - y_2) = W_1$$

$$\frac{W_2}{g} \ddot{y}_2 + C_2 \dot{y}_2 - C_1 (\dot{y}_1 - \dot{y}_2) + K_2 y_2 - K_1 (y_1 - y_2)$$

$$= W_2 + m \cdot r \cdot \omega^2 \cdot \sin \omega t$$

Simulation of drum motion aided by computer by utilizing this equation of motion draws curves as indicated in Fig. 4-4.

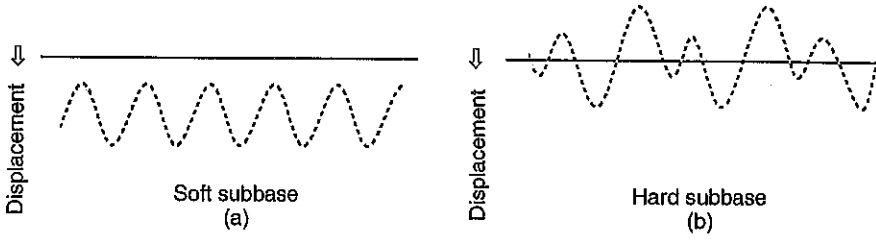


Fig. 4-4 Relationship between ground density and drum motion

When the ground is not yet sufficiently compacted, the drum retains a regular sinusoidal motion. As the soil is hardened, the drum motion changes from a regular curve to a distorted irregular one, finally the drum will start jumping. In this state, compaction is not effected, but reversely the ground will be loosened.

This condition indicates that the maximum contact pressure **P_{max}** has exceeded its allowable value. As can be seen from this, there are optimum relationships with each other among **W₁**, **W₂** and **F** to accomplish rational compaction. To achieve an effective compaction, each of these factors must neither be too large nor too small. Trials have also revealed that the shape of drum and amplitude have a far-reaching influence on the compaction effect.

Furthermore, **P_{max}** has also a definite correlation with the bearing capacity CBR. It is clear that **P_{max}** is attributed to the kinetic energy. Let the kinetic energy be **E**, then **E** is:

$$E = T + U$$

where, **T** = Kinetic energy in vibratory system

U = Potential energy

Practically, **E_{max} = T_{max}**

Hence **T_{max}** is the kinetic energy in the unsprung portion,

$$E_{\max} = T_{\max} = \frac{1}{2} \cdot m \cdot a^2 \cdot \omega^2$$

Concerning this **E_{max}**, Tanimoto describes in his report, "Mechanism of Soil Compaction and Compacting Equipment", that the vibratory compacting energy **E_v** is in proportion to the amplitude created by the vibratory mechanism of a vibrating roller.

$$E_v = 2 a \left(W_v + \frac{1}{2} \cdot F \right)$$

W_v is the unsprung weight.

For relationships between the vibrating energy **E_{max}** and compacting energy **E_v**, he derives the next relationship.

$$E_{max} \doteq 0.38 E_v$$

The compacting energy per unit area given by a vibrating roller is:

$$\begin{aligned}
 E &= E_v \cdot \frac{L}{V} \cdot n \cdot N \cdot \frac{1}{B \cdot L} \cdot Z \\
 &= 2a \left(W_v + \frac{1}{2} F \right) \cdot \frac{L}{V} \cdot n \cdot N \cdot \frac{1}{B \cdot L} \cdot Z
 \end{aligned}$$

where, **a** = Amplitude (half) (cm)
W_v = Unsprung weight (kg)
F = Vibratory force (kg)
L = Drum contact length (cm)
V = Travel speed (cm/min)
n = Vibratory frequency (vpm)
N = Number of passes
B = Drum width (cm)

The relationship between compacting energy **E** and degree of compaction is shown in Fig. 4-5.

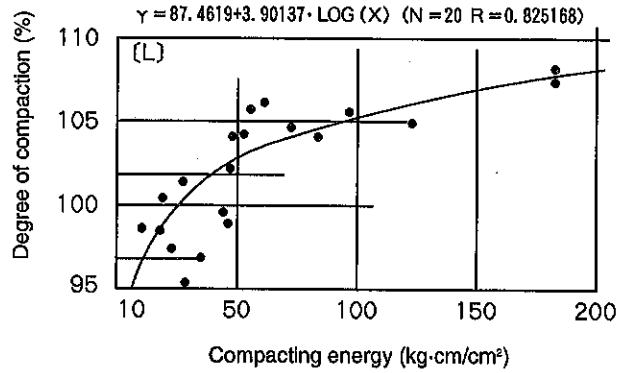


Fig. 4-5 Relationship between compacting energy and degree of compaction

On the other hand, the degree of compaction correlates with the bearing capacity CBR as Fig. 4-6 represents. From this correlation, the compacting energy/ CBR relationship can be obtained as in Fig. 4-7.

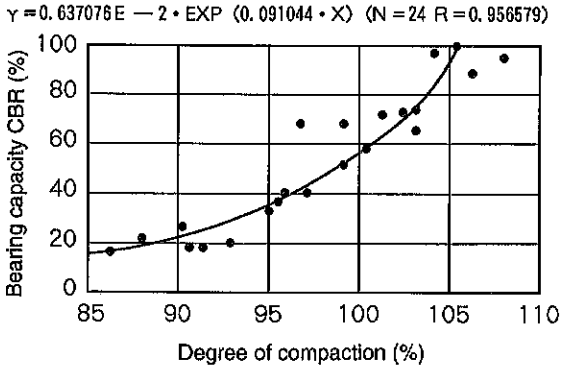


Fig. 4-6 Relationship between degree of compaction and CBR (P16)

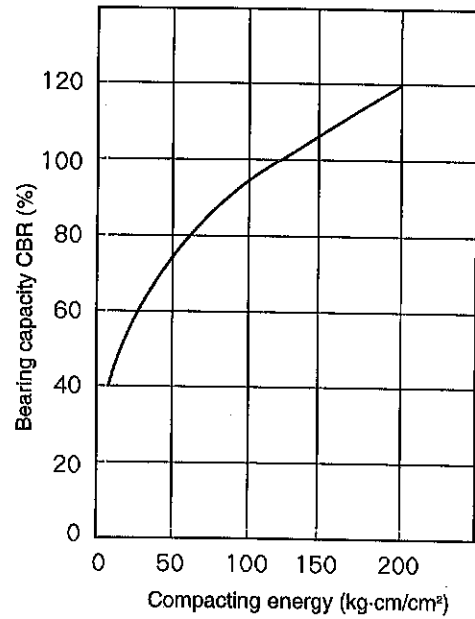


Fig. 4-7 Relationship between compacting energy and CBR

Figures 4-8 and 4-9 are other examples, obtained from extensive test results, of compacting energy/CBR relationship with compacting energy values plotted on the logarithm scale.

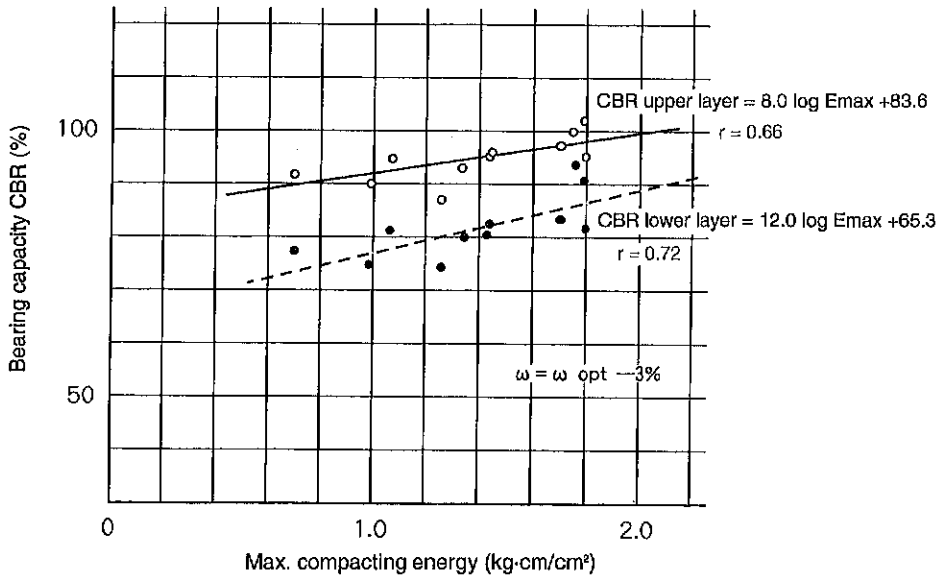


Fig. 4-8 Relationship between compacting energy and CBR (1)

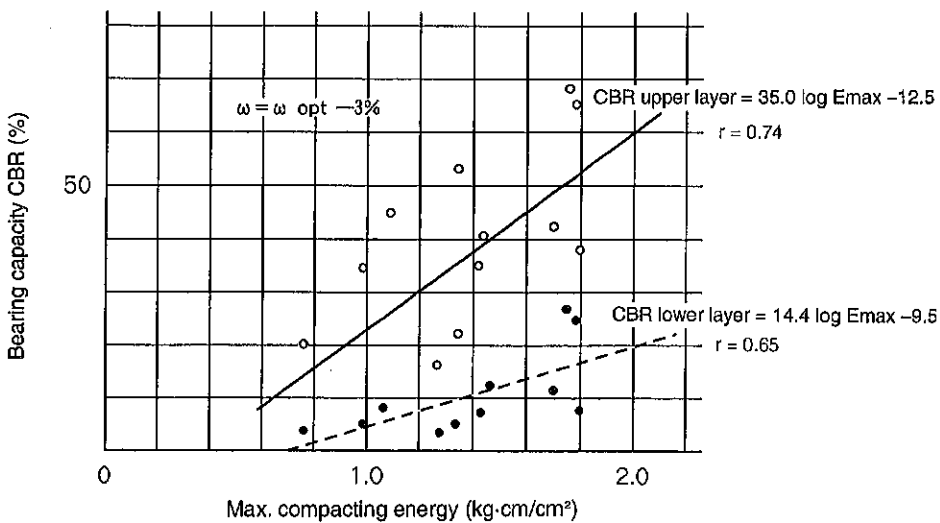


Fig. 4-9 Relationship between compacting energy and CBR (2)

There are definite correlations between compacting energy and bearing capacity CBR. The former is, therefore, of vital importance for an effective achievement of a compaction project.

Most of the vibrating rollers utilize a vibrator (or two vibrators) that creates vibration by the rotation of eccentric masses. In this system, the factor that exerts a great influence on compaction effect is the amplitude **a**. The magnitude of the amplitude depends upon that of the eccentric moment per unsprung weight. The vibration compelling power per amplitude is referred to as the Mechanical Impedance **Z** comparing to Electric Impedance used in the electrical engineering.

$$a = \frac{m \cdot r}{W_2}$$

$$F_v = m \cdot r \cdot \omega^2 \cdot \sin \omega t$$

$$Z = F_v/a$$

Because the mechanical impedance is in proportion to the eccentric mass, the former can take a larger value within the limit of its material strength. It can be said that the practical limit as viewed from both engineering and economical standpoints, governs this value. Or rather, it will be more adequate to say that the contact point between soil engineering/compaction technology and practical limits determines the value. In this respect, many problems remain unsolved in the analysis of vibratory compaction.

Many explanations have been offered in regard to compacting action by vibration. Two of them are easier to understand than the rest. One is the resonance theory and the other is the cyclic load theory. The two will be briefed here.

① Resonance theory

This theory assumes the soil has its own natural frequency as if it were an elastic body, and is based on the idea that the compacting effect is maximized when the vibration coincides with the natural frequency of the soil being compacted. In other words, maximized compaction is thought to occur when the whole system is in resonance.

In actual work the effect of resonance is conspicuous and can be analytically explained, but a question remains: how to maintain the condition of resonance. One will readily see that, as the soil becomes progressively denser, its natural frequency changes accordingly. How to detect this change and how to match and follow the frequency of the vibrator to the soil are practical problems yet to be solved.

Without doubt, kinetic energy delivered from the vibrator into the soil can be more effectively utilized if the system is in resonance, but this theory does not yet promise much for its practical application because of the above difficulties.

② Cyclic loading theory

This theory views the compacting effect as attributable to the sum total of cyclic compressive motions induced by the vibrator. This idea is regarded as acceptable by many for practical consideration where the frequency is comparatively low and the amplitude large. It is generally denied, however, for the frequency range from several hundred to several thousand per minute.

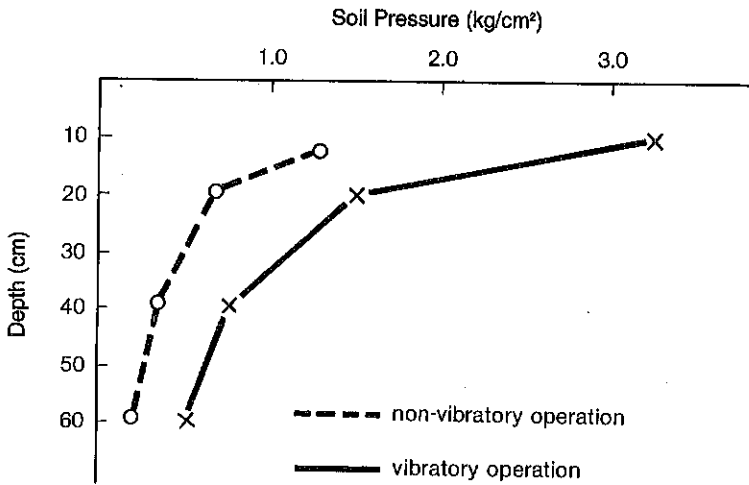
Some researcher has reported on a comparison between the result evaluated by the cyclic loading theory and test pieces which were compacted by the standard method. In terms of energy consumption, the former result was only one tenth of the latter. This indicates that the compacting action by vibrating motion is far more effective than the result evaluated by the summation of repeated loading.

Among other theories, there is one that is based on empirical findings and asserts that the vibration imparted to the soil drastically reduces its internal friction to minimize its internal resistance to shearing action: it does not take a large compressive force to pack the soil to a higher density.

It is common knowledge that shear resistance in the sand in vibrating condition is down to a small fraction. This resistance has been found to decrease to the order of hundredths. The same thing can be said of clay to a limited extent: If the vibratory acceleration is high, the internal shear resistance of the clay decreases appreciably. In the case of asphalt mixture, its shear resistance is said to decrease, on the average, to 1/5 or less.

It will be of quite practical interest for the contractor to know the steel roller equivalent of a vibrating roller. Only a rough rule can be laid down to equate the two in terms of performance if several conditions are given. For a given type of soil, a steel roller and a vibrating roller may be said to be equivalent to each other if their pressure-depth curves i.e. the pressure bulbs are qualitatively and quantitatively alike.

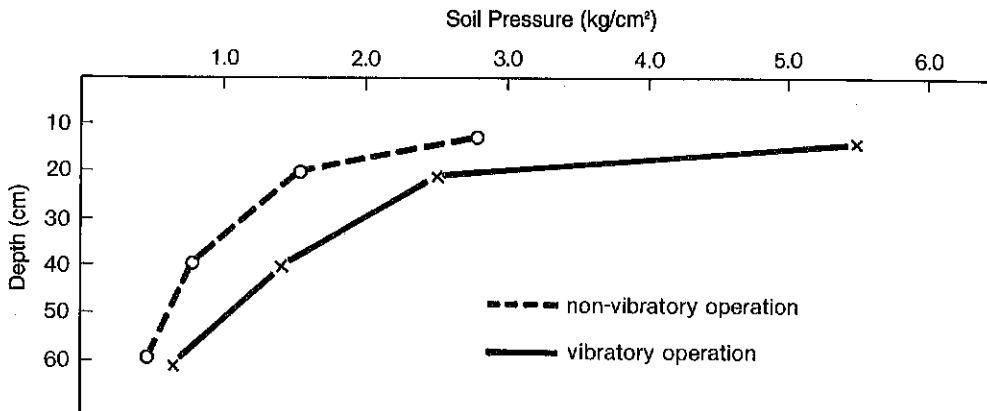
Since, in reality, these two types of compacting machines are basically different in compacting characteristic, a general rule of equivalence cannot be drawn. In this connection, the two pairs of curves shown in Fig. 4-10 and Fig. 4-11 will be meaningful: both curves in each case refer to the same vibrating roller, one curve stands for normal vibratory compacting operation and the other for operation with its vibrator shut down.



Drum diameter: $D = 750$ mm
 Drum width: $B = 1,400$ mm
 Drum weight: $W = 1,400$ kg
 Static linear pressure: $W/B = 10$ kg/cm

Frequency: $n = 2,300$ vpm
 Amplitude: $a = 1.2$ mm
 Vib. force: $F = 4,500$ kg

Fig. 4-10 Comparison between vibratory and non-vibratory operations (1)



Drum diameter: $D = 1,200$ mm
 Drum width: $B = 1,450$ mm
 Drum weight: $W = 3,300$ kg
 Static linear pressure: $W/B = 23$ kg/cm

Frequency: $n = 1,600$ vpm
 Amplitude: $a = 1.6$ mm
 Vib. force: $F = 8,000$ kg

Fig. 4-11 Comparison between vibratory and non-vibratory operations (2)



Base course compaction for New Takamatsu Airport runway

In both cases, the ratio of with/without vibratory run is roughly 1 to 2 in terms of compacting pressure. The roller in Fig. 4-11 is nearly twice as heavy as that in Fig. 4-10 and the curves indicate that the compacting pressure of the former is twice as high as that of the latter.

It may be noted in both figures that the vibratory operation curve of the roller of Fig. 4-10 roughly approximates the non-vibratory operation curve of the roller of Fig. 4-11. Accordingly, under those conditions, a vibrating roller provided with; $W_1 + W_2 + F = 1400 \text{ kg} + 4500 \text{ kg}$ can be equivalent to a static roller with a linear pressure of 23 kg/cm.

As mentioned previously, the degree of compaction depends on the pressure under the roller and the pressure is generally correlative with the amplitude under a certain frequency.

Under a certain given condition, maximum dry densities are variable with the frequencies and there can be an optimum frequency for attaining maximum density (Fig. 4-12). Under such a condition, the dry density is generally increased with the number of passes of the roller.

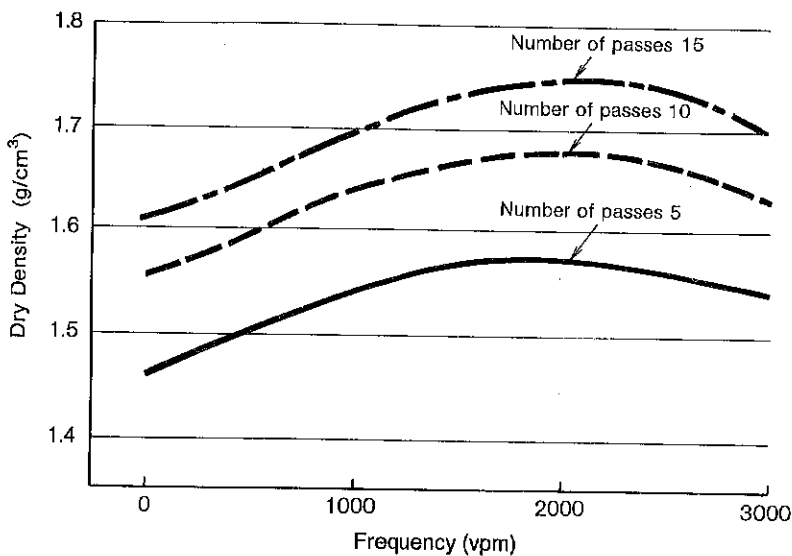


Fig. 4-12 Relationship between vibratory frequency and dry density for various numbers of passes

Here is another example showing the correlation of dry density (γ_d) vs. number of passes (P) compared with a static roller (Fig. 4-13).

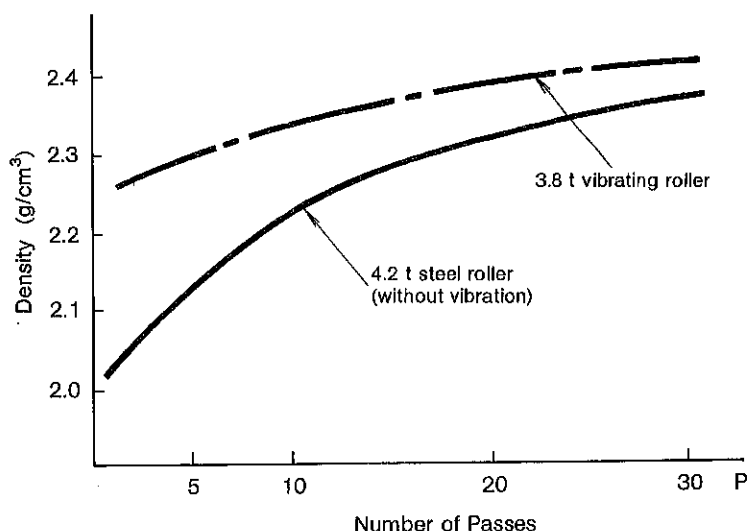


Fig. 4-13 Relationship between number of passes and density for two types of rollers

The dry density increases with an increase of P similarly in vibratory and static operations, but in this example, static operation requires a minimum of 12 P for the same γ_d . However, in the case of a vibratory roller, this is only 4 upto 6 P . It can therefore be appreciated that further compaction develops as it reaches a sufficient state.

2. Application of Vibrating Rollers

The range of applications of compacting operation using the vibrating roller is extremely wide, but it is particularly important to apply this theory with full understanding of the afore-mentioned characteristics. A few useful examples of test simulated to practical work are explained hereafter.

(1) Adaptability to granular material

When the base course material and subbase material of different compositions are compacted by various vibrating rollers, large or small, the following mutual relations must be fully understood.

- ① Number of passes and dry density of material being compressed
- ② Lift thickness and dry density
- ③ Correlations with aggregate
- ④ Correlations with bearing capacity of bottom subbase

Table 4-1 gives condensed specifications of eight models of vibrating rollers used for fields tests.

Table 4-1 Specifications of tested vibrating rollers

Utilized machine	Nominal weight (t)	Vibration force (t)	Static line-pressure (kg/cm)	Applicable SAKAI model
A	0.5 ~ 0.6	1.2	5 ~ 6	HV301/D (HV60, HV60S)
B	0.8 ~ 1.0	1.6 ~ 2.2	6 ~ 7	SV510/D, SV71 (SV500/D, SV-70/D)
D	4.0	2 ~ 4	6 ~ 19	SG500, SW5 (SW350, SW500)
E	7.2	5.5	26	SW70C
F	6 ~ 8	6 ~ 11	18 ~ 28	SW70
G	10 ~ 11	11 ~ 21	25 ~ 30	SW100, SV500 (SW750, TW100)
H	17.4	30	47	SV160D
I	18.8	35.5	56	

Table 4-2 Composition of given materials

#	Material	Maximum dry density (g/cm ³)	OMC (%)
1	Well-graded aggregate	2.17	7.2
2	M30	2.20	6.1
3	"	2.07	10.5
4	(Base course)	2.12	2.2
5	"	2.08	8.8
6	Sandy loam	1.88	14
7	(Subbase)	1.22	39

N.B. #6, #7 due to JIS A 1240 1.4 and others by 2.5.

Grain size distribution of the test materials are as shown below:

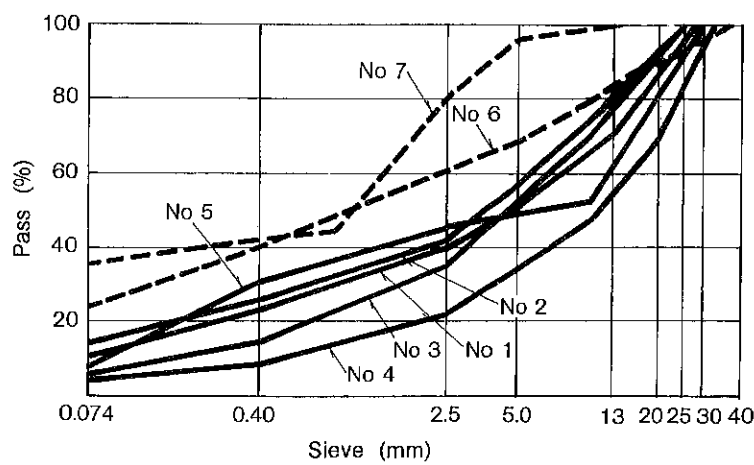


Fig. 4-14 Grain size distribution for soil samples

With static rollers, the minimum required value of 12 P was compacted roughly at 4 to 6 P by using the vibrating rollers, and further density can be expected. The same tendency applies to both the medium and heavy-duty type (Fig. 4-15).

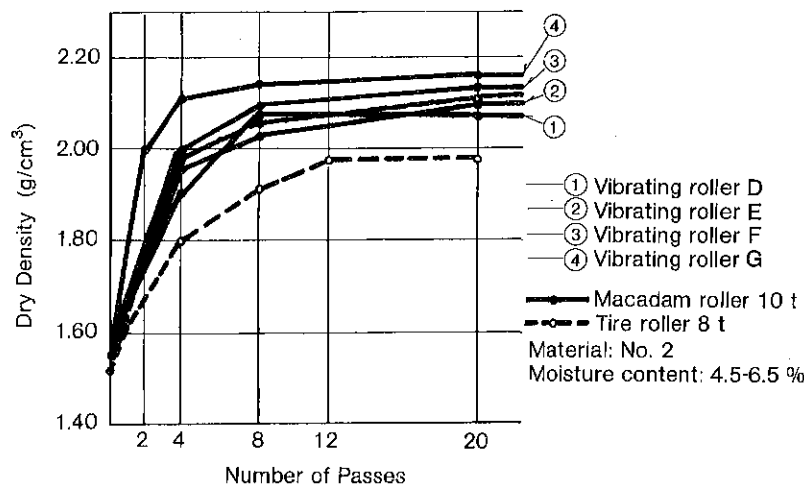


Fig. 4-15 Relationship between number of passes and dry density for various rollers

The heavy-duty rollers compact the soil obviously deeper than do the static rollers, but with 4 to 6 t type the effects appear on the surface layer only. Effects of weight are pronounced on the deeper layer (Fig. 4-16).

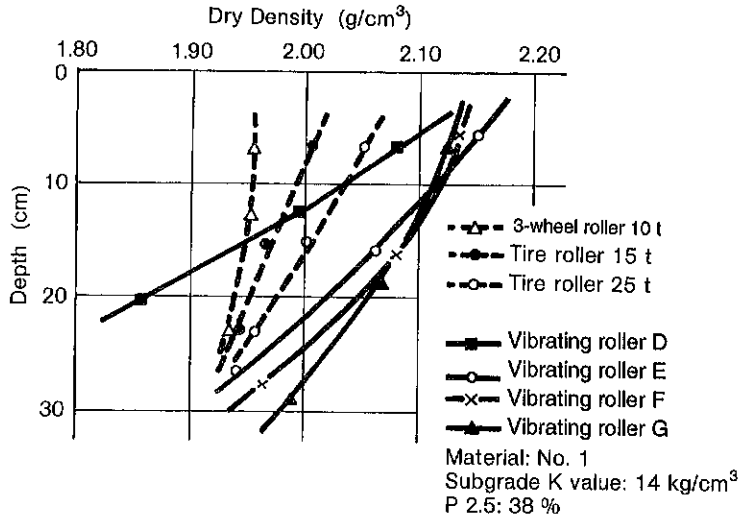


Fig. 4-16 Relationship between compacting depth and dry density for various rollers

Curves in Fig. 4-17 represent dry density/compacting depth relations with other material (Sample No. 2).

Over some materials, the order of vibratory roller size can be readily and clearly determined.

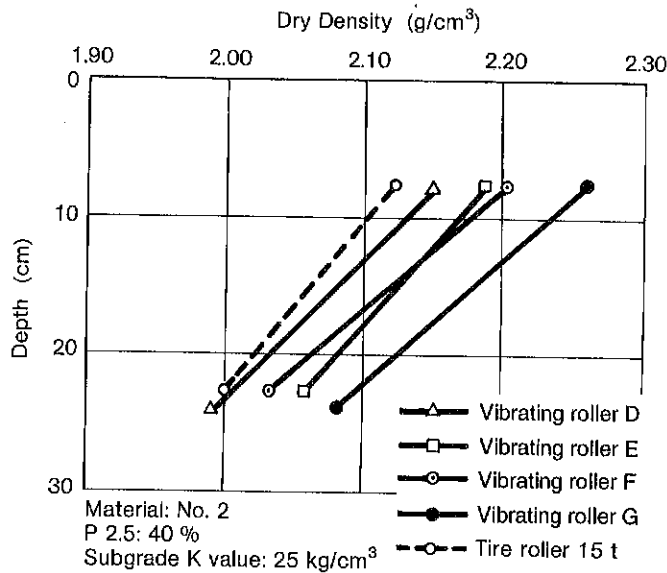


Fig. 4-17 Relationship between compacting depth and dry density for various rollers

The effects of a vibratory roller on the granular material are more pronounced than in the case of the static type. It is assumed that the optimum size and composing percentage are about 2.5 mm dia. and 30% respectively (Fig. 4-18).

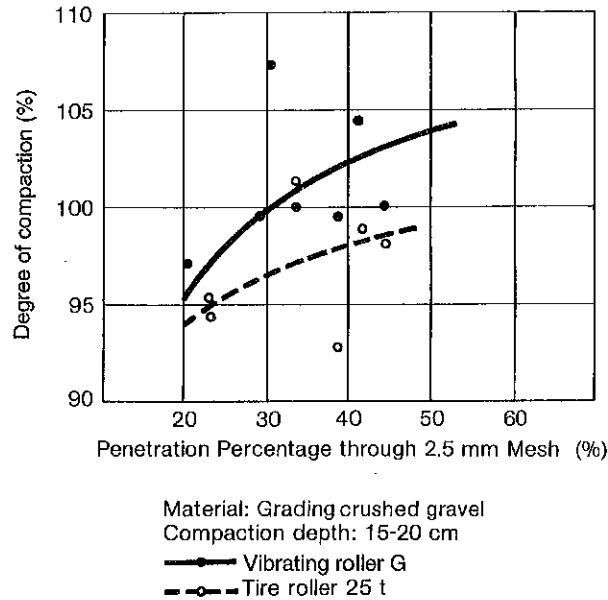


Fig. 4-18 Relationship between grading of materials being compacted and degree of compaction for vibratory and static compaction

Bearing capacity of the subbase affects considerably the compaction effects of a vibrating roller. Generally, satisfactory compaction effect will not be expected with K-value less than 7 kg/cm^3 (Fig. 4-19).

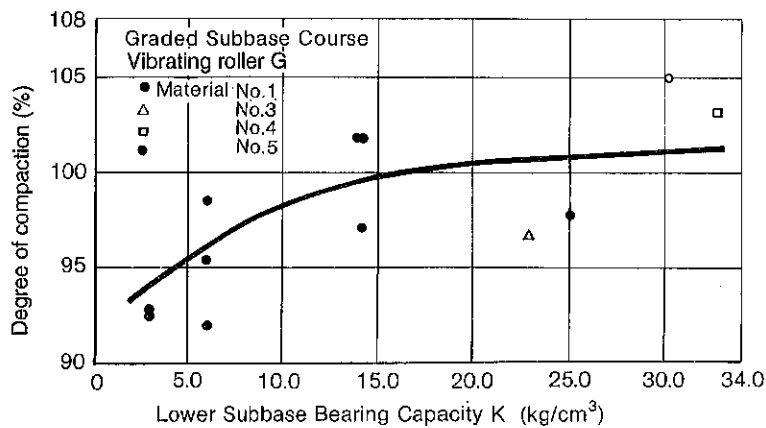


Fig. 4-19 Influence of bearing capacity of lower subbase on compaction effect of vibrating roller

The results of these studies of conventional, single-axis type vibrating rollers indicate roughly the following:

From the Standpoint of Material Composition

- ① The vibratory effects are reduced if aggregate size with 2.5 mm as maximum is less than 30%.
- ② The vibratory compaction cannot be effective on the subbase which has a bearing capacity K less than 7 kg/cm².
- ③ The effects are more significant at deeper than 20 cm.

From the Standpoint of Mechanical Characteristics

- ① Effects of heavy-duty vibrating roller are large on both granular materials and lime-stabilized soil.
- ② Optimum vibration frequency depends on the physical properties of material to be compacted and its bearing capacity. Also, from the standpoint of surface evenness, it is necessary to select a correlatively suitable frequency according to the speed of the roller.
- ③ Minimum required static linear pressure should be 25 kg/cm or more for subbase material when compacting with a vibrating roller.
- ④ Effects of vibrating acceleration are considerable. The roller capable of 4 to 5 G is sufficiently effective.

(2) Vibratory compaction of low-slump cement concrete (RCD)

To build a dam, there is a specific method called RCD method which spreads a low-slump cement concrete, and then compresses it with ordinary heavy-duty vibrating rollers with a view to constructing cost reduction.

Referring to the Experimental Study of Specific Cement Concrete Compacting Equipment conducted by the Construction Ministry, the pages that follow discuss the relationship between the compacting energy and compacting effect in relation to the paving cement concrete.

In the early part of this section, it was mentioned that

$$P_{\max} = W_1 + W_2 + F$$

determines generally the capacity of vibrating roller. This capacity generates dynamic energies resulting in compaction.

The compacting energies **E** discussed below are values calculated from the equation here.

$$\omega = \frac{2\pi n}{60}$$

$$F = \frac{M\omega^2}{g}$$

$$a = \frac{\sqrt{2} \alpha_{RMS}}{\omega^2} g$$

$$E = 2a \left(W + \frac{F}{2} \right) \frac{L}{V} \cdot n \cdot N \frac{1}{BL}$$

ω: Angular velocity (rad/s)

n: Frequency (vpm)

F: Vibrating force (kg)

M: Eccentric moment (kg·cm)

g: Gravity acceleration (980 cm/s²)

a: Amplitude; half (cm)

α_{RMS}: Effective value of vibratory acceleration (G)

E: Compacting energy (kg·cm/cm²)

W: Unsprung weight (kg)

L: Drum contact length (cm)

V: Compacting speed (cm/min)

N: Number of passes

B: Compacting width (cm)

Z: Number of vibratory drums

1) Test condition

Table 4-3 Test condition

Test No.	Composition	Lift (cm)	Frequency (vpm)	Vibrating force (t)	Passes	Applied machine
#1			1500	8	2 novib.	Sakai TW100 Weight: 10.5 t Vibratory force: 5~10 t Frequency: 2500 vpm
#2	W100	75	2100	15	12 vib.	
#3	C135		2100	8	2 novib.	
#4			3200	8		

2) Cement concrete mix design

Table 4-4 Composition of cement concrete

Gmax (mm)	VC (sec)	Air void (%)	W/C + F (%)	F/C + F (%)	S/a (%)	W	C + F	S	G	Pozo No. 8 (g)
						(kg)				
150	15 ± 5	1.5 ± 1	76.9	30	29	100	135	660	1509	1.44



RCD operation with SD450 on Urayama Dam site



RCD operation with SD450 on Urayama Dam site

Samples No. 1 and No. 3 are slightly high in density measurements with less deviations. Yet, it is hard to recognize these higher values. As far as vibratory frequency is concerned, suitable frequency seem to exist in the neighborhood of 2,000 vpm.

Because considerable deviations are noticeable with compressive strength measurements except for No. 3, No. 3 will be the only reasonable sample for evaluation.

4) Correlations between number of passes and surface settlement (Fig. 4-22)

With increasing number of passes, the surface consolidation settlement also increases. This sinking is caused by combinations of such factors as consolidation displacement, fluidity displacement and roadbed subsidence. For this reason, the amount of settlement is not equal to the compactive ability. However, it is meaningful as an evaluation standard on a work site.

On the other hand, care is needed to avoid the formation of surface unevenness.

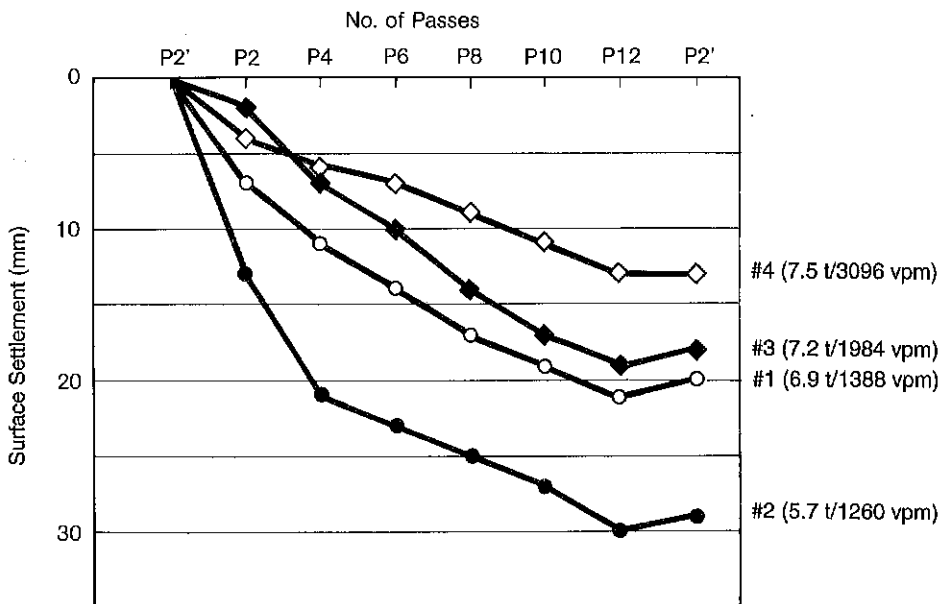


Fig. 4-22 Relationship between number of passes and surface settlement for various vibrating frequencies

5) Finalized table

The results of the tests are finalized and tabulated as follows (Table 4-6): The vibratory energies **E** are values calculated by the afore-mentioned equation, and frequency **n** is taken from graphically recorded vibratory acceleration. The values in parentheses are preset values of the test condition.

Table 4-6 Finalized table

Test No.		#1	#2	#3	#4
Applied Roller		SV500			
No. of Passes	P	12	12	12	12
Roller Speed (km/hr)	V	1.402	1.195	1.209	1.129
(cm/min)		2337	1992	2015	1882
Frequency (vpm)	n	1388	1260	1984	3096
		(1500)	(2100)	(2100)	(3200)
Angular Velocity (rad/s)	ω	145.35	131.95	207.06	324.21
Drum Dia. x Width (cm)	D x B	130 x 210			
Vib. Drum Axle Load (kg)	W	5600			
Eccentric Moment (kg-cm)	M	318.4	318.4	162.6	70.0
Vibrating Force (kg)	F	6864.1	—	7162.0	7508.1
		(8000)	(15000)	(8000)	(8000)
Vib. Acceleration (G)	α_{RMS}	5.45	4.35	4.16	3.24
		(1.43)	(2.68)	(1.43)	(1.43)
Amplitude 2a (cm)		0.7150	0.6926	0.2671	0.0854
Compaction Energy (kg-cm/cm ²)	E	219.2	—	138.0	75.1
Theoretical Max. Density (t/m ³)		2.400			
Core Density (t/m ³)	γ	2.386	2.375	2.381	2.360
± Deviation		±0.019	±0.016	±0.018	±0.023
Specific Density (%)	R	99.4	99.0	99.2	98.3
± Deviation		±0.8	±0.7	±0.8	±1.0
Core Observation (%)		68.4	58.2	52.7	35.1
(Excellent, good, fairly good)					
Surface Settlement (mm)		20	29	18	13
Core Strength (91 days) (kg/cm ²)		142	155	157	133
± Deviation		±20	±11	±8	±19

The relationship between vibrating frequency and compaction effects are as shown below:

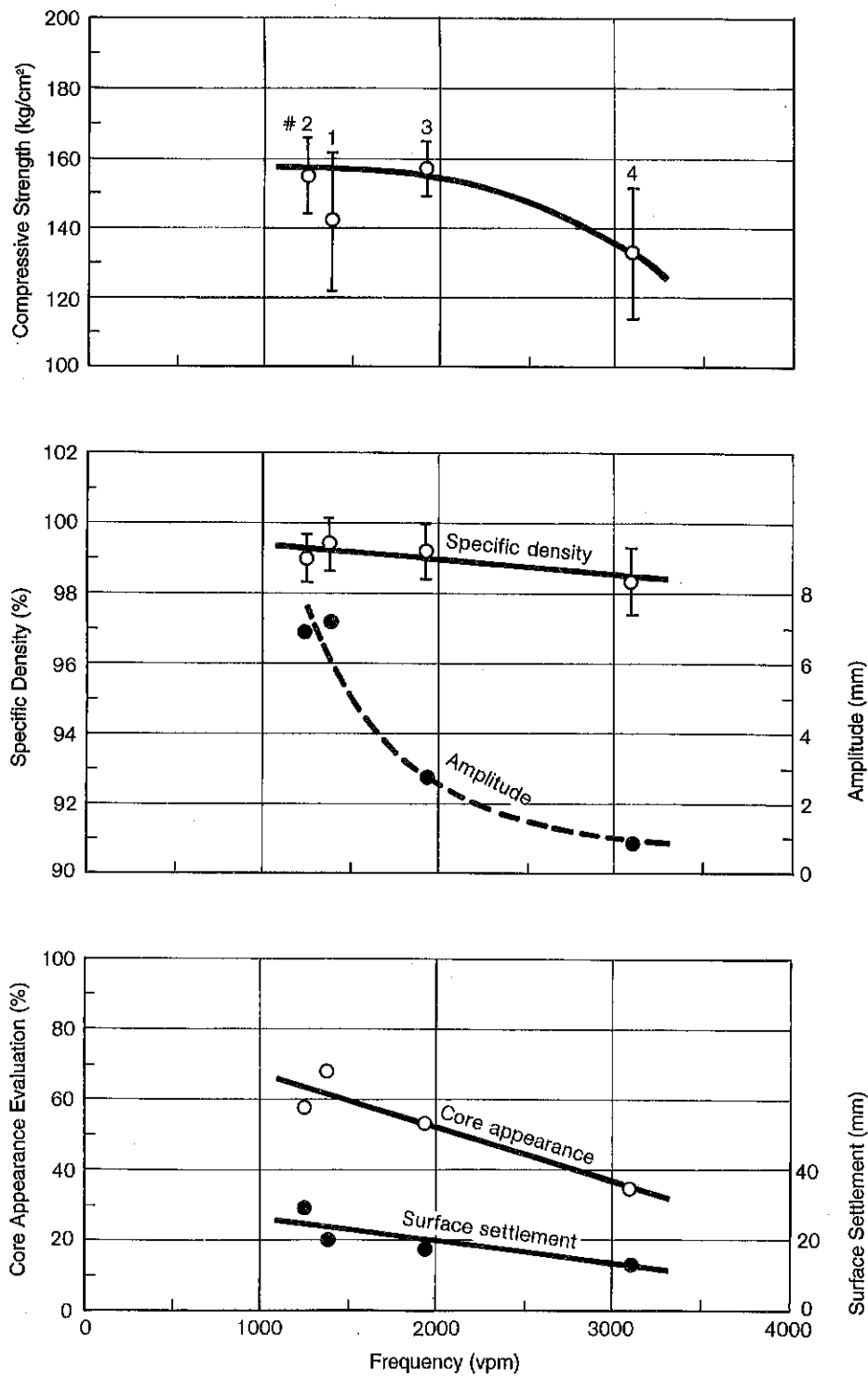


Fig. 4-23 Relationship between vibratory frequency and compaction effects



Surface compaction for RCD with the nutating roller

Judging from Fig. 4-23, compacting effects are large at lower frequency and high amplitude. This coincides with the result of $2a = 2$ mm or more required for attaining the density of more than 2.4 t/m^3 and the extent of the effects in excess of 98% in RCD compacting test with a lift of 35 cm.

Also, with lower amplitude, the core was good and the settlement showed a tendency to be greater (For RCCP, a simple evaluation is not acceptable).

The relationship between vibratory force and compacting effects are shown in Fig. 4-24.

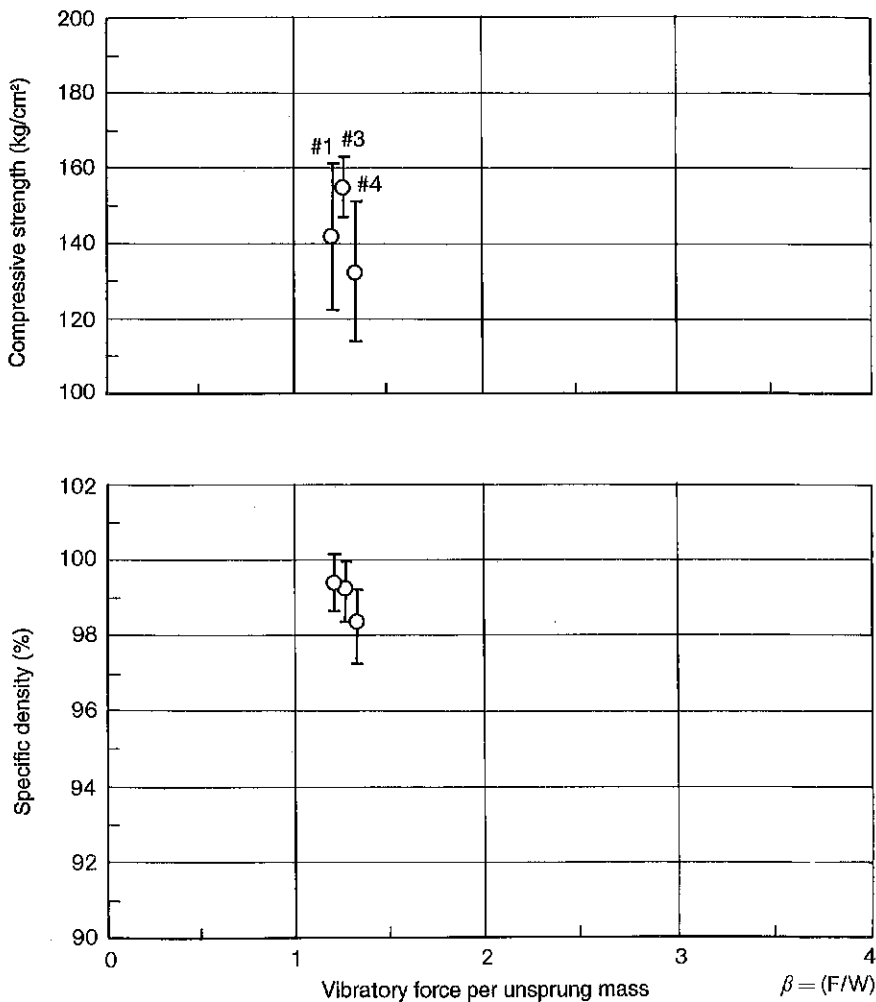


Fig. 4-24 Relationship between vibratory force and vibratory effects

NOTE: $\text{Vibratory force per unsprung mass} = \frac{\text{Vibratory force (kg)}}{\text{Unsprung weight (kg)}}$

Figure 4-25 illustrates the relationship between compacting energy and compacting effects.

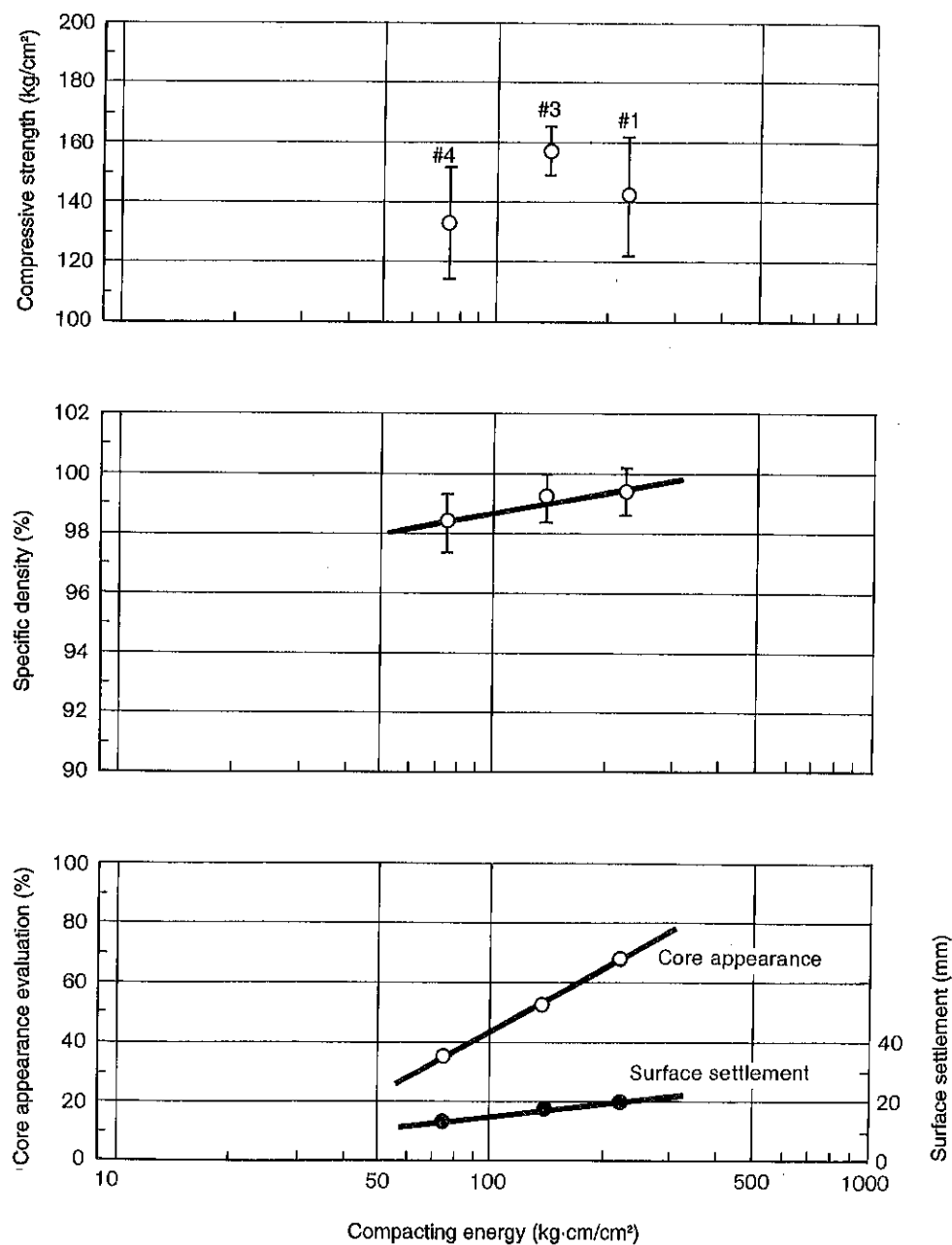


Fig. 4-25 Relationship between compacting energy and compacting effects



No considerable difference is observed in the vibratory acceleration/compacting depth relationship with different rollers (Fig. 4-26a). However, the compacting pressure/depth relationship differs widely with different machines. This indicates that effects of vibratory compaction stem rather from the pressure than the acceleration.

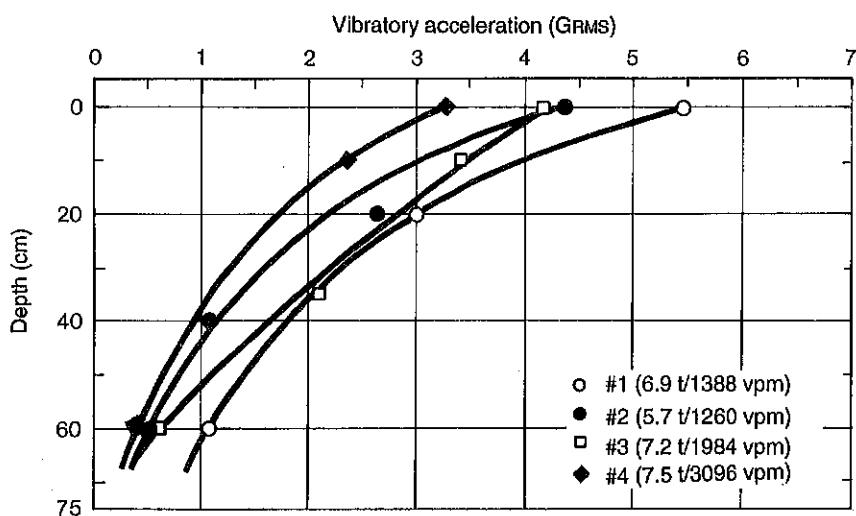


Fig. 4-26a Relationship between vibratory acceleration and compacting depth

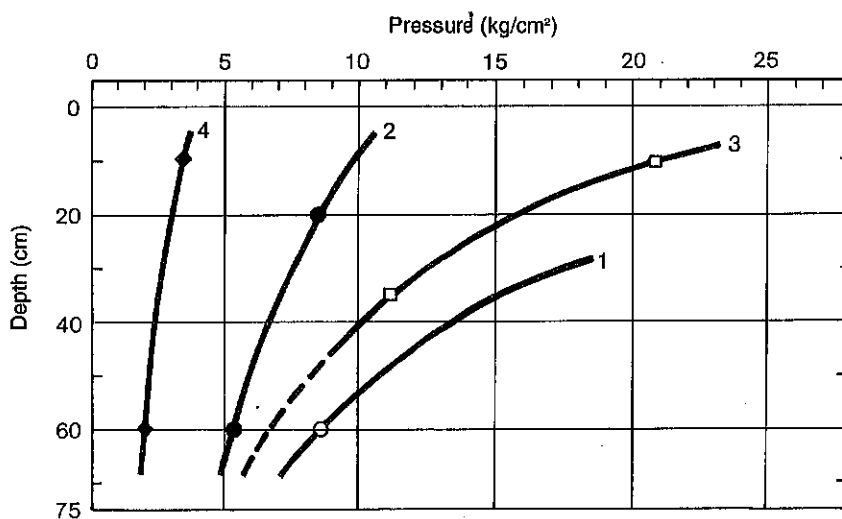


Fig. 4-26b Relationship between compacting pressure and compacting depth

It is apparent that the compacting pressure is not affected by the vibratory force, but is related to the amplitude. This also coincides with the relation between density and amplitude.

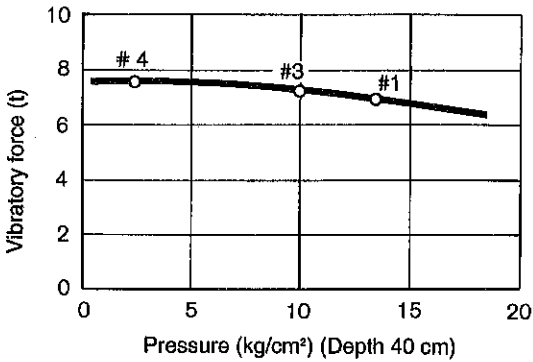


Fig. 4-27a Relationship between vibratory force and compacting pressure at a depth of 40 cm

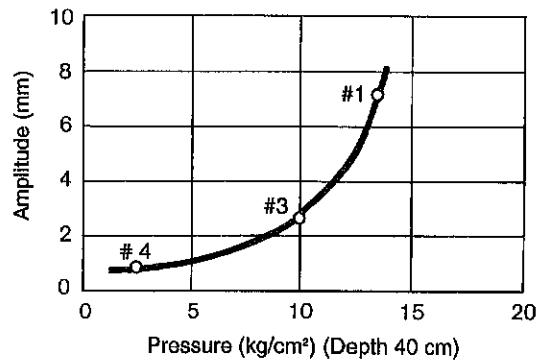


Fig. 4-27b Relationship between amplitude and compacting pressure at a depth of 40 cm

Figures 4-28a and 4-28b indicate the relationship between compacting energy, compressive strength and density.

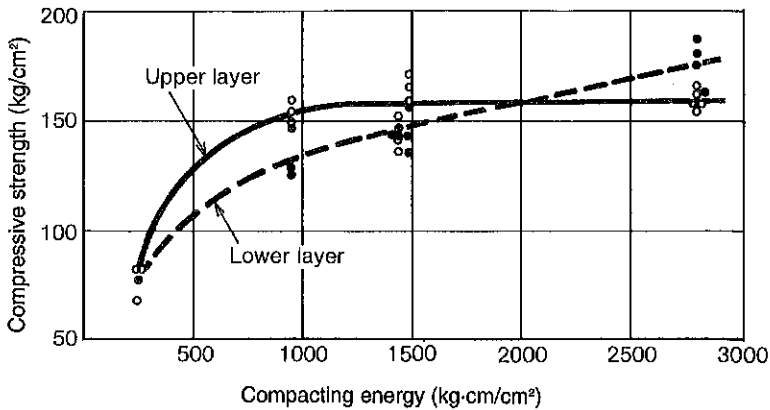


Fig. 4-28a Relationship between compacting energy and compressive strength

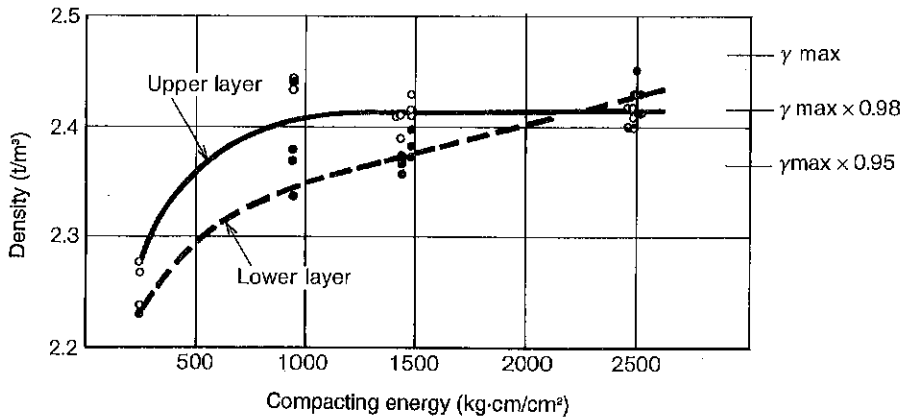


Fig. 4-28b Relationship between compacting energy and density

$$E_1 = 2a \left(W + \frac{1}{2} F \right) \frac{L}{V} n N \frac{1}{BL} Z$$

where, **E₁**: Compacting energy (kg·cm/cm²)
a: Amplitude (half cycle) (cm)
W: Vibrating mass (kg)
F: Vibrating force (kg)
V: Vehicle speed (cm/min)
L: Drum contact length (cm)
n: Vibratory frequency (vpm)
N: Number of passes
B: Drum width (cm)
Z: Number of vibrating drums
LxB: 1810 cm²

◇ **Summation**

- ① **As the compacting energy increases, the compressive strength also increase as a whole.**
- ② **Compressive strength of upper layer reaches the higher limit at a certain energy. After that, the strength cannot be increased even with the energy increased.**

- ③ On the other hand, the strength of lower layer gradually goes up with an increase in energy is this experiment.
- ④ From the above ② and ③, when the energy is not sufficient, an “upper strong but lower weak”, but “upper weak and lower strong” symptom occurs as the energy is in excess of a certain magnitude.
- ⑤ To cope with these particulars, variable amplitude mechanisms have been developed.

In a series of the foregoing experiment, considerable deviations in the strength were noticed probably due to segregation of the composed aggregates. It will not be correct to conclude from the test results that the existing problem is one of compaction only.

3. Development of a Roller (SD450) for RCD

Based on experimental researches as described in section 2-(2), a vibrating roller with a new mode has been developed for exclusive use in Roller-Compacted concrete Dams. Through an official examination, high performance of the model was officially recognized with a certificate (No. 9001) granted by the Japan Construction Mechanization Association that is an organization sanctioned by the Ministry of Construction.

Pages that follow provide technical information on the roller.

(1) Specification decision

In deciding design specifications, performance requirements were made clear as mentioned below based on the results of experimental analysis conducted.

- ① A comparatively heavy vibrating roller having high amplitude and frequency (i.e. high compactive energy) for effective compacting effort to reach deep into the material being compacted.
- ② A roller capable of maintaining straight travel while in compaction operation at creep speeds.
- ③ A roller excellent in riding comfort, keeping operator free from disagreeable vibrations and noise.
- ④ A roller excellent in maneuverability and trafficability for use on a thick layer of ready-mixed concrete materials.

To meet the above-mentioned requirements, the following specifications were selected on a trial basis:

Gross weight:	10,000 kg
On front axle:	5,000 kg
On rear axle:	5,000 kg
Amplitude (both drums):	1.4 mm
Frequency:	2,000 vpm
Vibrating system:	Vertical and mechanical vibration with 2-axis eccentric shafts
Wheel base:	As short as possible
Final density target:	105% of max. degree of compaction stipulated by JIS Standard (A-1201-1990)

(2) Vibrating system

Generally used, one-axis type vibrating system finds its limit in size of its structure and in its capability of delivering compacting energy. Particularly when compaction process approaches its final stage, propelling and steering maneuvers tend to become unstable. This tendency is noticeable at low vehicle speeds. If the roller body starts oscillating, jumping and shaking its head, the machine will be thrown into difficult operation with extreme lowering of compaction effects. Finally, the machine will be damaged. To prevent this irregular 3-dimension motion, rolling, pitching and yawing, a “vertical vibrating mode based on a 2-axis eccentric shaft principle” was chosen. In this mechanism, two identical eccentric shafts arranged in parallel with each other rotate synchronously in a mutually opposing direction and leave only vertical-motion elements, with horizontal-motion vectors cancelling each other (Fig. 4-29).

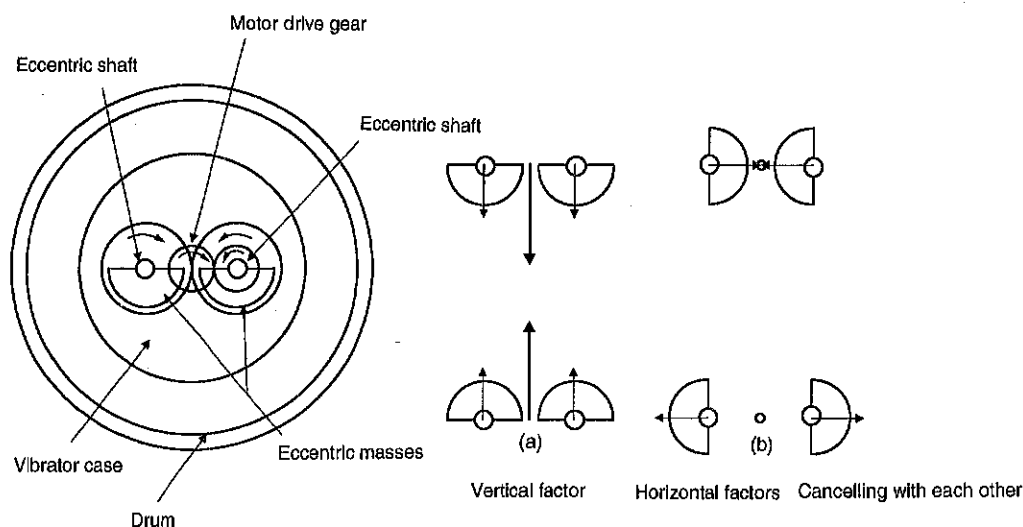


Fig. 4-29 Vertical mechanical vibration mode utilizing 2-axis eccentric shafts

(3) Soil compaction tests

To evaluate, on a general basis, the compacting performances of the prototype, a series of compacting tests were conducted on a standard sandy loam, prior to the RCD tests.

1) Sample soil analysis

Specific gravity

of soil particles: 2.82 g/cm^3

Type of soil: Sandy loam

Liquid limit: 27.0

Plastic limit: 17.9

Plasticity index: 9.1

Flow index: 5.0

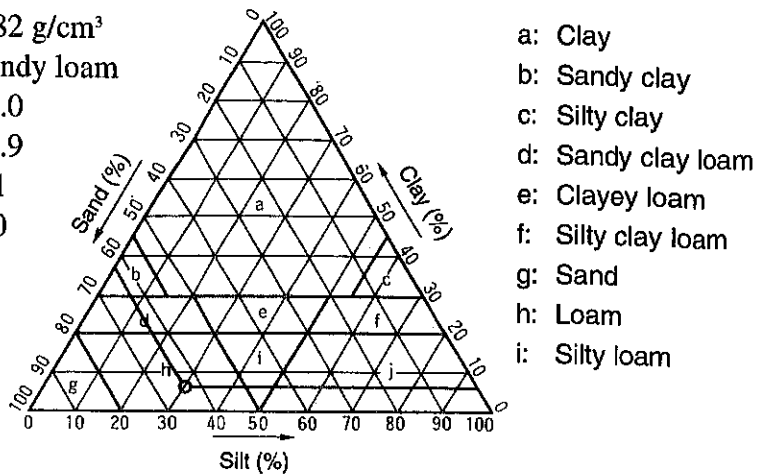


Fig. 4-30 Soil classification diagram

Figure 4-30 provides convenient classifications of soils. Figure 4-31 represents grain size distribution of soil samples.

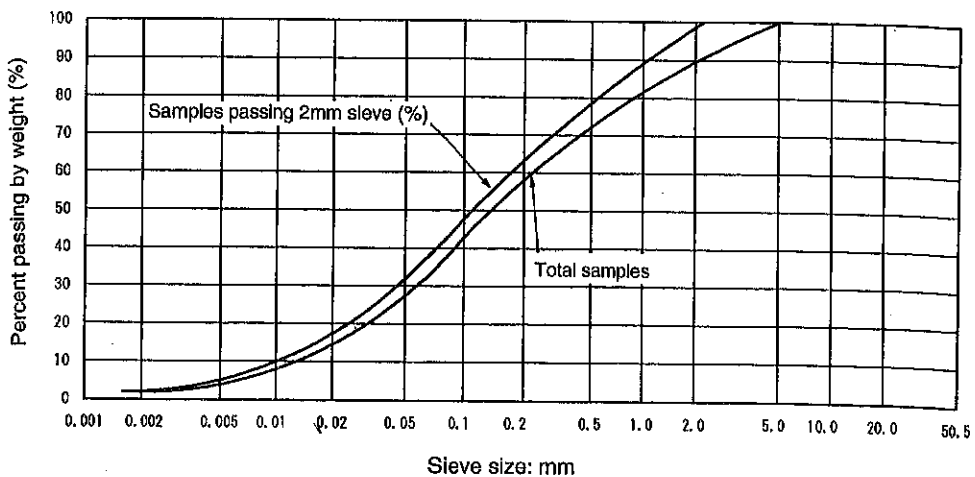


Fig. 4-31 Grain size distribution for soil samples

2) Conditions of sample soil

Spreading depth:	30 cm	Moisture content	
Optimum moisture content (OMC):	11.5%	Dry side:	Approx. 8%
Standard max. dry density: 1.995 g/cm ³		Proximity of OMC:	10%
Max. particle size:	5 mm	Wet side:	Approx. 12%
Max. number of passes:	16		

Under the above-listed conditions, measurements were taken of the degree of compaction, settlement in each pass, CBR, and vibratory acceleration.

3) Dry density

With 16 passes at a moisture content of 9%, a specific dry density of 108.5% was obtained. This value well clears the target value of 105%.

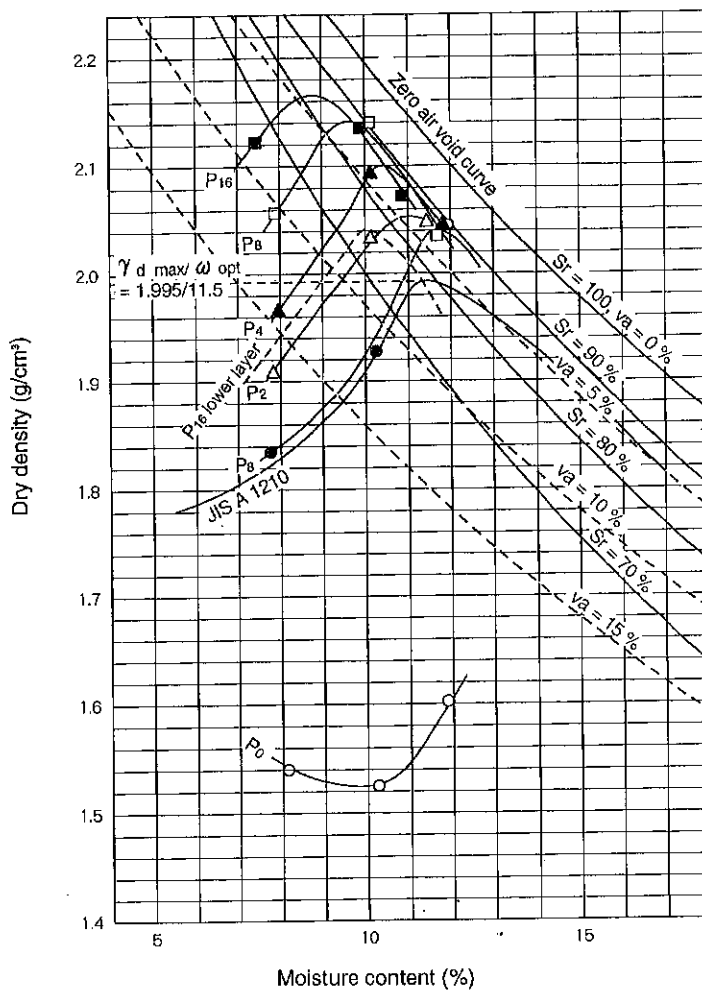


Fig. 4-32 Dry density/moisture content relationship

4) CBR measurement

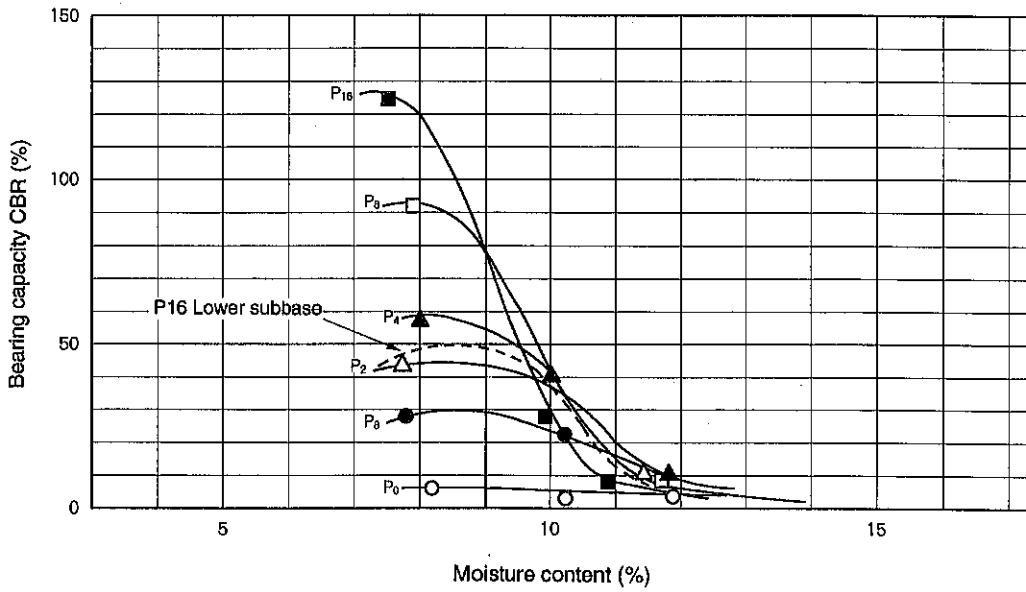


Fig. 4-33 CBR/moisture content relationship

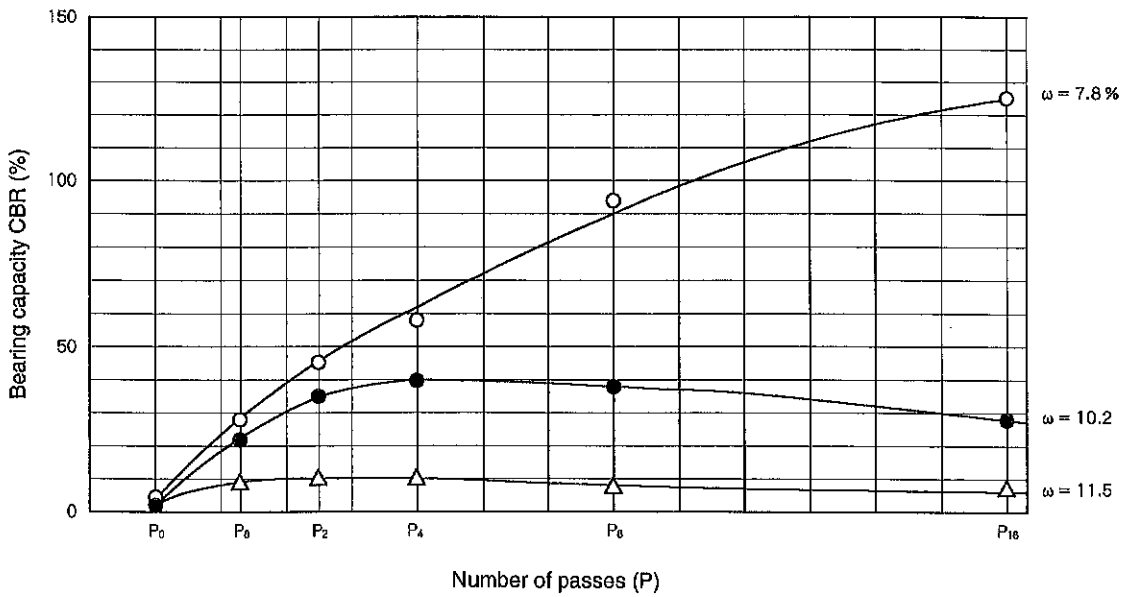


Fig. 4-34 CBR/number of passes relationship

5) Vibration factor measurement

With a vibratory acceleration sensor mounted on the vibratory drum (unsprung portion), frequency and acceleration readings were taken as follows:

Frequency: 2,600 ~ 2,700 vpm

Amplitude: 1.4 mm (integration of acceleration values)

It is clear from these values that they meet the design target. In addition, almost no acceleration values in the horizontal direction were noticed, proving that with the new mode that utilizes dual eccentric shaft, acceleration vectors in the horizontal direction cancel one another (Fig. 4-36).

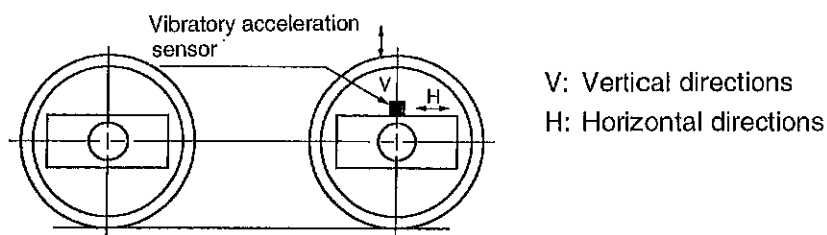


Fig. 4-35 Mounting location of vibratory acceleration sensor

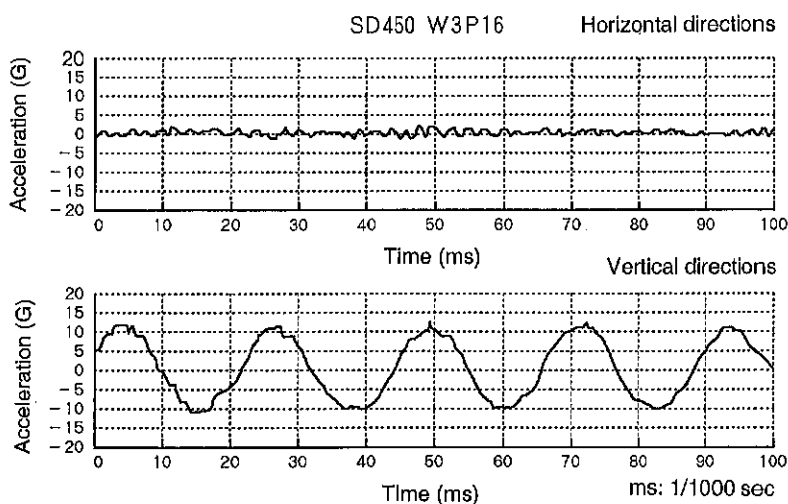


Fig. 4-36 Vibratory acceleration curves in horizontal and vertical directions

6) Compactive performance comparison with conventional models (soil compaction)

Figure 4-37 shows the performance curves in terms of maximum degree of compaction and maximum CBR obtained from a variety of experimental results in the past 10 or more years on conventional static rollers, pneumatics, tamping types and 1-axis vibrating rollers. Mark \odot represents a measurement of the SD450 with its new mode. As can be seen among other models, the SD450 ranks top in performances for soil compaction.

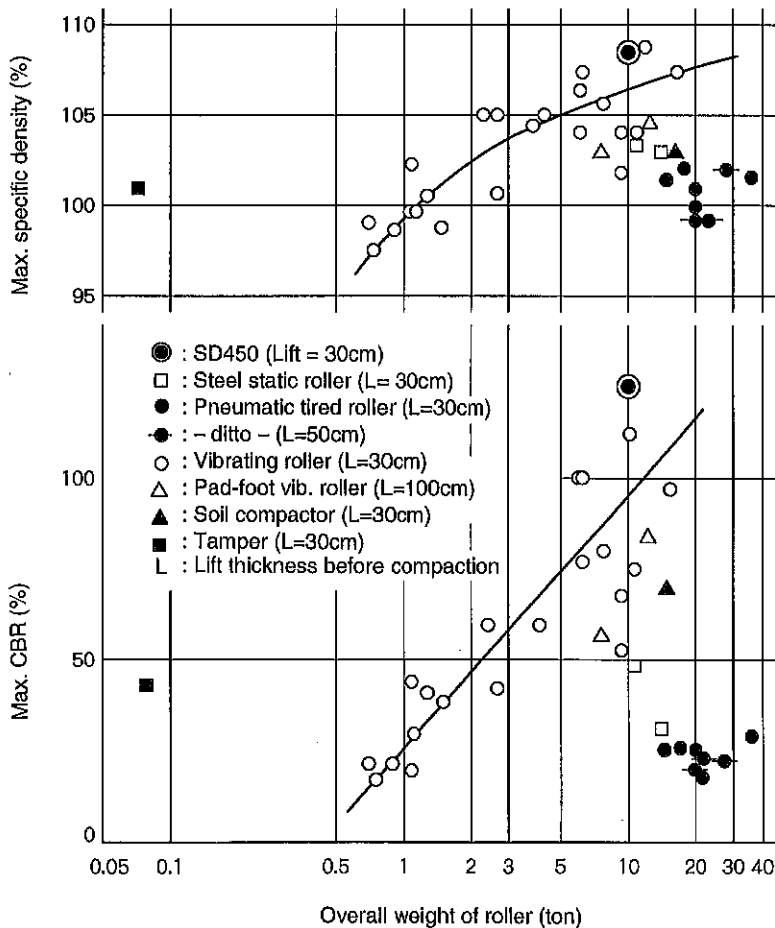


Fig. 4-37 Compacting performance comparison between SV450 and other conventional rollers

(4) RCD compaction tests

Following the soil compaction experiments, a series of RCD field tests - our primary object - was made at Ryumon Dam in Kyusyu by the Kyusyu Regional Construction Bureau on October, 1990 for the purpose of evaluating the performances of SD450.

To know the compactable depth limit of one layer of a zero-slump cement concrete mixture with the SD450 employed, 3 lifts (100, 125 and 150 cm in thickness) were prepared in addition to a 75cm-lift that had been proved to fall within the compactable limit.

In every compaction pass, measurements were taken of surface settlement caused by consolidation, R-I density, core density and core compressive strength. As part of the evaluations, appearance evaluation was also made on the sample cores after a curing period of 91 days.

1) Mix design

Table 4-7 Mix proportion

Max. size of aggregate	150 mm
VC-value	15 ~ 20 sec
Percentage of voids	15%
Water-cement ratio W/C	62.3 ~ 64.6%
Filler ratio S/a	28%
Moisture content W	81 ~ 84 kg/m ³
Cement (plus slag)	130 kg/m ³
Filler volume S	601 ~ 603 kg/m ³
Aggregate size/mixing amount	
80 ~ 150 mm	409 ~ 411 kg/m ³
40 ~ 80 mm	406 ~ 458 kg/m ³
20 ~ 40 mm	360 ~ 361 kg/m ³
5 ~ 20 mm	409 ~ 411 kg/m ³
Additives	0.325 kg/m ³
Max. theoretical density	2.488 ~ 2.494 t/m ³

2) Pressure distribution with depth

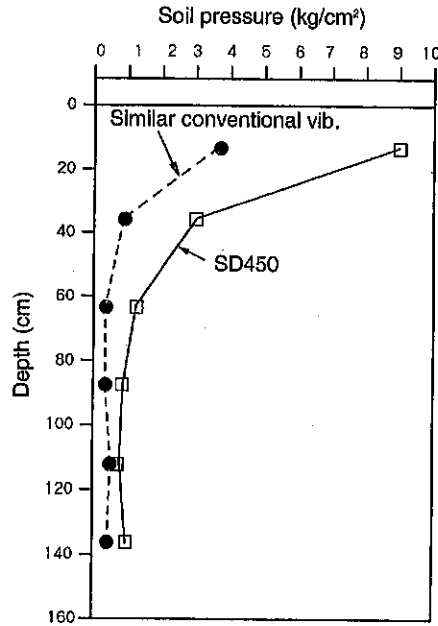


Fig. 4-38 Pressure/depth relationship

3) Compressive strength and density of sample cores

Two lanes were arranged in the test yard. Sections with different mat thickness were prepared in the lanes, 75, 100, 125 and 150 cm. Samples were taken from each section to determine the compressive strength and density. For 75 cm- and 100 cm-lifts, test specimen were collected from the surface and bottom of the layers. For 125 cm- and 150 cm-lifts, samples were taken from the surface, middle and bottom of the layers. Generally, the compressive strength and density obtained in laboratory tests show positive correlation, however, measurements of specimens taken from the job site after a fixed curing period tend to scatter widely. Such factors as aggregate segregation and measurement errors are responsible for the deviation. This, however, is another problem.

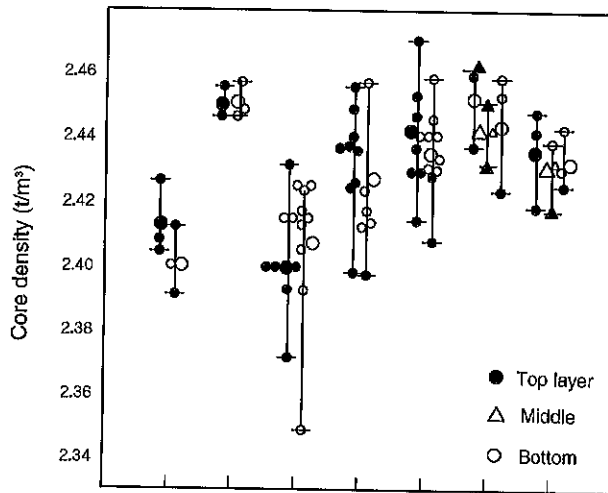
In Figs. 4-39 and 4-40, it is hard to recognize correlations as far as these measurements are concerned. It is, however, clear that density value dispersion in the SD450 is less than that of other models.



Cold profiling on the No. 3 Keihin Expressway



ER501F

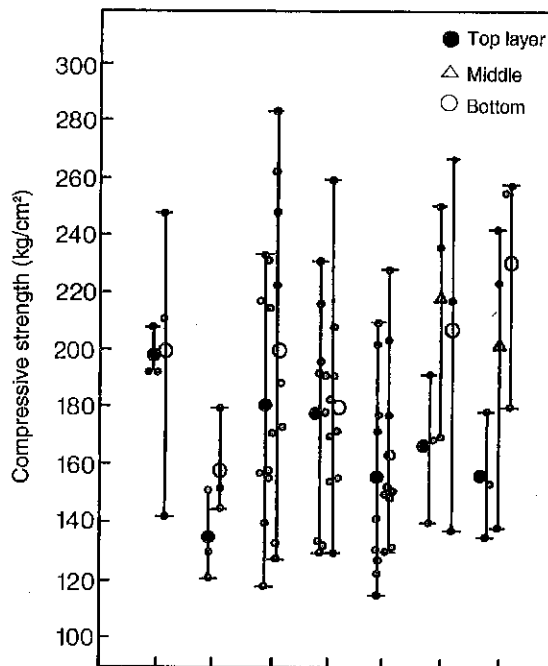


Lift (m)	0.75	0.75	1.0	1.0	1.0	1.25	1.5
Tested machine	OM	SD	OM	SD	SD	SD	SD
VC value	20	20	20	20	15	15	15

SD: SD450

OM: Other machine

Fig. 4-39 Core density/depth relationship



Lift (m)	0.75	0.75	1.0	1.0	1.0	1.25	1.5
Tested machine	OM	SD	OM	SD	SD	SD	SD
VC value	20	20	20	20	15	15	15

SD: SD450

OM: Other machine

Fig. 4-40 Compressive strength/depth relationship

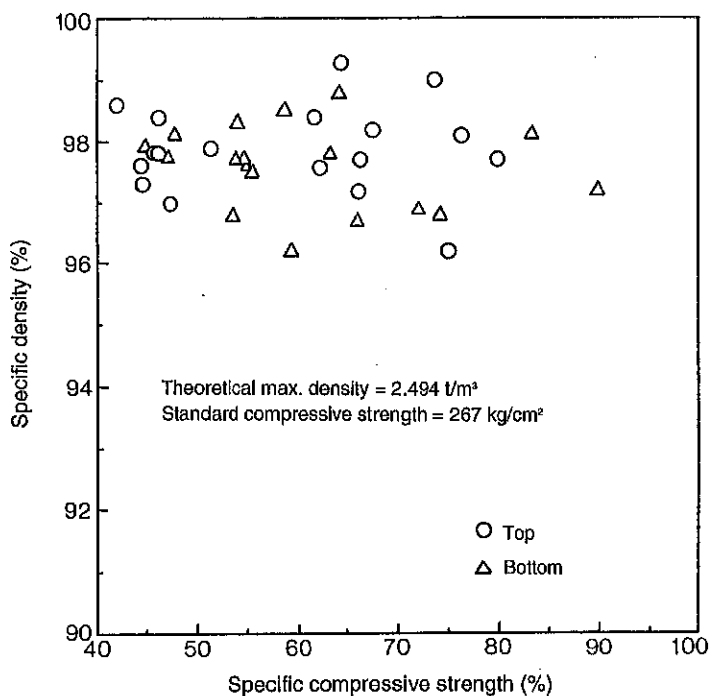


Fig. 4-41 Specific density/specific compressive strength relationship

4) Specific density and compacting energy

As can be seen from the above-mentioned results, the density values do not vary as widely as the compressive strength. Our experimental researches in the past 5 years confirmed that the correlations between the specific density and compacting energy are reliable as a performance evaluation factor.

Let us calculate key values by applying the formula described in the foregoing pages. Compacting energy E in each pass is expressed as:

$$E = 2a \left(Wv + \frac{1}{2} F \right) \frac{L}{V} n N \frac{1}{BL} Z \text{ (kg}\cdot\text{cm/cm}^2\text{)}$$

$$= 68.6 N \text{ (kg}\cdot\text{cm/cm}^2\text{)}$$

where, a = amplitude : 0.14 cm

W = axle load : 5,000 kg

F = Vibratory force : 23,000 kg

L = Contact length in rotating direction of vibratory drum

V = Rolling speed : 1,667 cm/min)

n = Vibratory frequency : 2,600 vpm

N = Number of passes

B = Rolling width (Vibratory drum width) : 210 cm

Z = Number of vibrating drums ($Z = 2$)

$E (N = 12) = 82.3 \text{ kg}\cdot\text{cm/cm}^2$

$E (N = 18) = 1234.8 \text{ kg}\cdot\text{cm/cm}^2$



Cold-paving in Chiba City

Relationships between the compacting energy and specific density with SD450 at different layer thickness are shown in Figs. 4-42a, 4-42b, 4-42c, 4-42d, 4-42e.

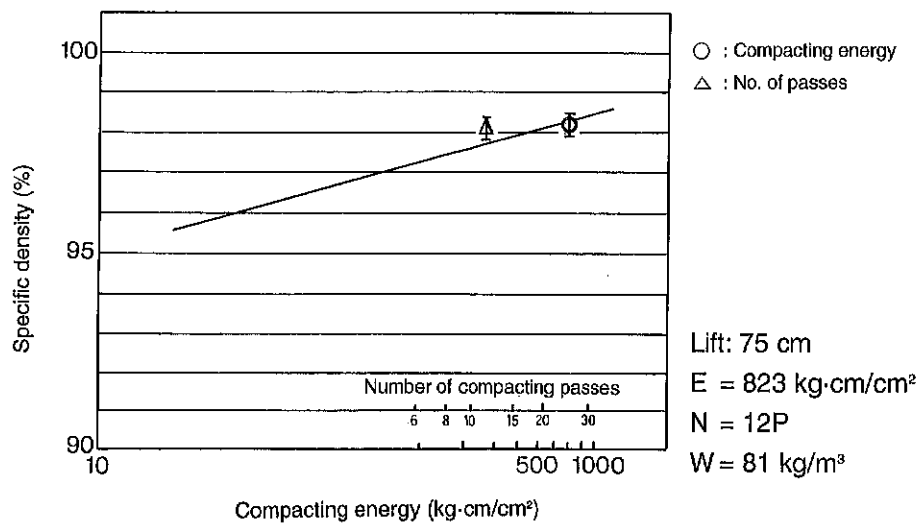


Fig. 4-42a Compacting energy/specific density relationship

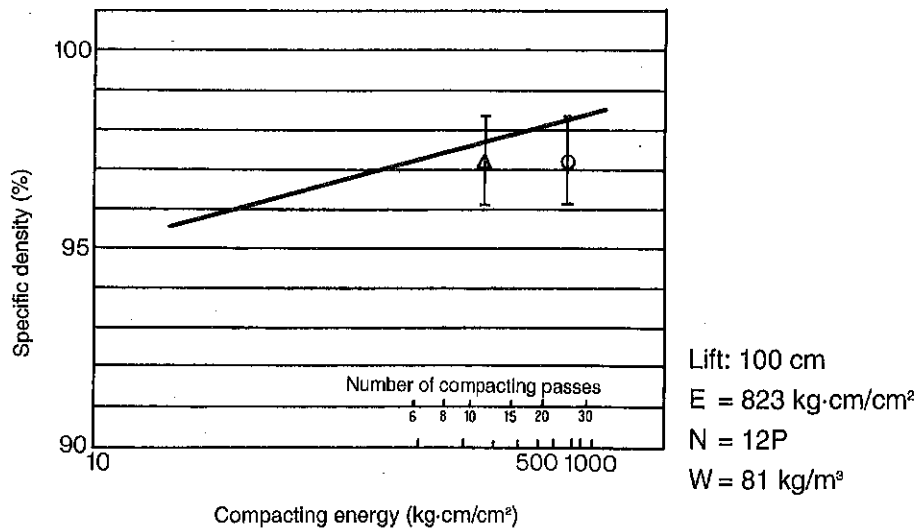


Fig. 4-42b Compacting energy/specific density relationship

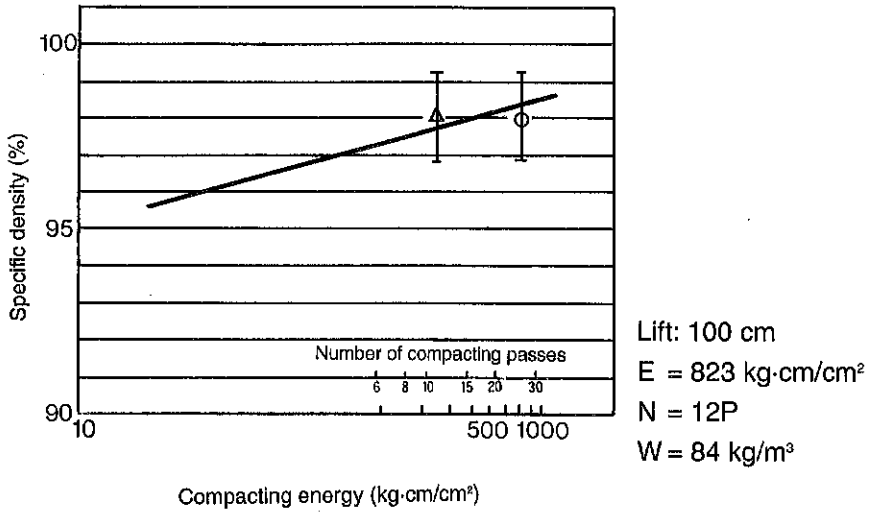


Fig. 4-42c Compacting energy/specific density relationship

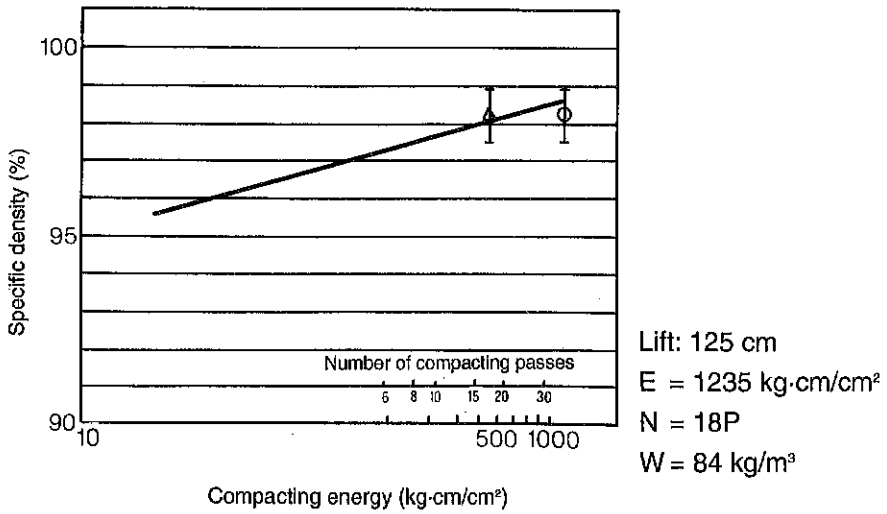


Fig. 4-42d Compacting energy/specific density relationship

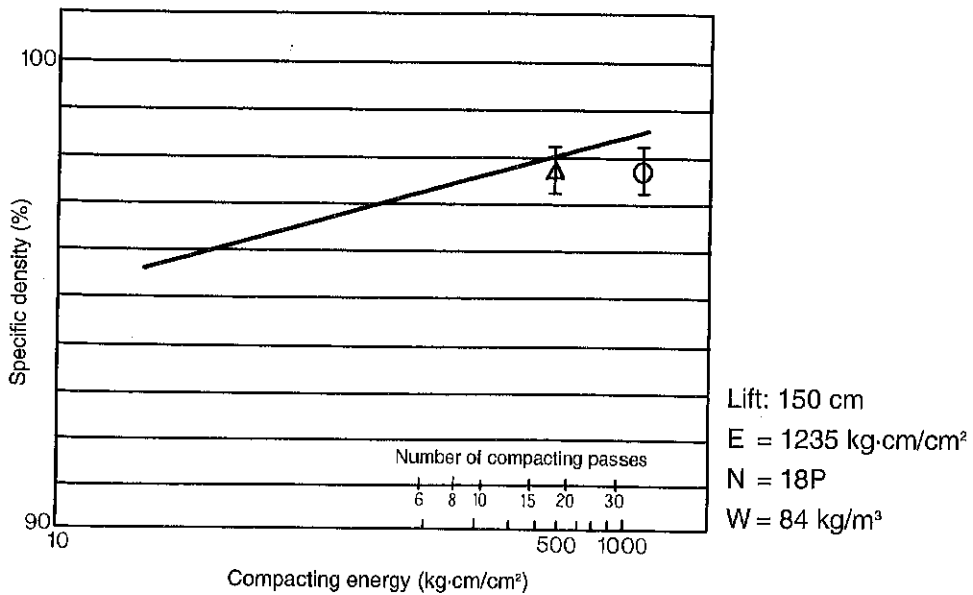


Fig. 4-42e Compacting energy/specific density relationship

5) Test result comparison with other models

Performance tests conducted with a view to comparing the SD450 with other same-class machines have revealed that, in general, SD450 maintains superiority over other rollers in respect to R-I density, core density and appearance evaluation. It has also come to light that the machine is capable of compacting roller-compacted concrete lifts about 100 cm thick, being quite within the bounds of possibility to compress thicker lifts upto 150 cm.

4. Development of a Roller for RCCP

Preceding pages have discussed the application of roller-compacted concrete to dam construction. Recently, this type of concrete has been finding its field in road building. Such pavement is referred to as "Roller-Compacted-Concrete Pavement", RCCP for short. In this method, a cement concrete of very low water content is spread, and compacted by road rollers. The concrete layer thus built is used as a surface layer or layers applied correspondingly.

This RCCP method aims at construction of quality pavements at low costs, making the most of excellent features existing in conventional cement concrete pavement structures.

RCCP dates back to 1941 when the U.S. engineer corps initiated it. After an interval of about 30 years, it came to be widely used in southern Europe centering around Spain. In Japan, the method was put to practical use in 1987.

(1) RCCP pavement

Completion of the development of the machine for RCD use accelerated the application of roller-compacted concrete to pavements. In the early period of the development, a conventional single-axis eccentric shaft mechanism was utilized. Later, however, a more excellent mode (dual-axis vertical vibratory mode) was adopted instead.

Working principle and basic mechanism of the new type vibrator unit were common to the RCD machine and the unit is built in the vibratory drum. This enabled the two models, conventional and new, to share the same drum module which is a key unit of the machines.

Following pages concern the vibratory output of conventional single-axis mode and that of the new dual-axis mode in terms of the vibratory acceleration and pressure in the roller-compacted concrete layers.

For single-axis mode and dual-axis mode, the SW750H and SW750V were submitted respectively to the tests.

Table 4-8

Item	SW750H (Conventional single-axis type)	SW750V (Dual-axis, vertical vibration type)
Gross weight	9,400 kg	9,150 kg
On front axle	4,520 kg	4,400 kg
On rear axle	4,880 kg	4,750 kg
Linear pressure		
Front drum	28.7 kg/cm	28.0 kg/cm
Rear drum	30.8 kg/cm	29.8 kg/cm
Vibratory force		
Low	6,000 kg	6,000 kg
High	10,000 kg	10,000 kg
Frequency	2,600 vpm	2,600 vpm
Overall length	4,220 mm	4,220 mm
Overall width	1,840 mm	1,840 mm
Wheelbase	3,000 mm	3,000 mm
Rolling width	1,680 mm	1,680 mm
Unsprung weight	2,230 kg	2,100 kg



Field test of permeable pavement
in a suburb of Niigata City



Vibrotless compaction operation with the
rotating roller in a residential area

As repeatedly discussed in the preceding pages, factors that constitute the vibratory output are not simple. However, the vibratory acceleration and pressure inside the layer being compacted act as factors that are easy to measure, and govern compaction results.

Figure 4-43 shows the relationships between the compaction pass and pressure inside the material being compressed. Both models demonstrate the same pressure effect for low and high vibratory forces, however, the pressure delivered to the material by V-type (vertical vibration) is about twice as high as that given by H-type (conventional vibration).

As these tests indicate, high pressure delivery is the outstanding feature of the new vertical vibratory mode.

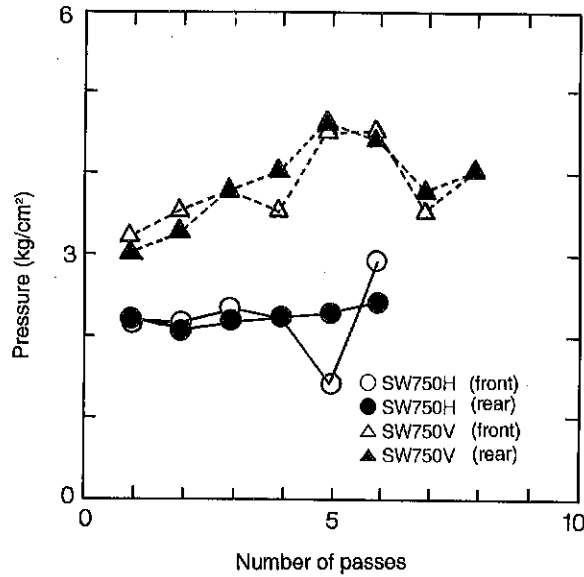


Fig. 4-43 Pressure/Compaction pass relationship

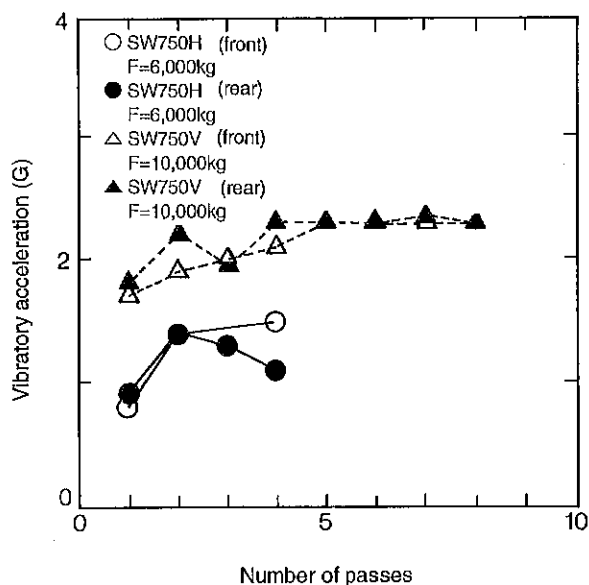


Fig. 4-44 Vibratory acceleration/compaction pass relationship

(2) Expanding the application field

Characterized by high pressure concentration features, the new vertical vibration mode has a high potential for application to a variety of newly-developed high-quality special paving mixtures that are hard to compact, or to diverse recycled materials. Today, new trials are in progress to advance into new field of application. On completion of analysis and evaluation of these test results, in-depth information will be made available.

V. NUTATING ROLLER (HORIZONTAL VIBRATING ROLLER)

1. Background of the Development

In some period after World War II when research and development of vibrating rollers were in high gear in Europe, we also started basic research on soil compaction mechanisms. Through the research, we were concerned with the fact that an application of a shearing stress to a soil specimen while simultaneously exerting a compressing stress greatly accelerates the consolidation of the soil, and that the optimum condition would exist in the ratio of intensity between the two stresses.

On the other hand, in the laboratory of professor Brown and other investigators at Nottingham University, they had been forwarding analysis of the same theme. They presented the results of their research to an international conference in Pais in 1978. The main points of the research are:

- ① **Both-direction shearing stresses given to a test material consisting of aggregates of uniform grain size with a simple shear test machine brought a substantial increase in compacting effects.**
- ② **If compacted with a vibratory roller, application of horizontal vibration coupled with vertical oscillation will prove more effective.**

Figure 5-1 illustrates the simple shear test principle.

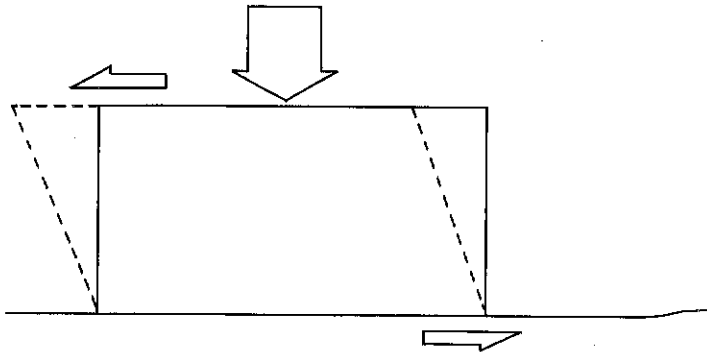


Fig. 5-1 Simple shear testing principle

Refer to the right-hand side drum in Fig. 3-5. The self-propelled drum is driven by a drive torque, $M = U \cdot R$. The compacting pressure just under the drum can be

divided into 3 vectors; vertical stress, horizontal stress and vertical/horizontal shearing stress. The vertical stress is created by gravitational reaction Q . The horizontal stress is generated by reaction R_x of the drive torque. These factors bring a shearing stress that is the main factor greatly contributing to compaction effects. These effective stresses, however, act on the ground only 2 times in 2 passes (forward and reverse) of the drum. This requires many rolling passes to achieve satisfactory results.

Figure 5-2 represents relations between shearing load frequency and permanent strain revealed by tests made by Dr. Prof. Brown and other investigators mentioned above.

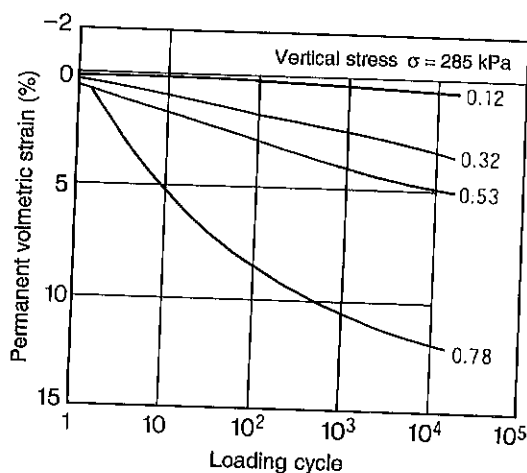


Fig. 5-2 Shearing load cycle/permanent strain relationship

With the curve for a parameter of 0.78 in this figure, the permanent strain, or the settlement due to consolidation, reaches 12% with the shearing load applied 10^4 times. If taken simple, this will require 10,000 compaction passes for a static roller. A horizontal vibration mode vibrating roller is supposed to accomplish this in a few minutes.

With these excellent characteristics taken into account, a vibrating roller (nutating roller) with an entirely new, horizontal vibration mode has come into being.

2. Principle of Nutating Motion

Authoritative dictionaries define “Nutation” as a phenomenon that the axis around which the earth spins changes its direction at a relatively short period.

Hold a bar vertically with one hand supporting the middle portion of the bar. Let the top of the bar make a circular motion with the other hand. Then, its bottom end will also draw a circle. Combinations of the holding point and the top motion will create a variety of movements on the bottom end.

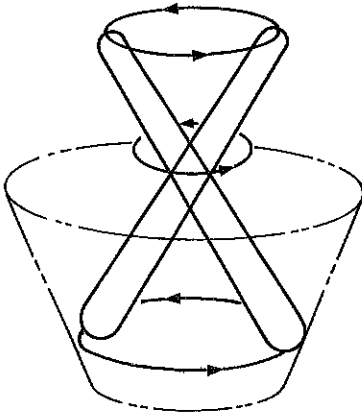


Fig. 5-3 Nutating motion

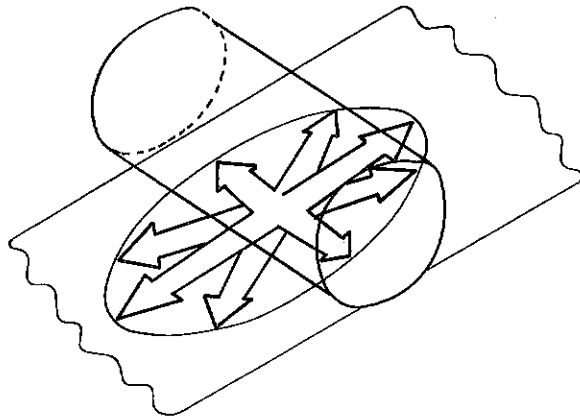


Fig. 5-4 Nutating motion with a drum

A drum of a vibrating roller with this new mode incorporated exerts forces on the ground as shown in Fig. 5-4 in the form of an oval that is long in forward-backward directions. Compared with a vibratory pattern in forward-backward directions only or that in sidewise directions alone, this new combined direction mode gives better compaction results.

Such a multi-direction motion in a horizontal plane is referred to as Nutating Motion. The roller that applies this principle is called a Nutating Roller as another name.

A nutating roller has a mechanism that mechanically generates combined motions as described above, delivering them cyclically to the vibratory drums.

Figure 5-4a illustrates propagation of horizontal vibration combined with normal static pressure with other factors omitted for simplified consideration.

Figure 5-4b shows cyclically applied horizontal forces in drum rolling directions alone (cyclic torque vibration).

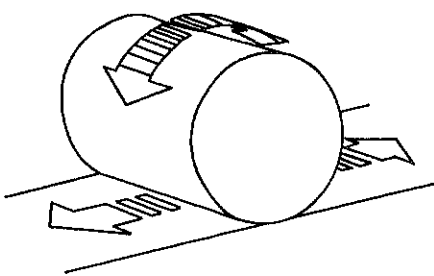
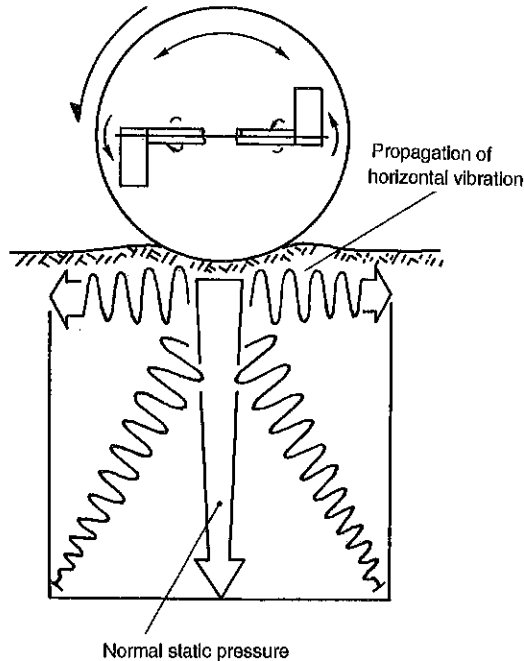


Fig. 5-6 Cyclically applied horizontal force (Forces in longitudinal direction only are shown)

Fig. 5-5 Propagation of horizontal vibration and normal static pressure

3. Characteristics of Nutating Roller

Figure 5-7 shows the soil pressure created immediately under the drum passing point. When the drum is approaching the point, the pressure fluctuates due to the vertical component of the horizontal vibration, however, when it comes to the point there is no more pressure wave, but only the static pressure remains due to the static weight of the drum axis.

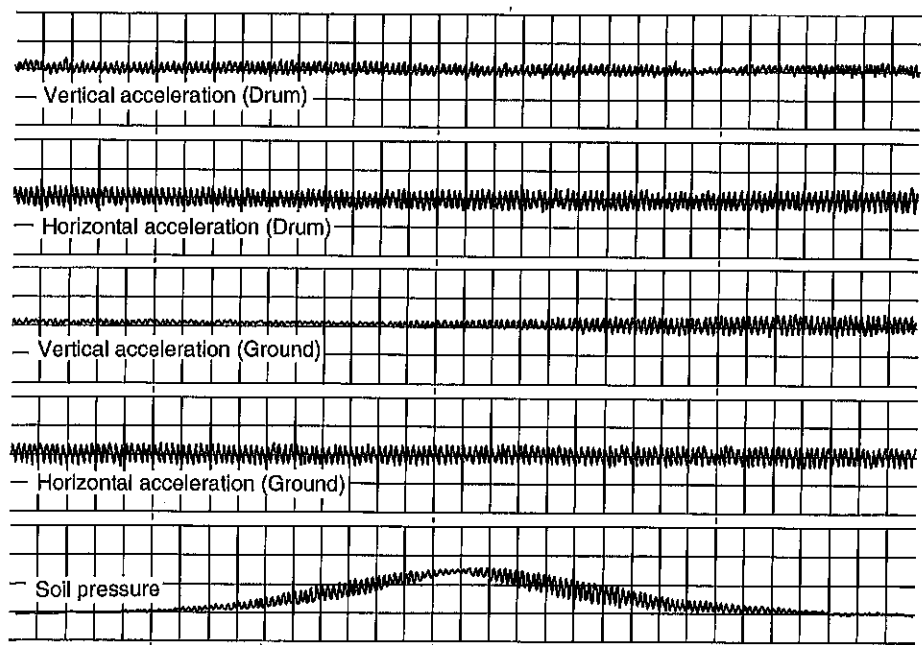


Fig. 5-7 Soil pressure created just under drum passing point

Based upon the test data, let us compare the performances of the nutating roller with conventional mode rollers.

The first performance tests on the nutating roller date back to April of 1984 when we conducted a series of experiments on a prototype small-sized machine under joint research with the Laboratory of Science and Engineering in Waseda University. Based on the data obtained from these tests, model SW60N was built on a trial basis in September of 1985. On October of the same year, a series of tests were made at the Construction Machinery Research Laboratory. A variety of experiments followed; Tests at the Sakai test ground in April of 1986, tests at the Construction Machinery Research Laboratory in May of the same year and tests at the Sakai Laboratory in a period from January to July of 1987. Our customers, Kajima Doro, Fukuda Doro and Kinki Kensetsu also conducted a variety of tests independently.

Measurements were taken on various items in the tests mentioned above. Of them, ground vibration, propelling power, surface finish grade and degree of compaction shall be taken up here for discussion. Many reports rate the machine highly for a low ground vibration nature. Here are some reports that evaluate the machine on a numerical basis.

① **Performance test report on a model SW60N in April, 1986**
(No. of 0210-00119)

Compared with a conventional vibrating roller, the vibration level in a up-and-down and right-and-left directions on the ground on the right-hand side of the nutating roller's drum is lower by 15 ~ 20 dB. A maximum difference of about 30 dB in up-and-down vibration level is noticeable at a point on the ground 1 m away from the drum's right end (Fig. 5-8).

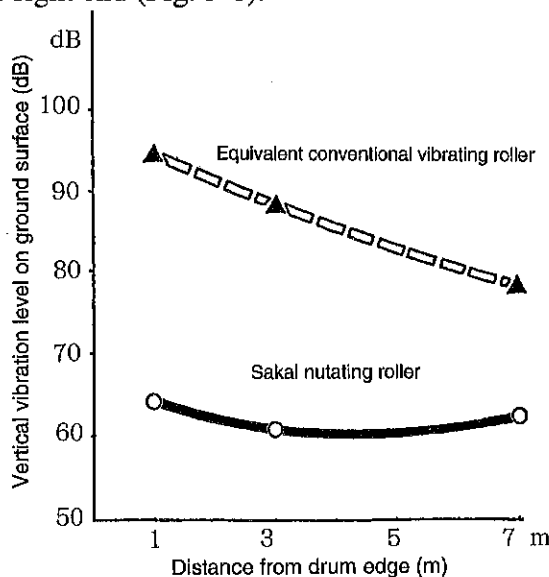


Fig. 5-8 Comparison of vibration propagation on ground surface

② **Data from an asphalt mix compaction test, conducted at the test course at Sakai Technical Laboratory in March, 1987**

Measuring equipment was set close to the drum. One of the measurements indicated a difference of 15.4 dB in an up-and-down vibration level between the conventional type (SW60) and the nutating type (SW60N), as shown in the table below:

Table 5-1 Vertical vibration level comparison

Machine	Vertical vibration level on ground surface with 8 passes
SW60 (Conventional vibration)	100 dB
SW60N (Horizontal vibration)	84.6 dB

③ **Data from a performance test made at Kinki Construction Company in July, 1990**

In this test, vertical vibration levels were measured at a spot 2 m away from the center of each machine. Table 5-2 shows the results.

For subbase material compaction, 430N (horizontal vibrating roller) is less noisy by 9 dB than SW70 (conventional vibrating roller).

For asphalt mix compaction, the vibrating level of 430N is lower by 8 to 12 dB when compared with TW70H (combined roller).

Table 5-2 Ground vibration comparison

Subbase material			Asphalt mix		
Machine Pass	430N (Vertical vibrating)	SW70 (Tandem vibrating)	Machine Pass	430N (Vertical vibrating)	TW70H (Combined)
P8	80 dB	80 dB	P3	81 dB	93 dB
P12	80.5 dB	89.5 dB	P4	82 dB	94 dB
P16	79 dB	87.5 dB	P5	84 dB	92 dB
			P6	84 dB	92 dB

④ **Others**

With numerical data not given, a report dated January of 1987 presented by Nihon Hodo Co., or articles carried on technical magazines claim that the nutating roller effectively lowers the noise level.

Actually, the machine has gained recognition from contractors as a roller characterizing low noise level, since almost no vibrations are felt even in the proximity of the work sites.

In addition, the Technical Guide for Roller-compacted Concrete Pavement and the latest revised edition of the Manual for Asphalt Pavement have added the horizontal vibrating type to a series of recommendable machines for pavement building because of its low noise feature.

4. Power Consumption to Drive Vibrator

The direct measurement of the power required to drive the vibrator shaft is not yet realized, however, a reasonable assumption can be made by measuring the hydraulic pressure in the vibrator drive motor. The measurement of the pressure in question was taken in tests at Sakai's Technical Laboratory in 1986 and 1987. The test results showed that the hydraulic pressure in the horizontal vibrating type increases to a lesser degree with increasing vibrating frequency when compared with the conventional vibrating mode. This indicates that under normal conditions, the power consumption to drive the vibrator is lower with the horizontal vibrating roller. In other words, the horizontal vibrating roller is an energy saving machine.

Figure 5-9 represents the relationships between the hydraulic pressure in the motor and engine RPM. Figure 5-10 is a schematic diagram presentation of the power consumption comparison.

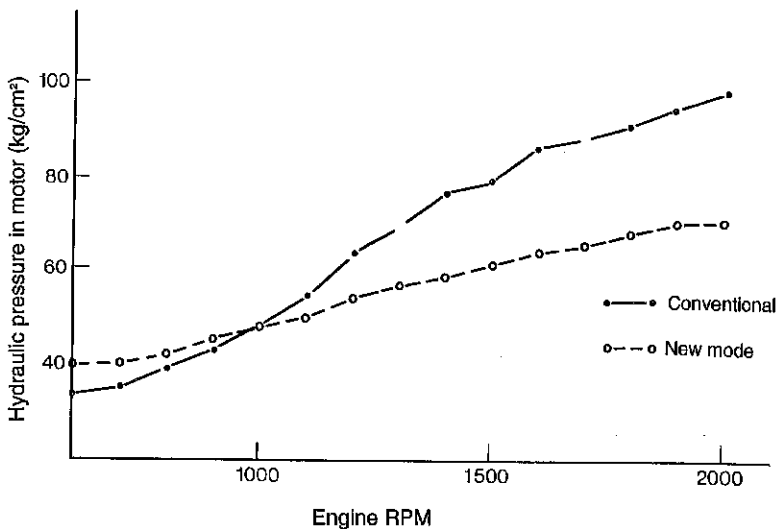


Fig. 5-9 Motor pressure/engine RPM relationship

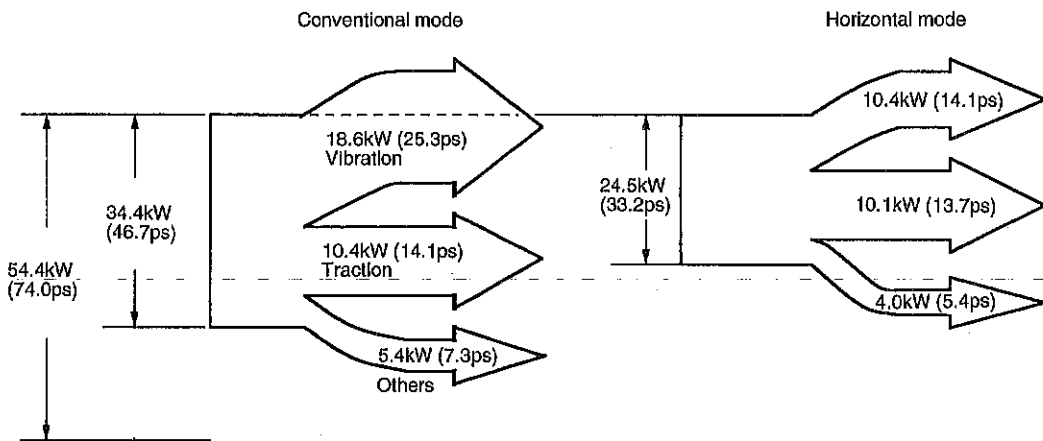


Fig. 5-10 Power consumption comparison

As shown in Fig. 5-10, the power consumption of the new mode roller stands at 24.5 kW (33.2 PS), lower than the 34.5 kW (46.7 PS) of a conventional type. Most of this power saving is attributable to a reduction of power needed to generate vibration. This extra energy consumed by the conventional mode is lost as useless energy, presents noise problems, and spoils riding comfort with unpleasant vibrations transmitted to the operator's station.

5. Experimental Comparison Between Compaction Effects

Discussion needs to concentrate on the problem of practical compaction effects offered by the new mode as compared with the conventional mode. What more can be done to the conventional vibrating roller? Most of the manufacturers, and users also, feel that the vibrating roller in the conventional mode is already the optimum in design, with little scope left for further development.

On the contrary, much potential is expected for applications of the horizontal vibration roller.

Studies have been conducted at Sakai's laboratory on the correlation between the magnitude of cyclic torque applied at the ground contact area and the normal static linear pressure. As of today, we have grasped various peculiarities that the new mode has. The horizontal vibration roller shows a variety of characteristics different from those of the conventional model.

Figures 5-11a and 5-11b show differences in compacting effect between the conventional mode roller with a prototype drum unit and additional ballast weights and the new mode machine. On the whole, the degree of compaction is higher than the conventional mode. In the asphalt compaction test, the degree of compaction reaches approx. 96% at about four passes.

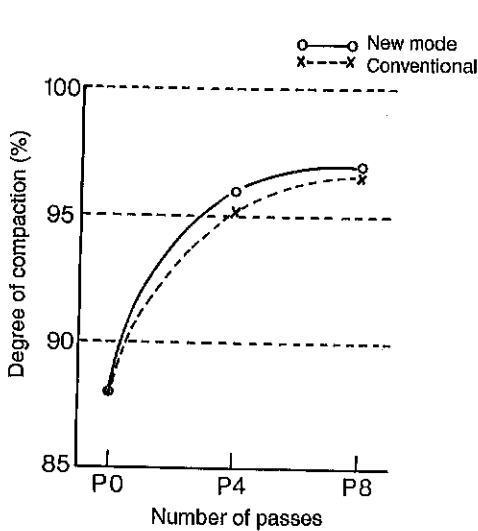


Fig. 5-11a Relationship between degree of compaction and number of passes (Asphalt mix)

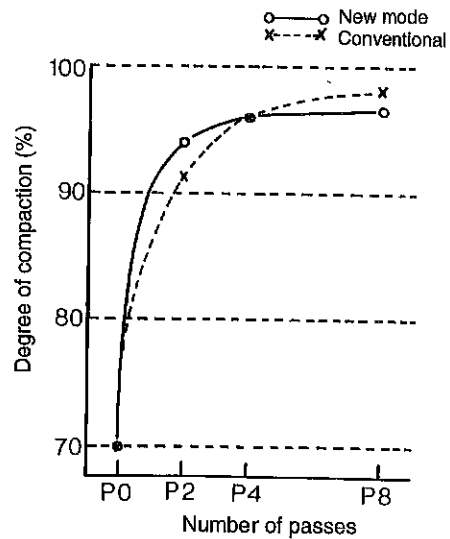


Fig. 5-11b Relationship between degree of compaction and number of passes (Soil)

6. Field Tests to Determine Compacting Effects

The following pages describe test results on the new mode roller used for subbase course compaction (By courtesy of Kinki Construction Company).

(1) Weight and travel speed of test machines

Table 5-3 Vehicle weight and travel speed

Weight and speed Type of roller	Weight (kg)	High speed* (km/h)	Low speed* (km/h)
Pneumatic	12,760	7.3	4.0
3-Wheel	10,380	5.5	3.0
Combined	3,600	5.7	2.8
4-ton combined	6,200	6.0	2.8
4-ton horizontal vibrating	6,880	6.2	2.8
7-ton tandem drum vibrating	7,860	5.2	2.9
Walk-behind	920	3.1	1.8

*: Measured values

(2) Settlement rate and number of passes

For a reasonable comparison between rollers, each roller's compacting characteristics were analyzed, with the surface settlement converted into a settlement rate.

$$\text{Settlement rate} = \frac{\text{Settlement } \Delta \ell \text{ (mm)}}{\text{Spreading lift } \ell \text{ (mm)}} \times 100 (\%)$$

where, **Settlement $\Delta \ell$ (mm)** = (Standard height after spreading) – (Standard height after compaction)

Spreading lift ℓ (mm) = (Standard height after spreading) – (Standard height of subgrade)

Little unevenness in density in the precompaction stage was noticeable thanks to the use of a base paver for mix spreading.

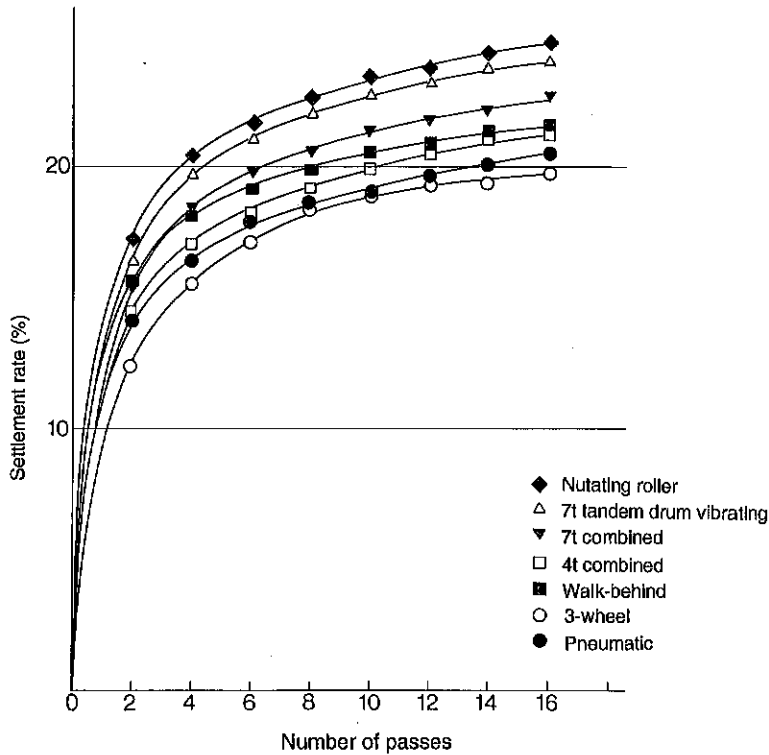


Fig. 5-12 Relationship between number of passes and settlement rate

(3) Degree of compaction

The degree of compaction measured on the first day when the test material was delivered to the test site was designated the standard value, because laboratory compaction tests revealed that with the test material there were no noticeable changes in quality.

Standard value: $d_{\max} = 2.215 \text{ g/cm}^3$ $\omega_{\text{opt}} = 5.85\%$

where, d_{\max} = Max. dry density

ω_{opt} = Optimum moisture content

Figure 5-16 represents the relationship between number of passes and degree of compaction for each roller with values obtained using the RI (Radio-isotopic) density measurement method.

Like the settlement measure, values of degree of compaction were averaged for high and low speeds.

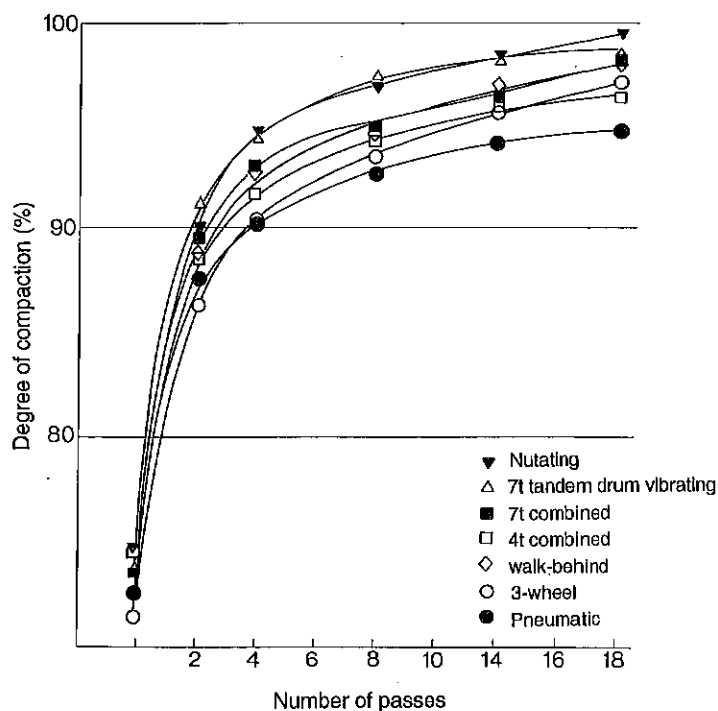


Fig. 5-13 Relationship between number of passes and degree of compaction

(4) Compaction characteristics

As shown in Fig. 5-13, vibrating rollers offer a high degree of compaction. Particularly the 7-ton tandem vibrating and horizontal vibrating rollers are excellent. The same tendency can be noted in the settlement ratio characteristics as shown in Fig. 5-12.

Concerning the compaction characteristics of the 7-ton and horizontal vibrating rollers, Fig. 5-13 confirms that:

With the nutating roller, the degree of compaction increases in approximate proportion to the number of passes after 6 passes. In the 7-ton tandem, however, its curve tends to become flat after 10 passes. Very little increase is noticeable between 12 and 16 passes with the degree of compaction registering 98.2% and 98.5% for 12 passes and 16 passes respectively.

The main reason for this tendency is thought to be that:

With the 7-ton tandem, rise of material left behind the passing roller is higher

than with other machines. Furthermore, the surface tends to become loose due to the presence of small stone particles that come to float due to vibration.

This trend is low with the new mode machine thanks to vibrations acting in circumferential directions.

7. Summation of Features

The nutating roller is quite different from the conventional mode. The latter utilizes vertical component vibrating forces, and has a history more than half a century ranging from the inchoate stage of research to the highly-developed step today at which numerous quality machines have been put into practical use.

In the previous pages, we have described experimental analysis of cyclically applied shearing stress and field test results to clarify the influence of this new vibratory mode on materials being compressed.

The unique characteristics of the roller using this new mode has gradually come to gain recognition from construction quarters.

The new mode roller is now at a historical stage at which a variety of trial have been made with the advancement of research and development of compaction materials as given below:

- ① **Emulsified composite material for cement and asphalt, slug basecourse material, etc.**
- ② **Stability treatment material for soil, recycled mix such as loam fluidization treatment soil, etc.**
- ③ **Fiber reinforcement material, natural material, mixture containing large-sized aggregates, etc.**
- ④ **Permeable mixture, ambient temperature mixture, etc.**

Such being the case, we are now not in a position to introduce more field test examples. However, extensive analyses based on a variety of experiments made in the past make us establish a summation on the new mode as described below:

- ① **Operator and working environment are protected from irritating noise and vibration.**
- ② **Most of the vibratory energies turn into an effective and useful compacting energy.**
- ③ **The horizontal vibration eliminates the risk of crushing brittle materials.**
- ④ **The pore water pressure in the soil is not surged up.**

VI. AUTOMATIC CONTROL FOR COMPACTION PROCESSES

1. Evaluation of Compaction Operation

In construction of structures, such as roadways, compaction aims at improving, using the mechanical consolidation processes, freshly spread materials to reinforced materials that satisfy specifications.

The processes to gain target results should be under pertinent and economical control. For qualitative and quantitative enforcement of the control, evaluation of work results must be as objective as practical.

For detailed evaluation methods, refer to relevant technical books available.

For evaluation indexes, however, the dry density, specific density, compressive strength, CBR and K-values, etc. have been used as key factors in the previous chapters to discuss characteristics of compacting equipment.

The management cycle loop closes through processes as given below:

Compaction work ⇒ Work results ⇒ Measurement and testing ⇒ Evaluation ⇒ Study ⇒ Setting of optimum machine condition ⇒ Machine adjustment and selection ⇒ Compaction work ⇒ Work results ⇒ Measurement and testing ⇒ Evaluation ⇒ Study ⇒ Return to the first item, "Compaction work".

This cycle includes appreciable discontinuances of processes and requires subjective and objective judgement based on accumulated experimental results and rules of thumb.

Hereupon, we naturally come to an idea of automated control which realizes instant completion of a loop made up of non-destructive, real time measurements on the spot, its evaluation and feedback of the information to give the optimum maneuver of the relevant machine.

Machines that bear the possibility to realize this automated control will be vibrating rollers utilizing an electro-hydro-dynamic system to drive their auxiliary equipment.

2. Compaction Meter

For real time measurement and evaluation of compaction results on the job site without the need to disturb the ground for specimen excavation, equipment called "Compaction Meter" (Geodynamik AB) is available which has been put to practical use under some limited conditions of use.

In an early stage of a compaction process, vibration given by a vibrating roller will form regular sinusoidal curves. As compaction proceeds, reactions from the

ground will change, distorting the regular sinusoidal curves to convert to random vibration.

The compaction meter picks up this change as a change in displacement and acceleration of the vibrating roller.

Figure 6-1 is an example of its application to a standard vibrating roller. With an assumption that the vibratory drum frame (the unsprung portion) shares vibratory behavior with the ground, a vertical acceleration sensor is mounted there to indicate real time values on gages. The CDS (Compaction Documentation System) is a system that displays on a monitor the vibration waves picked up at every spot on the ground while the roller is rolling.

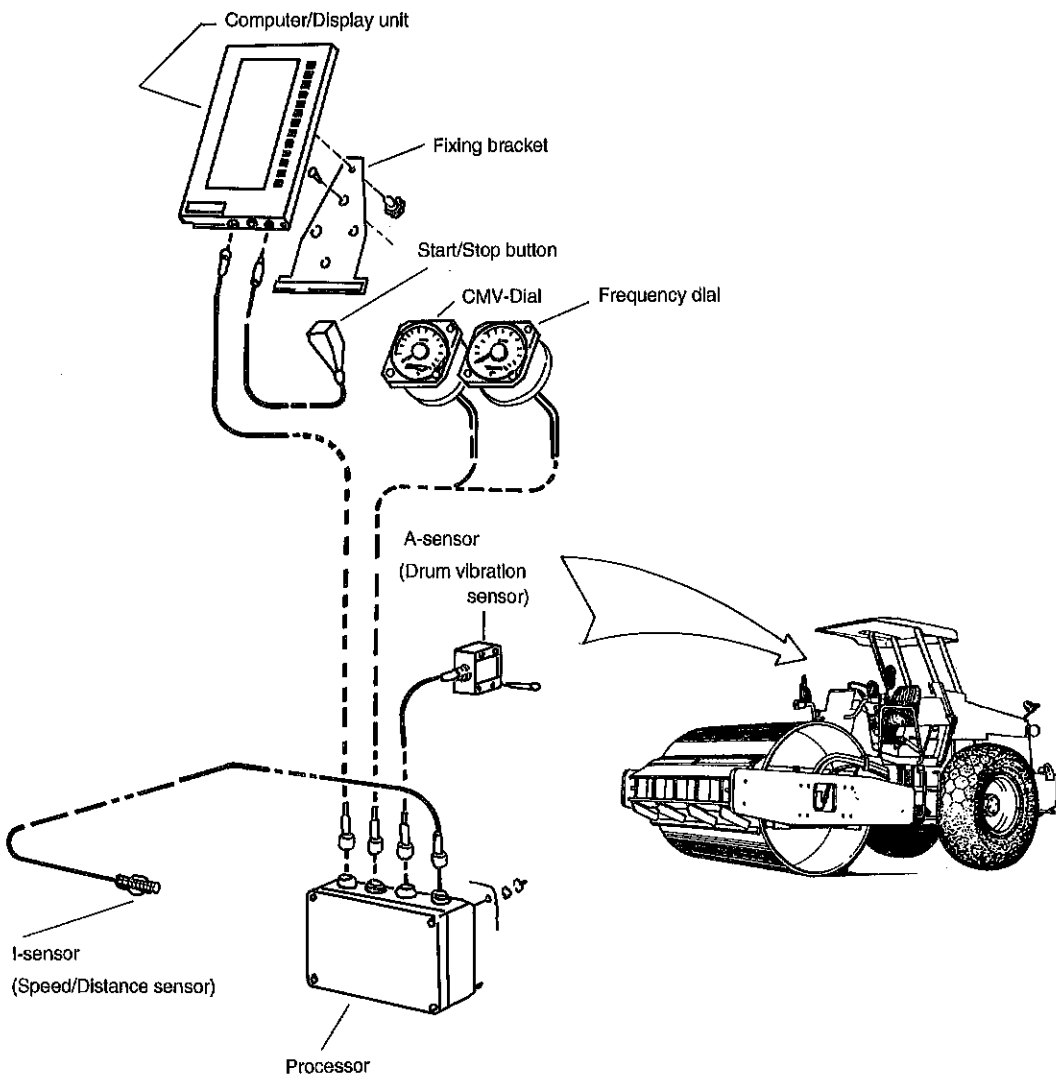


Fig. 6-1 Compaction documentation system (CDS)

Figure 6-2 is another example based on a similar principle. In this system, field-obtained data are inputted into a memory card, and then the data card is carried to the execution management post for analysis.

Figure 6-3 illustrates a system that graphically processes input data from 2-dimension figures to 3-dimension ones.

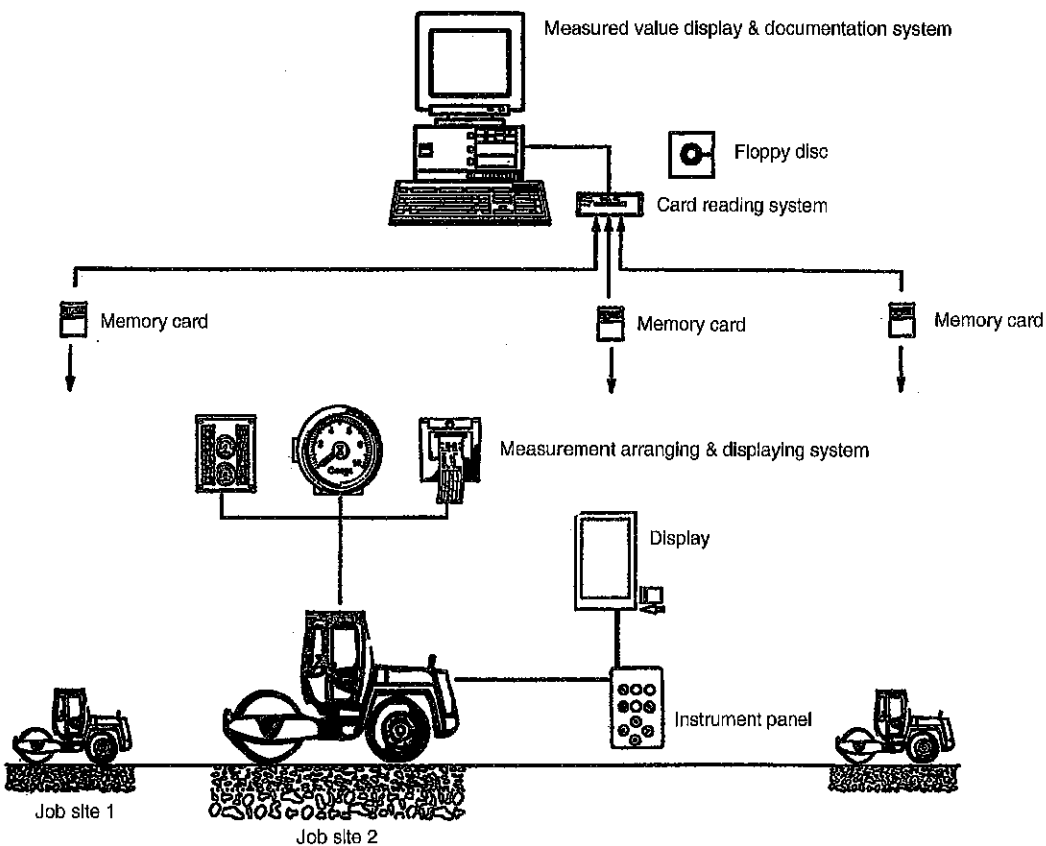


Fig. 6-2 Field data recording system

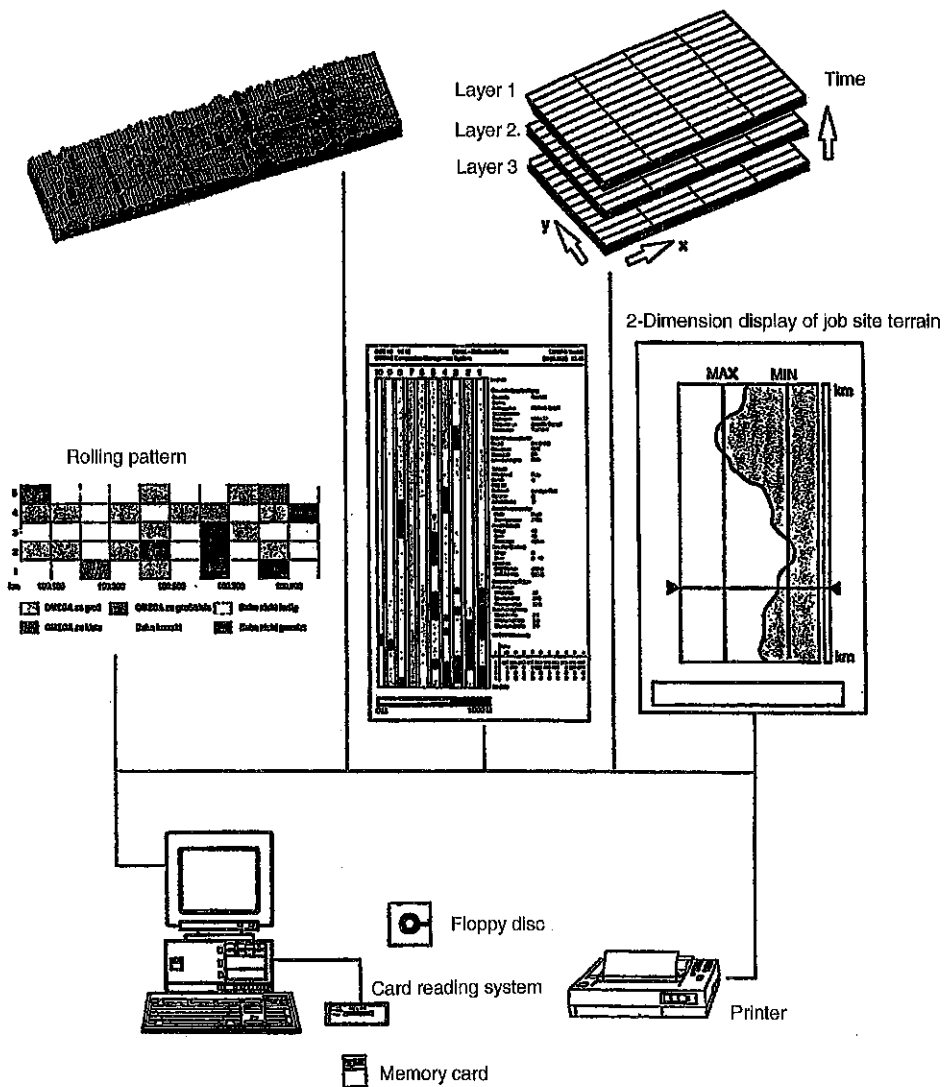


Fig. 6-3 2-dimension to 3-dimension graphic system

3. Compaction Simulation

It is not practical to evaluate compaction processes and compaction effects in such a manner that tests are conducted first then the results are feedback to the machine to meet work specifications. Such a method needs arduous work to analyze a variety of parameters. An ideal means to cope with this problem will be automated control of compaction operations. Simulation of compaction with the use of computers is now on its way to development.

Concerning this subject, professor Wolfgang Poppy and other investigators in Berlin Technical College introduced, in ISTVS magazine (November, 1992), two

calculation models to express the correlation between a roller in motion and a soil being compacted by the roller:

- ① **A roller analysis model: A model dealing with physical numerical values such as vibratory frequency and amplitude that are factors governing vibratory compaction.**
- ② **A mathematical model to express characteristics of soil: A mathematical model that deals with such factors as density, elasto-plasticity and damping coefficients of soil.**

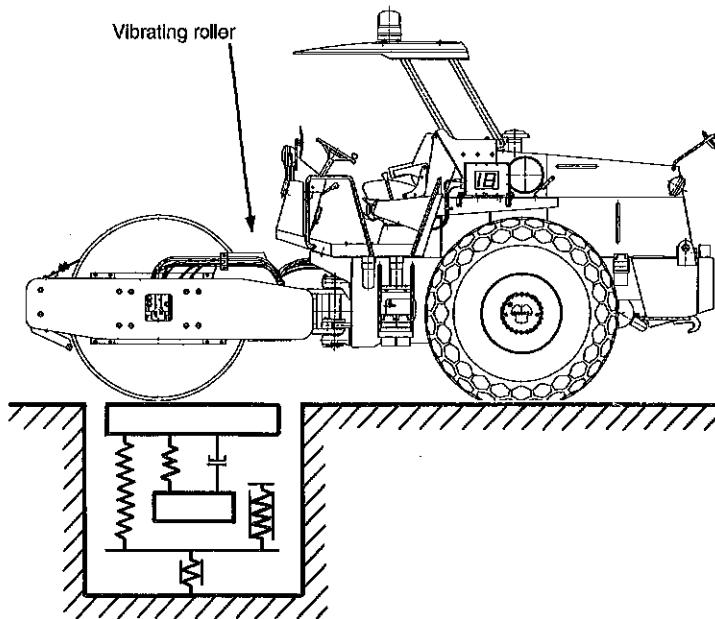


Fig. 6-4 Diagraming of vibratory compaction

In defining these mathematical models, they distinguished between a roller jumping condition and a condition of ground contact in a like manner as the analysis for the relationship between elastic deformation and non-elastic deformation of the ground, since roller motion and ground deformation are in a linear correlation. In addition, they (investigators) developed a calculation system by definitely fixing the range (mass) that is under the influence of roller vibrations.

The vibrating roller and soil are expressed in a closed-loop circuit. Therefore the response of each system cannot be discussed separately.

This report concludes that the simulation results verify that the mathematical model dealing with a roller/soil system is capable of mathematically determining

the relationship between vibratory behavior and compaction effects.

This is considered to suggest the possibility to calculate, with the use of a computer, the feedback circuit that optimizes parameters of roller structure and job condition. However, it is impossible to directly indicate the density of the material being rolled without compaction trials to determine the correlation between the density of the material and actual gage readings. To know this relationship, huge amounts of field data and their analyses will be required.

4. Automated Control of Compaction Process

In the foregoing pages in this chapter, the existing circumstances of automatic control of the compaction process have been discussed from the standpoint of software development. Many investigations for the automated control are left as future problems. On the other hand, in the respect of hardware, difficult problems do not exist to draw the optimum conditions from the data summarized on a real time basis during the compaction operation.

The realization of the automated control is limited to the use of a vibrating roller having variable factors related to vibration.

Variable factors possible are vibratory frequency and amplitude. Some machines with a definitely variable mechanism already exist. However, automated control needs an infinitely variable system.

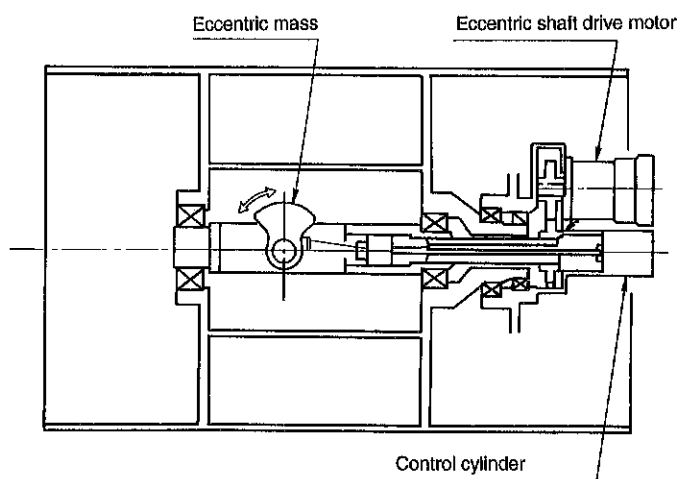


Fig. 6-5 Sakai variable amplitude mechanism

VII. INDUCTIVE ESTIMATE OF COMPACTION RESULTS

As a compacting equipment manufacturer, Sakai has consistently been occupied with the development and manufacture of compacting equipment since its foundation in 1918. Various types of machines have come into development particularly after the year 1950. In the course of these developing periods, Sakai has accumulated extensive experiment-based technical data.

Utilizing much of these data and those of other manufacturers, trials have been made to establish successful inductive formulae to estimate compaction results.

Based upon experiment results from 28 models of vibrating rollers as a data base, mechanical specifications having higher correlations with compacting performance were selected. Then, with both recurrent and non-recurrent methods employed, recurrent analysis results were obtained for density and maximum CBR values corresponding to dynamic and static linear pressure, compactive energy and rolling passes. The compaction pass/density formulae are to be applied to general vibrating rollers of large and small size. Needless to say, estimated values from these formulae are deductively not associated with the mechanical specifications. However, they are useful in that these measurements make estimate possible with some deviations admitted.

1. Prediction Formulas of Dry Density (for General Vibrating Rollers)

(1) Basic formula

This equation applies to general vibrating rollers with linear pressures:

Dynamic linear pressure: 15 to 18 kg/cm

Static linear pressure: 5 to 32 kg/cm

Total linear pressure: 15 to 105 kg/cm

$$D_n = D_{\max} \frac{n}{A + Bn} + D_0 \dots\dots\dots(1)$$

where, **D_n**: The soil density after n times of compaction passes by tested rollers (g/cm³)

D_{max}: Maximum dry density of the soil from test JISA-1200 (g/cm³)

D₀: The minimum value of the soil density after preparation compaction passes (g/cm³)

n: Number of compaction passes by tested roller;

A: Regression coefficient which can be calculated from formulas shown later

B: Regression coefficient which can be calculated from formulas shown later.

(2) Basic coefficient formulas

$$\bar{A} = 2.82205 - 0.013997 \frac{F + Wv}{Bw} \dots\dots\dots(2)$$

$$\text{when, } \frac{F + Wv}{Bw} \leq 83.5$$

or

$$\bar{A} = 11.33096 - 0.236157 \frac{F + Wv}{Bw} + 0.00143968 \left(\frac{F + Wv}{Bw} \right)^2 \dots\dots\dots(3)$$

$$\text{when, } \frac{F + Wv}{Bw} > 83.5$$

$$\bar{B} = 3.57 - 0.53407E^{1.21768} \times 10^{-4} \dots\dots\dots(4)$$

where **F:** Centrifugal force (kg)
Wv: Axle weight of vibrating drum (kg)
Bw: Width of vibrating drum (cm)
E: Compaction energy of the roller (kg·cm)

$$E = 2a \left(\frac{F}{2} + Wv \right) \dots\dots\dots(5)$$

where **a:** Amplitude of vibration (half) (cm)

(3) Modified coefficient formulas

$$A = \xi_a \bar{A} \dots\dots\dots(6)$$

$$B = \xi_b \bar{B} \dots\dots\dots(7)$$

- where \bar{A}, \bar{B} : Basic coefficients which can be calculated from eqns. (2), (3) and (4),
 A, B : Modified coefficients which can be used in basic prediction formula,
 $\xi a, \xi b$: modified coefficients for different number of vibrating drums.

$$\xi a = 1 \text{ and } \xi b = 1.0 \text{(8)}$$

for single vibratory drum.

$$\xi a = 0.5 \text{ and } \xi b = 1.0 \text{(9)}$$

for dual vibratory drums.

2. Prediction Formulas of Dry Density (for Small-sized Rollers under 2 tons)

(1) Basic formula

$$D_n = D_{max} \frac{n}{A + Bn} + D_o \text{(10)}$$

See formula (1) for D_n , D_{max} , n , A , Bn and D_o .

(2) Basic coefficient formulas

$$\bar{A} = \alpha_a \frac{F+W_v}{Bw} + \beta_a \left(\frac{F+W_v}{Bw} \right)^2 + \gamma_a \left(\frac{F+W_v}{Bw} \right)^3 \text{(11)}$$

$$\bar{B} = \frac{F+W_v}{Bw} (\alpha_b + \beta_b \left(\frac{F+W_v}{Bw} \right) + \gamma_b \left(\frac{F+W_v}{Bw} \right)^2)^{-1} \text{(12)}$$

- where F : Centrifugal force (kg),
 W_v : Axle weight of vibrating drum (kg),
 Bw : Width of vibrating drum (cm),
 $\alpha_a = 0.128 \times 10$
 $\beta_a = -0.882 \times 10^{-1}$
 $\gamma_a = 0.169 \times 10^{-2}$
 $\alpha_b = -0.121 \times 10^2$
 $\beta_b = 1.477$
 $\gamma_b = -0.029$

(3) Modified coefficient formulas

$$A = \xi_a A \dots\dots\dots(13)$$

$$B = \xi_b B \dots\dots\dots(14)$$

where, **A, B:** Basic coefficients which can be calculated from eqns. (11) and (12),

A, B: Modified coefficients which can be used in basic prediction formula

ξ_a, ξ_b : Modified coefficients for different number of vibrating drums:

$$\xi_a = 1 \text{ and } \xi_b = 1 \dots\dots\dots(15)$$

for single vibratory drum.

$$\xi_a = 0.536 \text{ and } \xi_b = 1.383 \dots\dots\dots(16)$$

for dual vibratory drums.

3. Prediction Formulas of CBR (for General Vibrating Rollers)

(1) Prediction formula

$$CBR_{16} = 52.0374 + 1.0066 \left(\frac{F}{Bw} \right)^2 + 0.498899 \left(a \left(\frac{F}{2} + Wv \right) - 6.7341 \right)^2 \dots\dots\dots(17)$$

where, **CBR₁₆**: CBR value after 16 passes of roller

F: Centrifugal force (ton)

Bw: Wheel width (m)

Wv: Weight of vibrating wheel (ton)

a: Amplitude (mm)

(2) Calculation example

1) Machinery parameters

$$F = 5.6 \text{ ton}$$

$$Wv = 4.12 \text{ ton}$$

$$f = 2200 \text{ vpm}$$

$$Bw = 1.677 \text{ m}$$

$$a = 0.25 \text{ mm}$$

$$a \left(\frac{F}{2} + Wv \right) = 1.73 \text{ ton} \cdot \text{mm}$$

$$\frac{F}{Bw} = 3.339296$$

2) Calculation

$$\begin{aligned} CBR_{16} &= 52.0374 + 1.0066 \times (3.339296)^2 \\ &\quad + 0.498899 \times (1.73 - 6.7341)^2 \\ &= 75.755 \end{aligned}$$

(3) Comparison between the test data and prediction value

Prediction	75.755
Tested data	74
Error	-2.37%

(4) Other examples

Roller Type	CBR Test Data	Prediction	Error
SV510	120.000	121.679200	-1.679153
SV70	111.000	108.780100	2.219925
SV100	74.000	73.065110	0.934891
SG500	70.000	71.475670	-1.475670

4. Summary

For selection of machines that satisfy finish specifications in compaction process, there is no alternative as general means except for dependance upon a rule of thumb.

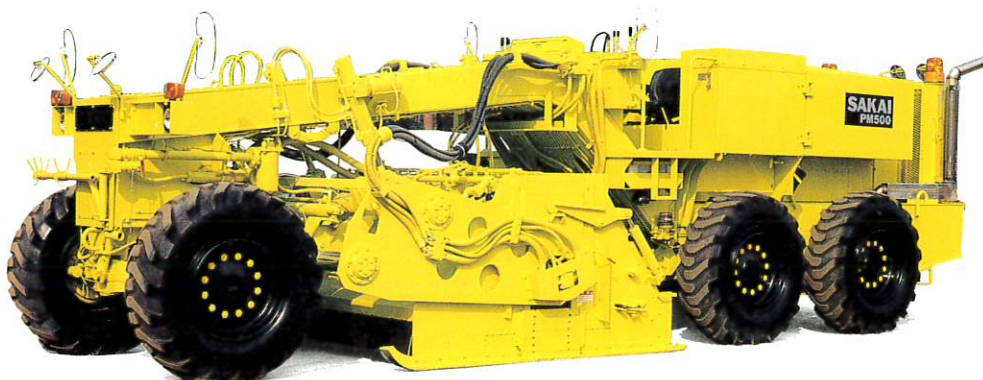
It is ideal to gain required machine conditions through simulation into which all work conditions like specification requirements and soil properties should be input. This rational method, however, is still in the experimental stage.

Under these circumstances, the inductive prediction method stated above is useful as a general use of rule of thumb. Establishing corrective formulae by forging the basic formulae through repeated use of the inductive method will boost accuracy, leading to expansion of application scope.

However, from the standpoint of the question of technology, results of inductive method need to be deductively verified.



Subbase stabilization in Matsuyama City



PM500

CONCLUSION

The first edition, issued in 1985, concluded that continuous research and experiment in future will unveil the whole picture of the problem which will provide a significant key to the optimum condition for high-quality compaction operation.

Significant achievements have since been made through a variety of researches and developments during the course of the last ten years. To discuss the progress in the field of compaction, we now offer this revised edition with added information which is mentioned in the preface of this book as in the following:

- ① **Analysis by elasto-plasticity finite element method for compacting results of steel rollers**
- ② **Prevention of mix pick up on roll surfaces**
- ③ **Development of a roller for RCD**
- ④ **Development of a roller for RCCP**
- ⑤ **Nutating roller**
- ⑥ **Automatic control for compaction process**
- ⑦ **Inductive estimate of compaction results**

The above-mentioned problems are considered to develop in the future as described below: Enclosed numbers of the above-mentioned items correspond to those of the below-mentioned descriptions.

① In this theme, research will inevitably advance from the current static analysis to the dynamic, i.e. vibratory application. However, it is still an unknown field.

② In spite of its importance, this problem has not drawn attention. It is an object of study of physical properties on the microscopic basis hereafter.

③ and ④ Both will be required to cope with increased demand for larger-scale and thicker-lift compaction projects.

⑤ It is long since the new mode roller was put into practical use. But, the model still does not win a high evaluation. The reason is that the basic characteristics of nutating motion is not yet seized sufficiently. With the completion of compaction facilities at our laboratory, the direct approach to the further development is expected. Judging from the trend in which paving materials are increasingly diversified, for new compaction technologies to develop, mechanization based upon new principles will be required.

⑥ The automated control of compaction process is the ultimate theme to attain in our discussion. The problem is classified into two categories as described below:

- ☆ **Controlling the posture of location of the compacting equipment**
- ☆ **Optimum control of machine elements for providing qualitatively compacted materials**

The latter is the main arguing point. This problem has been mentioned in the final part of this edition. At the current investigation level, however, it is not yet decided on what basis the compaction quality is evaluated. Furthermore, it will be impossible to put real-time information of compaction results into the control circuit of rollers while clinging to the paradigm of the current method. For this reason, it is necessary to change the point of view of study to adopt a new alternative.

As a member concerned in this field, the writer takes a great interest in how this problem will develop before the third edition is issued in the future.

The writer would like to thank a number of individuals who united their efforts for this revised edition.

Diffinitions

◆ **Binder** — General term for materials used for the bonding of aggregate particles to each other. Generally, asphalt materials and other special materials mainly utilized for pavement mixes.

◆ **CBR value** — CBR Test is a test to determine the bearing capacity of a material. A plunger of 5 cm in diameter is penetrated into the material by means of a hydraulic jack. A dial gauge indicates the penetration of the plunger, while the proving ring measures the load. The relationship between the load and the penetration is examined. CBR value is given as the ratio of standard load (1,370 kg) at a given penetration (normally 2.5 mm) to applied test load at the penetration (2.5 mm).

$$\text{CBR} = \frac{\text{Applied test load (kg)}}{\text{Standard load (kg)}} \times 100 (\%)$$

◆ **Consolidation** — Soils existing in a natural stage contain voids in them. Air and water occupy the voids. Under load, the air and water in the voids will be pressed out to lead to a decrease in volume and an increase in density of the soils. This phenomenon is “Consolidation”.

◆ **Damping Coefficient** — Fix a spring having a spring constant K , and a dashpot (an enclosed cylinder, filled with a highly viscous oil, with a piston having a small through hole) in parallel to an object having a mass m . Pull the object to extend the spring and then release. At this instance, the object is subject to a spring pull that tends to get the object back to its original position, and at the same time, a resisting force created by the dashpot. The resisting force is in proportion to the speed at which the object moves. Let the modulus of proportion in this case be “ c ”, and the distance that the object has moved be “ x ”, then its equation of motion is given by:

$$m\ddot{x} + k\dot{x} + cx = 0$$

The constant “ c ” is referred to as the “Damping Coefficient”. Depending on the magnitude of c , motion of the object can be periodic motion, damping motion or simple harmonic motion.

◆ **Degree of Compaction** — A standard to determine density, after compaction, of materials such as soils and asphalt mixes. Indicated by a ratio of laboratory-made specimen density to density of a field-compacted specimen.

Degree of compaction (Soil) =

$$\frac{\text{Dry density of field-compacted soil}}{\text{Dry density of laboratory-made soil}} \times 100 (\%)$$

Degree of compaction (Asphalt mix) =

$$\frac{\text{Density of field-compacted mix}}{\text{Density of laboratory-made mix}} \times 100 (\%)$$

◆ **Dry Density** — Weight of dry material per unit volume

◆ **Electric Impedance** — Total electric resistances in an alternating current circuit.

◆ **Filler** — Among aggregates used for asphalt mixes, a material containing more than 65 percent of solid particles smaller than 0.074 mm is called “Filler”.

◆ **Flow Index** — A test soil mixed with water is put in a cup. Then the soil is divided into two sections by grooving tools so that a groove across the soil pat may separate the two sections leaving a given distance. The cup is repeatedly dropped through a height of 1 cm at a frequency of two times a second until the bottom edges of the groove come in contact along a distance of 13 mm. Repetition of this procedure for the same soil while varying its moisture content also exerts influence on the number of blows required to close the groove. Plotting of the moisture content and corresponding number of blows gives a straight line curve on a semi-logarithm graph paper. This curve is called a “Flow Curve”. Inclination of the flow curve is referred to as the “Flow Index”. From this curve, moisture content at which the groove should close in 25 blows can be obtained. This moisture content represents the liquid limit of the soil specimen. Flow index indicates intensity of change in shearing stress corresponding to changes in moisture content.

◆ **K Value** — There is a test to determine the bearing capacity of ground. A load is applied by means of a hydraulic jack on the test material through a loading plate (30, 40, 50, or 75 cm in diameter. Normally 30cm diameter is used.) placed on the material. Relationships between applied load and plate settlement are examined. K value which indicates the bearing capacity of the ground is given by:

$$K = \frac{\text{Applied Test Load (kg/cm}^2\text{)}}{\text{Plate settlement (cm)}} \text{ (kg/cm}^3\text{)}$$

◆ **Liquid Limit** — Moisture content at which soil passes from plastic state to liquid condition as determined by liquid limit test. Liquid limit is used for evaluation of quality of such materials as base course material.

◆ **Modulus of Deformation** — For an object such as a rock in which stress-strain relations are not necessarily rectilinear, the ratio of stress to strain is called “Modulus of Deformation”.

◆ **Modulus of Elasticity** — With an elastic body, strain is in proportion to stress within its proportion limit. The constant of this proportion in such a material is generally called the “Modulus of Elasticity”.

◆ **Moisture Content** — A percentage by weight of water present in a material such as soil. Expressed as a ratio of water to dry material.

Moisture content =

$$\frac{\text{Weight of water in material}}{\text{Weight of solids in the same material}} \times 100 (\%)$$

◆ **Optimum Moisture Content** — Percentage of moisture in a material such as soil at which maximum dry density is obtained for a given compactive effort. A soil compacted at maximum moisture content will retain a stable condition even if it rains.

◆ **Percentage Voids** — Ratio of volume of voids to total volume of material, given by:

$$\text{Percentage voids} = \frac{\text{Total volume of voids}}{\text{Total volume of material}} \times 100 (\%)$$

◆ **Plastic Index** — A value that indicates range in which a soil remains in plastic state as given by the following relationship: See “Liquid Limit” and “Plastic Limit”. Liquid limit and plastic limit are obtained by a given test method.

$$\text{Plastic Index} = \text{Liquid Limit} - \text{Plastic Limit (\%)}$$

◆ **Plastic Limit** — Moisture content at which soil passes from semi-solid state to plastic condition as determined by plastic limit test. Plastic limit is used for the evaluation of such materials as base course material.

◆ **Proctor Density** — The Proctor Test was developed by R.R. Proctor in 1933 to check the density of earthfill dams. A test soil is placed, in 3 layers, in a mould of 934 cm³ capacity. Each layer is compacted by 25 blows of a 2.5 kg rammer dropped through a height of 305 mm. The density of a specimen determined in this test method is called the “Proctor Density”.

◆ **Rockfill Dam** — Among dams composed of soils, sands, gravels and rocks, etc., a dam in which rocks occupy more than half the volume of it is referred to as “Rockfill Dam”.

◆ **Sealing** — A process to make a ground surface texture fine for such a purpose as prevention of rain water permeability. That is to build an impermeable layer.

◆ **Single and Dual Vibrating Shafts** — Vibration generating methods of a vibratory roller. With single vibrating shaft method, vibratory force acts radially in a 360 pattern. In dual vibrating shaft method, two identical vibrating shafts eliminate horizontal (backward and forward) vibratory forces, leaving vibrations in vertical direction alone. The latter is suitable for thick layer compaction.

◆ **Spring Constant** — Strength of a spring, or a force required to compress or stretch a spring to a unit length. Generally, its unit is kg/mm.

◆ **Stability** — Asphalt mixes support loads (buildings and traffic loads, etc.) by resisting to such loads while being subject to a change in shape. This resistibility accompanied by a deformation indicates strength of the mixes, and is referred to as “Stability”. The Marshall Test is one of the tests that determine stability of asphalt mixes, widely used for mix designs. A test sample with a diameter of 10 cm, and a thickness of 6.3 cm is compressed by arc-shaped loading plates at a loading rate of 5 cm per minute. Maximum load indicated before the sample collapses is “Marshall Stability”. The amount of deformation at the time when maximum load is applied gives the “Flow” value of the specimen.

◆ **Standard Deviation** — With such a distribution of scholastic marks statistically supposed to fall into a normal distribution, each mark can indicate, based on standard deviation, how far it deviates from a mean score. The value thus indicated is “Deviation”. “Standard Deviation” and “Deviation” are given by:

$$\text{Standard deviation} = \sqrt{\frac{\text{Sum of (each score — mean score)}^2}{\text{Number of examinees}}}$$

$$\text{Deviation} = \frac{10 \times (\text{each score} - \text{mean score})}{\text{Standard deviation}} + 50$$

◆ **Well-graded Crushed Stones** — Crushed stones adjusted to a proper grading for use in base courses.

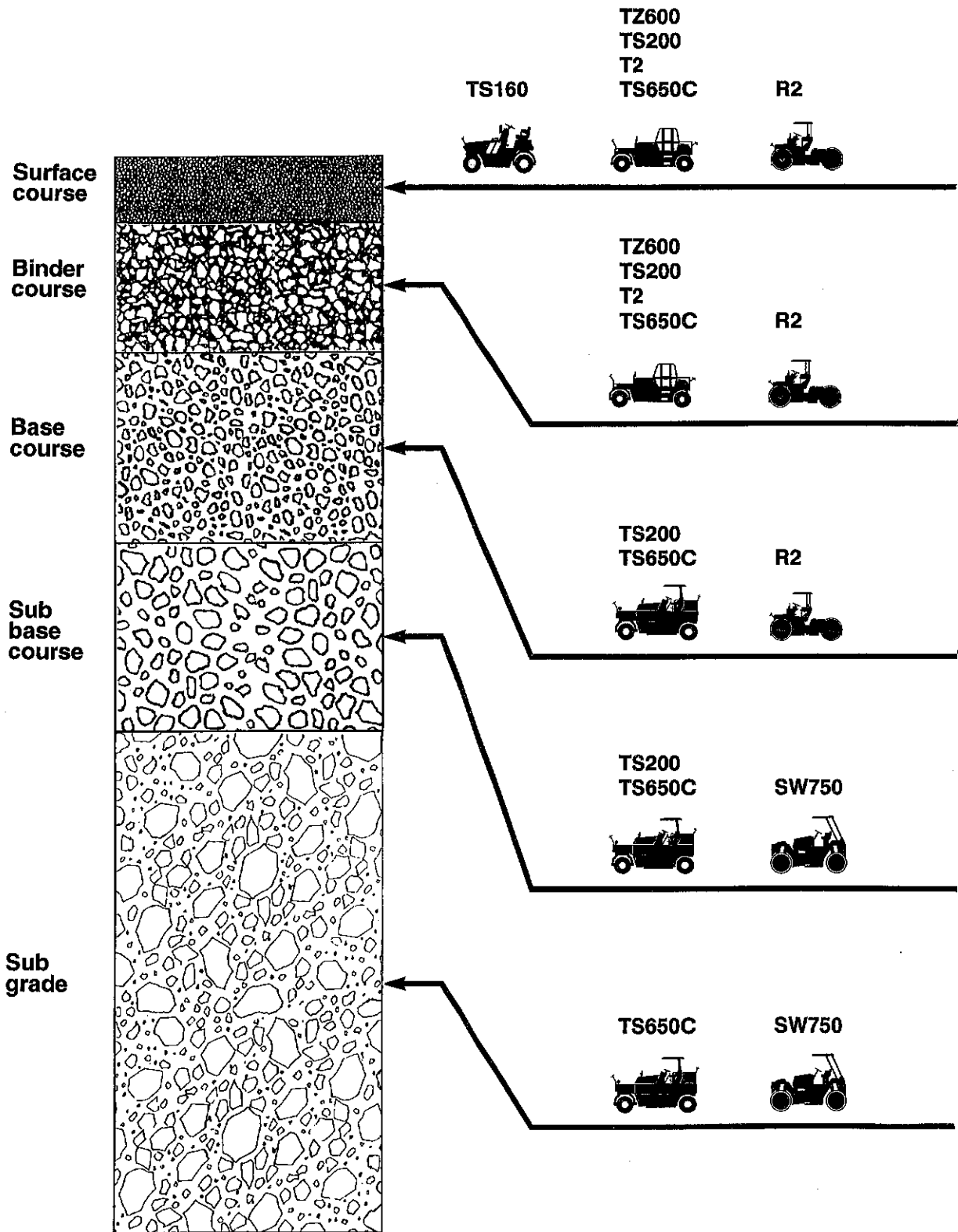
References

- 1) М. Н. Летошнев: "Колесне пвоэки" 1936 Теория и производство сельскохозяйственных машин
- 2) M. G. Bekker: "Theory of Land Locomotion"
- 3) J. Theiner: "Untersuchungen der Walzverdichtungsvorgänge mit gezogenen und Selbstfahrenden Glattwalzen auf kohäsionlosem und bindigem Boden" AACHEN
- 4) Colin Vallies: Hyster, The Earthmover Nov. 1974
- 5) 建設機械化研究所性能試験報告書「サカイ・ハム前輪駆動タンDEMローラ」昭和40年12月
- 6) "Some aspects of the design and operation of the 3-wheeled road roller" THE INSTITUTION OF MECHANICAL ENGINEERS
- 7) Söhne: "Druckverteilung im Boden und Bodenverformung unter Schlepperreifen"
- 8) 沢田健吉: トラフイカピリテイ、土木技術資料、Vol. 8, No. 4~5
- 9) Н. Я. Хархута: "Влияние давления вшинах катков на уплотнение грунтов" Строительное и Дорожное Машиностроение No 11, 1959
- 10) D. R. Freitag, M.E. Smith: "Center-line deflection of pneumatic tires moving in dry sand" Journal of Terramechanics Vol.3, No.1, 1966.
- 11) Dr. Ing. K. Banaschek u. Ing. F. Fischer:
"Der Einsatz von Gummiradwalzen mit Erdbau und im bituminösen Straßenbau".
- 12) Dott. Ing. Domenighetti:
The Elementary Technology of Compaction
- 13) 藤本義一、根本忠: 建設機械化研究所 "建設機械用タイヤ性能"
- 14) E. Bauer, Köln: Straßen-u. Tiefbau Heft 8/1967
"Vorverdichtung von bituminösen Mischgut beim Einbauvorgang".
- 15) Dipl. Ing. Klaus Schulze, TH München: Zeitschrift Straßen-u. Tiefbau, 1966.
"Die Walzverdichtung bituminöser Fahrbahndecken u. Tragschichten" 1965
"Einflußfaktoren auf die Ebenheit bituminöser Fahrbahnbeläge".
- 16) Lars Forsblad: ACTA POLYTECHNICA SCANDINAVICA
"Investigations of Soil Compaction by Vibration".
- 17) 根本忠ほか、建設機械化研究所 "振動ローラの締固め特性"
- 18) 高野漢、桃井徹: 道路建設 55/9
- 19) (財) 国土開発技術研究センター: "RCDコンクリート締固め実験調査報告書" 53/3
- 20) S.F. Brown, University of Nottingham. P. Ansell, Sir William & Partners
"The influence of repeated shear reversal on the compaction of granular material"
- 21) SAKAI "VIBROLESS" VIBRATING ROLLER IN NEW MODE
- 22) 「新しい振動ローラによる試験施工について」
ダム技術 増刊第一号 1991
- 23) 転圧コンクリート舗装技術指針 (案) 平2・10 (社) 日本道路協会
- 24) アスファルト舗装要綱 平成5年1・16第2版 同上

- 25) 大槻・加形「転圧コンクリートの試験施工の一例」 舗装 88・4
- 26) 岩隈 「章動ローラの開発」 建設機械 88・10
- 27) 坪田・玉井「ローラ機種の違いによる締固め効果の検討」 舗装91・10
- 28) 加形「RCCPの締固め要因」 同上
- 29) 後町・松井「締固め機械と管理装置」 同上
- 30) 三井・宮崎「締固め機械の振動装置」 公開特許 昭62-25004
- 31) 「SD450型振動ローラ技術審査証明報告書」 平2.9 (社) 日本建設機械化協会
- 32) 「RCCPの試験施工結果」平成5年5月 福田道路(株)
- 33) Dieter Pietzsch & Wolfgang Poppy
“SIMULATION OF SOIL COMPACTION WITH VIBRATORY ROLLER”
Journal of Terramechanics. Vol.29, No.6 pp.585-597, 1992
- 34) Rudolf Floss, Andreas Reuther
“Vergleichsuntersuchungen über die Wirkung von vibrierend und oszillierend arbeitender Verdichtungswalze” München 1990
- 35) 能勢・橋口・上野・内山・Jarzebowski・小山・亀井・住吉
「車輪走行現象の解析」農業機械シンポジウム論文集 (1992) p 86 ~ 102
- 36) 内山・能勢・Jarzebowski・橋口・上野
「車輪と土の相互作用に関する数値解析」テラメカニクス 第12号 p 73 ~ 78
- 37) 橋口公一：「最新弾塑性学」朝倉書店 1990. 5. 20
- 38) 三好俊郎：「有限要素法入門」
- 39) C.S.デサイ/J.F.A アーベル 山本善之訳
「マトリックス有限要素法 ― 基礎理論とその応用 ―」
- 40) O.C. Zienkiewicz
The Finite Element Method-3rd Edition-
- 41) 根本・佐々木：土の締固め特性 建設機械化研究所
創立30周年記念論文集 1994. 6.10
- 42) 馮副教授 中国上海同済大学
Prediction Formulas of Dry Density for the Vibration Roller
- 43) Messtechnik für die Verdichtungskontrolle. Strassen u. Tiefbau 6 '94

APPENDIX

APPLICATION RANGE for SAKAI COMPACTION EQUIPMENT



SW250
SW350
SW500
SW650
SW750



TW250
TW350
TW500
TW650
TW750



SG350
SG500



TG350
TG500



PM500



ER501F



SW650
SW750



TW650
TW750



PM500



ER501F



SW650
SW750



TW650
TW750



SV70
SV500
SV510D



SV70TF
SV500DF
SV500TF



PM500



SV70
SV500
SV510D
SV160D



SV70TF
SV500DF
SV500TF



PM500



SV70D
SV500D
SV510D
SV160D



SV70T
SV500T
SV510T
SV160T



SV70TF
SV500DF
SV500TF



1. PNEUMATIC TIRED ROLLER

MODEL	WEIGHTS kg		WEIGHT DISTRIBUTION / TIRE (OPERATING) kgf		NUMBER OF TIRES		WIDTH (TIRE) mm	DRIVE SYSTEM
	EMPTY	OPERATING	FRONT	REAR	FRONT	REAR		
TS160	2,800	3,000	445	407	4	3	243	HYDROSTATIC
TZ600	8,500	15,000	2,133	2,150	3	4	370	HYDROSTATIC
TS200	8,500	15,000	1,575	1,740	4	5	260	MECHANICAL
T2	8,500	15,500	2,200	2,225	3	4	370	MECHANICAL
TS600C	8,500	15,000	1,600	1,720	4	5	260	HYDRODYNAMIC
T600C	8,500	15,500	2,233	2,200	3	4	370	HYDRODYNAMIC
TS600	8,500	15,000	1,575	1,740	4	5	260	HYDROSTATIC
T600	8,500	15,500	2,200	2,225	3	4	370	HYDROSTATIC
TS650C	12,750	25,050	3,540	3,608	3	4	314	HYDRODYNAMIC

2. THREE WHEEL ROLLER

MODEL	WEIGHTS kg	PRESSURE kgf/cm		DRUM DIMENSION (DIAMETER x WIDTH) mm		REMARKS
		FRONT	REAR	FRONT	REAR	
R2	9,950	44.3	46.2	1,620×550	1,620×1,100	STANDARD
R2H	14,000	61.9	65.4	1,620×550	1,620×1,100	HEAVY WEIGHT
R2B	11,850	51.4	56.4	1,620×550	1,620×550×2	SEPARATE (REAR DRUM)
R2F	11,200	48.4	53.5	1,620×550	1,620×1,100	TILT (FRONT DRUM)
R2V	11,200	48.4	53.5	1,620×550	1,620×1,100	VIBRATORY (FRONT DRUM)
R2W	14,000	55.9	61.2	1,620×650	1,620×1,100	WIDE DRUM (FRONT DRUM)

3. VIBRATING ROLLER

3-1. PAVING TANDEM VIBRATORY ROLLER (ARTICULATED)

MODEL	WEIGHTS kg	LINEAR PRESSURE kgf/cm		DRUM (DIAMETER x WIDTH) mm	VIBRATING FORCE kgf	FREQU- ENCY vpm	REMARKS
		FRONT	REAR				
SW200	1,330	8.6	8.0	558×800	670	3,150	
SW230	1,480	8.4	8.0	558×900	840	3,150	
SW250	1,550	8.0	7.5	558×1,000	940	3,150	
SW350	2,780	11.6	11.6	675×1,200	2,100	3,300	
SW500	4,150	15.6	16.3	800×1,300	2,500	3,300	STANDARD
SW500N	4,470	16.8	17.5	800×1,300	6,400	3,300	(≡OSCILLATORY) ROLLER
SW650	7,200	23.3	25.3	1,070×1,480	3,750/7,000	3,100	STANDARD
SW650B	8,000	26.0	28.0	1,070×740×2	3,750/7,000	3,100	SEPARATE (DRUM)
SW650N	7,500	24.3	26.4	1,070×1,480	11,000	3,100	(≡OSCILLATORY) ROLLER
SW650V	7,700	25.0	27.0	1,070×1,480	4,500/8,000	3,100	VERTICAL VIBRATORY
SW750	9,150	26.2	28.3	1,220×1,680	6,000/8,000	3,000	STANDARD
SW750B	9,950	28.6	30.7	1,220×840×2	6,000/8,000	3,000	SEPARATE (DRUM)
SW750N	9,150	26.2	28.3	1,220×1,680	14,500	3,000	(≡OSCILLATORY) ROLLER
SW750V	9,640	28.0	29.4	1,220×1,680	6,000/10,000	2,600	VERTICAL VIBRATORY
SW750H	10,000	28.6	31.0	1,220×1,680	6,000/10,000	2,600	HEAVY DUTY

3-2. PAVING COMBINED ROLLER (ARTICULATED)

MODEL	WEIGHTS kg	FRONT DRUM		VIBRATING FORCE kgf	FREQU- ENCY vpm	REAR TIRE			REMARKS
		LINEAR PRESSURE kgf/cm	(DIAMETER x WIDTH) mm			WEIGHTS ON TIRE kgf	NUMBER OF TIRES	WIDTH (TIRE) mm	
TW200	1,230	8.6	558×800	670	3,150	180	3	210	
TW230	1,310	8.4	558×900	840	3,150	183	3	210	
TW250	1,380	8.0	558×1,000	940	3,150	145	4	210	
TW350	2,450	11.5	675×1,200	2,100	3,300	268	4	243	
TW450	3,530	15.2	750×1,270	2,200	3,300	400	4	224	STANDARD
TW450W	3,550	15.2	750×1,270	2,200	3,300	405	4	275	WIDE TIRE
TW500	3,600	15.2	800×1,300	2,500	3,300	408	4	224	STANDARD
TW500W	3,620	15.2	800×1,300	2,500	3,300	413	4	275	WIDE TIRE
TW650	6,500	23.0	1,070×1,480	3,750/7,000	3,100	775	4	260	
TW750	8,000	26.2	1,220×1,680	6,000/8,000	3,000	900	4	314	

3-3. PAVING TANDEM VIBRATORY ROLLER (REAR DRUM STEERING)

MODEL	WEIGHTS kg	FRONT DRUM		CENTRI- FUGAL FORCE kgf	FREQU- ENCY vpm	REAR DRUM		REAR TIRE			REMARKS
		LINEARY PRESSURE kgf/cm	(DIAMETER WIDTH) mm			LINEARY PRESSURE kgf/cm	(DIAMETER WIDTH) mm	WEIGHTS ON TIRE kgf	NUMBER OF TIRES	WIDTH (TIRE) mm	
SG350	2,750	14.0	850×1,200	2,600	3,200	11.3	720×950				
TG350	2,550	14.0	850×1,200	2,600	3,200			290	3	243	COMBINED ROLLER
SG500	4,000	18.7	950×1,350	4,300	3,200	14.5	820×1,020				
TG500	3,900	19.0	950×1,350	4,300	3,200			335	4	224	COMBINED ROLLER

4. EARTH WORK VIBRATORY ROLLER

MODEL	WEIGHTS kg	FRONT DRUM			CENTRIFUGAL FORCE kgf	FREQUEN- CY vpm	REMARKS (S=Smooth drum) (T=Tamping drum)
		ON AXLE kgf	LINEAR PRESSURE kgf/cm	(DIAMETER x WIDTH) mm			
SV200D	4,050	2,000	16.1	940×1,240	5,200	1,800	ALL WHEEL DRIVE
SV200T	4,250	2,200		1,000×1,240	6,500	1,800	TAMPING ROLL
SV200TB	4,450	2,450		1,000×1,240	6,500	1,800	TAMPING WITH BLADE
SV70	6,500	3,100	18.2	1,250×1,700	6,000/11,000	1,800	REAR WHEEL DRIVE
SV70D	6,600	3,200	18.8	1,250×1,700	6,000/11,000	1,800	ALL WHEEL DRIVE
SV70T	7,300	3,950		1,400×1,700	13,000	1,800	TAMPING ROLL
SV70TB	7,650	4,400		1,400×1,700	13,000	1,800	TAMPING WITH BLADE
SV70TF	8,950	5,750	26.7	φ1,450×1,700	13,000	1,800	(S) & (T) EXCHANGEABLE
SV500	10,000	5,400	25.1	1,530×2,150	8,500/21,000	1,300/2,400	REAR WHEEL DRIVE
SV500D	10,200	5,600	26.0	1,530×2,150	8,500/21,000	1,300/2,400	ALL WHEEL DRIVE
SV500DF	11,600	7,100		φ1,710×2,150	17,000/21,000	1,800/2,400	(T) & (S) EXCHANGEABLE
SV500T	10,500	5,900		1,600×2,150	25,000	1,800	TAMPING ROLL
SV500TF	12,800	8,300	38.6	φ1,650×2,150	25,000	1,800	(S) & (T) EXCHANGEABLE
SV510D	10,500	5,600	26.0	1,530×2,150	17,000/21,000	1,800/2,400	ALL WHEEL DRIVE
SV510T	10,900	5,900		1,600×2,150	25,000	1,800	TAMPING ROLL
SV510DV	11,400	6,500	30.2	1,530×2,150	17,000/23,000	1,800/2,400	VERTICAL VIBRATORY (S)
SV510TV	11,700	6,700		1,600×2,150	17,000/23,000	1,800/2,400	VERTICAL VIBRATORY (T)
SV160D	17,400	10,000	46.5	1,700×2,150	21,000/30,000	1,700	ALL WHEEL DRIVE
SV160T	17,400	10,000		1,760×2,150	30,000	1,700	TAMPING ROLL
SV160DV	17,600	10,200	47.4	1,700×2,150	21,000/30,000	1,700/2,400	VERTICAL VIBRATORY (S)
SV160TV	17,700	10,300		1,760×2,150	21,000/30,000	1,700/2,400	VERTICAL VIBRATORY (T)
SD451	11,000	前 5,250	25.0	1,000×2,100	17,000/23,000	2,600	VERTICAL VIBRATORY
		後 5,750	27.4	1,000×2,100	17,000/23,000	2,600	(TANDEM VIBRATORY)

5. SURFACE CUTTER

MODEL	CAPACITY			OPERATING WEIGHT kg	CUTTER UNIT DRUM OFF-SET		LOADER mm	VEHICLE
	WORKING SPEED m/min	CUTTING WIDTH mm	Max. DEPTH mm		LEFT-HAND-SIDE mm	RIGHT-HAND-SIDE mm		
ER501F	0 ~ 30	2,100	160	26,100	450	450	3,400	PNEUMATIC TIRE

6. ROAD STABILIZER (RECLAIMER)

MODEL	CAPACITY			OPERATING WEIGHT kg	CUTTER UNIT MIXING ROTOR OFF-SET		CARRIER
	WORKING SPEED m/min	MIXING WIDTH mm	MAX. MIX-DEPTH mm		LEFT-HAND-SIDE mm	RIGHT-HAND-SIDE mm	
PM500	0 ~ 50	2,000	400	21,000	500	500	PNEUMATIC TIRE

SAKAI HEAVY INDUSTRIES, LTD.

Head Office:	1-4-8, Shiba Daimon, Minato-ku, Tokyo, Japan
Telephone:	+81-3-3431-9971
Facsimile:	+81-3-3436-6212
Technical Laboratory:	2626, Takayanagi, Kurihashi-machi, Kitakatsushika-gun, Saitama Prefecture
Telephone:	+81-480-52-6131
Facsimile:	+81-480-52-0117

Printed in Japan ©

